RECYCLING SMC WASTE THROUGH PYROLYSIS FOR SUSTAINABLE PRODUCTION OF AUTOMOTIVE COMPONENTS

A THESIS SUBMITTED TO
THE GRADUATE SCHOOL OF NATURAL AND APPLIED SCIENCES
OF
MIDDLE EAST TECHNICAL UNIVERSITY

BY

BARKIN DURMUŞ

IN PARTIAL FULFILLMENT OF THE REQUIREMENTS
FOR
THE DEGREE OF MASTER OF SCIENCE
IN
MICRO AND NANOTECHNOLOGY

JANUARY 2025

Approval of the thesis:

RECYCLING SMC WASTE THROUGH PYROLYSIS FOR SUSTAINABLE PRODUCTION OF AUTOMOTIVE COMPONENTS

submitted by **BARKIN DURMUŞ** in partial fulfillment of the requirements for the degree of **Master of Science in Micro and Nanotechnology, Middle East Technical University** by,

Prof. Dr. Naci Emre Altun
Dean, **Graduate School of Natural and Applied Sciences** _____

Prof. Dr. Deniz Üner
Head of the Department, **Micro and Nanotechnology** _____

Prof. Dr. Almıla Güvenç Yazıcıoğlu
Supervisor, **Micro and Nanotechnology, METU** _____

Dr. Feyza Kazanç Özerinç
Co-Supervisor, **Prairie Research Institute, UIUC** _____

Examining Committee Members:

Prof. Dr. Cevdet Kaynak
Metallurgical and Materials Eng., METU _____

Prof. Dr. Almıla Güvenç Yazıcıoğlu
Mechanical Engineering, METU _____

Prof. Dr. Burcu Akata Kurç
Micro and Nanotechnology, METU _____

Prof. Dr. Hüsnü Emrah Ünalan
Metallurgical and Materials Eng., METU. _____

Assoc. Prof. Dr. Kadriye Özlem Hamaloğlu
Chemical Engineering., Hacettepe University _____

Date: 10.01.2025

I hereby declare that all information in this document has been obtained and presented in accordance with academic rules and ethical conduct. I also declare that, as required by these rules and conduct, I have fully cited and referenced all material and results that are not original to this work.

Name Last name : Barkın Durmuş

Signature :

ABSTRACT

RECYCLING SMC WASTE THROUGH PYROLYSIS FOR SUSTAINABLE PRODUCTION OF AUTOMOTIVE COMPONENTS

Durmuş, Barkın
Master of Science, Micro and Nanotechnology
Supervisor: Prof. Dr. Almıla GÜVENÇ YAZICIOĞLU
Co-Supervisor: Dr. Feyza KAZANÇ ÖZERİNÇ

January 2025, 122 pages

Due to their crosslinked structure, conventional methods cannot reuse thermoset composites, and recycling methods are expensive or harmful. These composites contain valuable inorganic components crucial for a circular economy and sustainable production. Employing products derived from the polymer matrix also supports these objectives. This study develops a method to recycle sheet molding compound (SMC) waste from tractor manufacturing and vehicles, enabling the reuse of recovered solids in tractor applications. Liquid products are characterized, and potential uses are proposed, while a literature review informs the reuse of gaseous products.

Laboratory-scale trials evaluate pyrolysis, oxidation, and pyrolysis followed by oxidation. Pyrolysis employs a 15 °C/min heating rate, while oxidation heats samples to 500 °C at 10 °C/min with a 50-minute hold. Based on the results, pyrolysis is selected, eliminating the need for fiber cleaning. A pilot-scale process is implemented, collecting condensable products, and employing a new protocol: heating to 400 °C at 10 °C/min with a 10-minute hold, followed by 600 °C at 5 °C/min with a 60-minute hold, avoiding $CaCO_3$ decomposition. Recovered glass

fibers and solids replace $CaCO_3$ in bulk molding compound (BMC) at 5%, 10%, and 15%. Mechanical testing identifies 10% as the optimal substitution, enabling the fabrication of a tractor component that meets the required specifications.

Characterization methods for solids include TGA, DSC, FTIR, XRD, XRF, EDX, SEM, and optical microscopy, while GC-MS and a bomb calorimeter are used for liquids. Finally, simulation and bump testing validate the recycled tractor part.

Keywords: Pyrolysis, Automotive, Sustainability, SMC, Recycling

ÖZ

PİROLİZ YOLUYLA SMC ATIKLARININ GERİ DÖNÜŞÜMÜ İLE OTOMOTİV BİLEŞENLERİNİN SÜRDÜRÜLEBİLİR ÜRETİMİ

Durmuş, Barkın
Yüksek Lisans, Mikro ve Nanoteknoloji
Tez Yöneticisi: Prof. Dr. Almıla GÜVENÇ YAZICIOĞLU
Ortak Tez Yöneticisi: Dr. Feyza KAZANÇ ÖZERİNÇ

Ocak 2025, 122 sayfa

Çapraz bağlı yapılarından dolayı, termoset kompozitler geleneksel yöntemlerle yeniden kullanılamaz ve geri dönüşüm yöntemleri maliyetli veya çevreye zararlıdır. Bu kompozitler, döngüsel ekonomi ve sürdürülebilir üretim için kritik öneme sahip değerli inorganik bileşenler içermektedir. Ayrıca, polimer matrisinden elde edilen ürünlerin kullanımı da bu hedefleri desteklemektedir. Bu çalışma, traktör üretimi ve hurda parçalardan kaynaklanan sac kalıplama bileşiği (SMC) atıklarının geri dönüştürülmesi için bir yöntem geliştirmekte ve geri kazanılan katıların traktör uygulamalarında yeniden kullanılmasını sağlamaktadır. Sıvı ürünler karakterize edilerek potansiyel kullanım alanları önerilmiş ve gaz ürünlerin yeniden kullanımına ilişkin literatür incelemesi yapılmıştır.

Laboratuvar ölçekli denemeler, piroliz, oksidasyon ve piroliz ardından oksidasyon süreçlerini değerlendirmiştir. Piroliz, 15 °C/dakikalık bir ısıtma oranıyla gerçekleştirilirken, oksidasyon 10 °C/dakikalık bir ısıtma oranıyla numunelerin 500 °C'ye kadar ısıtılmasını ve 50 dakika süreyle bekletilmesini içermiştir. Sonuçlara dayanarak, fiber temizleme ihtiyacını ortadan kaldıran piroliz yöntemi tercih edilmiştir. Pilot ölçekli bir süreç uygulanmış, yoğunlaşabilir ürünler toplanmış ve yeni bir protokol benimsenmiştir: 10 °C/dakikalık bir ısıtma oranıyla numunelerin

400 °C'ye kadar ısıtılması ve 10 dakika bekletilmesi, ardından 5 °C/dakikalık bir ısıtma oranıyla 600 °C'ye kadar çıkarılması ve 60 dakika bekletilmesi, $CaCO_3$'ün bozunması önlenmiştir. Geri kazanılan cam elyaf ve katılar, toplu kalıplama bileşiği (BMC) içinde %5, %10 ve %15 oranlarında $CaCO_3$ yerine kullanılmıştır. Mekanik testler, %10'luk bir oranı en uygun ikame olarak belirlemiş ve gerekli spesifikasyonları karşılayan bir traktör bileşeninin üretilmesini sağlamıştır.

Katılar için karakterizasyon yöntemleri arasında TGA, DSC, FTIR, XRD, XRF, EDX, SEM ve optik mikroskobi bulunurken, sıvılar için GC-MS ve bomba kalorimetresi kullanılmıştır. Son olarak, simülasyon ve çarpma testleri geri dönüştürülmüş traktör parçasını doğrulamıştır.

Anahtar Kelimeler: Piroliz, Otomotiv, Sürdürülebilirlik, SMC, Geri Dönüşüm.

to my lovely family

ACKNOWLEDGMENTS

I would like to begin by expressing my deepest gratitude to my supervisor, Prof. Dr. Almıla Güvenç Yazıcıoğlu, for her understanding, thoughtful mentorship, timely support during critical moments, and the dedicated effort she invested in ensuring the completeness of this thesis.

I am also sincerely thankful to my co-supervisor, Dr. Feyza Kazanç, for her guidance, and contributions, which made it possible for me to begin and continue this thesis work.

The completion of this thesis was made possible by TürkTraktör, including funding, as part of my professional work. I am especially grateful to Dr. Hakan Mencek for his guidance and mentorship and to Özgür Gündüz and İdil Ünver for their continuous support and friendship.

I would also like to acknowledge the collaboration and contributions of Erdem Mutlu and I-Carbon, as well as Fatma Aydın and CTP Composite, during various stages of this thesis project.

I am grateful to Selin Erdoğan, with whom I have collaborated since the beginning of my undergraduate education, for her support and role in enabling me to complete this work.

I am also thankful to Furkan Bahadır Elik, Ozan Can Demirtaş, Yağmur Karahan, Şeyda Elif Asan and Alptuğ Okkan for their friendships, openness to exchanging ideas, and assistance in overcoming challenges.

I wish to thank my lab colleagues, Süleyman Şener Akın, Ali Bertan Kır, Umut Güçlü, and Alican Akgül, for their constant help and friendships.

I owe a profound debt of gratitude to my family, Sabahattin Durmuş, Süreyya Durmuş, and Ada Durmuş, who laid the foundation for everything I have achieved in life, supported me through challenges, and shared in my successes.

I am thankful to Vini, whose presence always made me smile.

Finally, I admire Yaşar Kemal, whose words about humanity overcoming despair inspired me, and Joaquín Rodrigo, whose compositions provided solace and focus throughout this journey.

TABLE OF CONTENTS

LIST OF TABLES

TABLES

LIST OF FIGURES

FIGURES

LIST OF ABBREVIATIONS

ABBREVIATIONS

BMC	Bulk Molding Compound
CAE	Computer-Aided Engineering
CCTL	Clean Combustion Technologies Laboratory
CF	Carbon Fiber
DMC	Dough Molding Compound
DSC	Differential Scanning Calorimetry
DTA	Differential Thermal Analysis
DTG	Derivative Thermogravimetry
EDX	Energy-Dispersive X-ray Spectroscopy
ELV	End-of-Life Vehicles
EU	European Union
FBAS	Flex Body Analysis and Simulation
FE	Field Emission
FRP	Fiber Reinforced Polymer
FTIR	Fourier Transform Infrared Spectroscopy
GC-MS	Gas Chromatography-Mass Spectrometry
GCV	Gross Calorific Value
GF	Glass Fiber
HCL	Hydrochloric Acid
HTC	Horizontal Tube Furnace

MBD	Multi Body Dynamics
PO	Pyrolysis Followed by Oxidation
RCRA	Resource Conservation and Recovery Act
RPM	Rotation per Minute
SEM	Scanning Electron Microscopy
SMC	Sheet Molding Compound
TGA	Thermogravimetric Analysis
US	United States
UV	Ultra-violet
XRD	X-ray Diffraction
XRF	X-ray Fluorescence

CHAPTER 1

INTRODUCTION

Sustainability concerns and the regulations stemming from them currently hold significant importance in the strategies of policymakers and companies. The term "sustainability" originates from the French word "soutenir" and has its roots in forestry, based on the principle that the amount of wood harvested should not exceed the number of trees that can regrow. In the modern era, this philosophy has evolved to mean that humans maintain themselves by protecting their safety, health, and non-renewable natural resources, [1,2] Transitioning from fossil-based sources to renewable resources, reducing our waste, and establishing a regenerative system has become essential for the security of future generations. [2]

1.1 Global Plastic Recycling: Current Practices and International Responsibilities

From the beginning of industrial production in 1950 until 2015, 8,300 million tons of virgin plastic have been produced, resulting in 6,300 million tons of plastic waste. Only 9% of this waste has been recycled, 12% incinerated, and the remaining 79% either landfilled or dispersed into the environment. Although efforts have been made over the past decade to increase recycling rates through regulations, estimates predict that plastic waste will reach 33,000 million tons by 2050, with a recycling rate of 44%. [3]

According to Plastics Europe, the production of plastics in 2022 alone was 400.3 million tons, with thermosets constituting approximately 11% or 42 million tons of

this total. [4] This situation lays the groundwork for regulations and inspections to be implemented on this issue, making it essential to increase the recycling rate.

Supported by international agreements and the European Union's climate targets aiming for carbon neutrality by 2050, addressing waste management has become a priority in all sectors, including agricultural machinery manufacturing and the automotive industry. The European Union's Waste Framework Directive (2008/98/EC) establishes a waste management hierarchy that imposes the principles of prevention, reuse, and recycling to minimize environmental. [5] Additionally, the End-of-Life Vehicles (ELV) Directive (2000/53/EC) mandates the same principles for the automotive sector, directing companies to set targets and promoting the reuse of components and recycling of materials. Although these regulations and directives apply to passenger vehicles, they set a regulatory example affecting similar sectors, such as tractor production, indicating future regulations these sectors may face. [6]

In the United States, regulations like the Resource Conservation and Recovery Act (RCRA) similarly govern waste management and encourage the development of recycling technologies for materials that are difficult to recycle, such as thermosets. [7]

1.2 Agricultural Machinery: Current Status and Driving Motivation

In Turkey, TürkTraktör is the market leader in tractor production and has the largest production capacity, maintaining a leading position in the field of agricultural machinery for many years. [8] TürkTraktör is a joint venture of Koç Holding and CNH Industrial and sells its products to markets such as the EU and the US. [9] Therefore, it must comply with these countries' regulations and align with its parent companies' sustainability commitments. Koç Holding has adopted the EU's 2050 carbon-neutral target. [10] Similarly, CNH Industrial has embraced comparable targets within the scope of its global sustainability program and is taking measures

towards these goals. [11] For these reasons, it is necessary for TürkTraktör to take actions that are aligned with the directives and regulations mentioned in this section.

TürkTraktör has an effective sustainability policy. In this policy, environmental impacts in areas such as production, logistics, and transportation are examined, and solutions are developed for more sustainable operations and production. So far, efforts have been made to make logistics operations more sustainable by making wooden pallets recyclable and reusable, preventing the consumption of natural resources, and transitioning to recyclable materials in packaging, with ongoing efforts in this area. However, currently, none of the plastic parts on the tractors produced are made from recycled materials, nor are they recycled by the company when they become post-consumer waste or production scrap. [12]

Numerous polymer-based parts are on the tractor. One of the components with the highest production and waste capacity is the sheet molding compound (SMC) used in body and fender parts. It is a thermoset composite composed of a polyester matrix and fiberglass reinforcement.

1.3 Composites

Throughout human history, composite materials have played a significant role in numerous fields, ranging from fundamental construction techniques to space-age materials, thereby benefiting humanity. Composites are formed by the combination of at least two distinct materials. The objective of composite production is to create a new material that exhibits superior performance compared to the individual properties of its constituent components. [13–17]

Furthermore, polymers have been integrated into our lives over the past several decades. Replacing metal and ceramic materials in numerous fields, they perform better in specific material properties tailored to their application areas. At the same time, they offer economic advantages. [15,18]

However, polymers alone may be inadequate in strength, stiffness, and other properties required for certain applications. In areas where polymers fall short, polymer composites have been developed. Fiber-reinforced polymer composites hold a significant position among the most common types of polymer composites. These composite materials replace metal and ceramic materials in construction, aerospace, automotive, marine, sports, transportation, and many other fields. [2,15,19–22]

In Fiber Reinforced Polymer (FRP) composites, materials such as epoxy, phenolic, polyester, and vinyl ester are commonly used as the matrix element. At the same time, glass fibers, carbon fibers, and natural fibers can be utilized as reinforcement elements. These fibers act as the primary load-bearing components within the composite, whereas the polymer matrix holds the fibers together and distributes the load among them. Compared to metals, FRPs offer advantages such as higher specific strength and stiffness, resistance to corrosion, chemicals, and weathering, superior fatigue strength, the ability to tailor electrical and thermal properties, greater design flexibility, ease of manufacturing, and low-cost production. These benefits make FRPs a preferred material in many fields. [15,19,20,23–26]

The attainment of these properties primarily depends on the type of matrix and reinforcement materials used, the additives incorporated, the micro- and macro-structure, the structural orientation, and the interfacial mechanisms between fibers and polymers. Extensive research has been conducted in these areas within the literature, and the number of studies focusing on different types of composites, their production and testing techniques, and their applications continues to grow steadily. [17,19,20,23–25,27–69]

Composite materials can be classified in several ways based on their two primary constituents: the matrix and the reinforcement. The fundamental principle underlying composites is that reinforcement is incorporated into a given matrix to impart or enhance mechanical properties that are absent or deficient in the matrix

material. The following diagrams also illustrate the classification of composites, first based on their matrix and then on their reinforcement. [70,71]

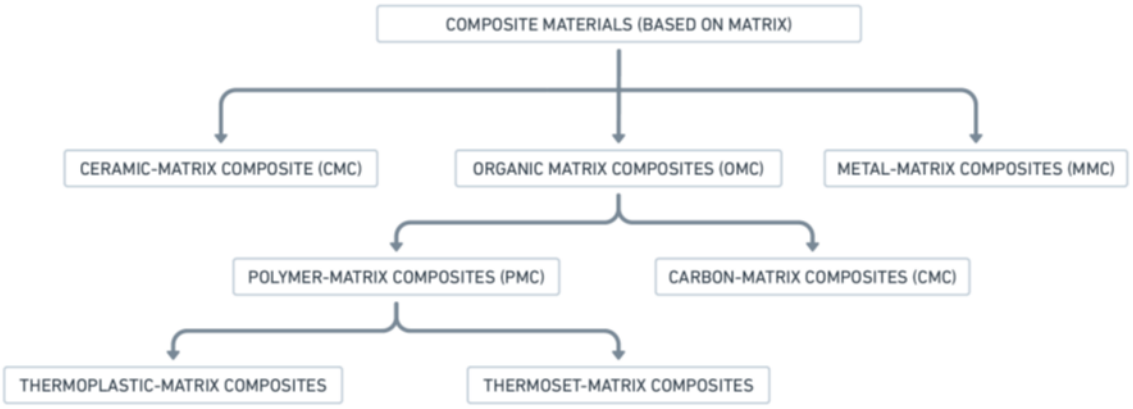

Figure 1.1. Composite Materials (Based on Matrix) [70,71]

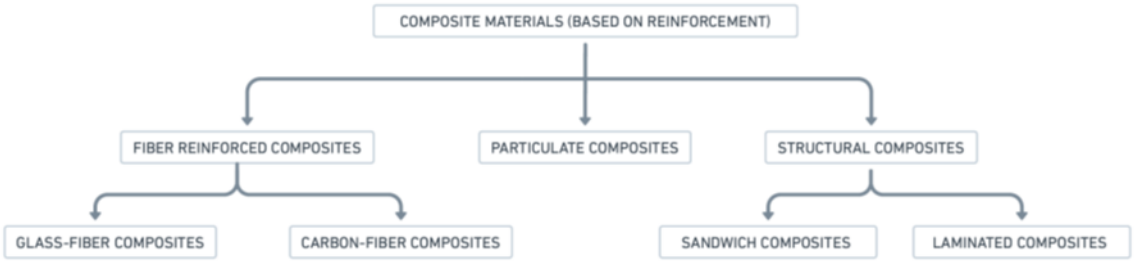

Figure 1.2. Composite materials (based on reinforcement) [70,71]

B. De et al. have also proposed an alternative framework specifically designed to categorize and illustrate the different types of Fiber Reinforced Polymer (FRP) composites. [15]

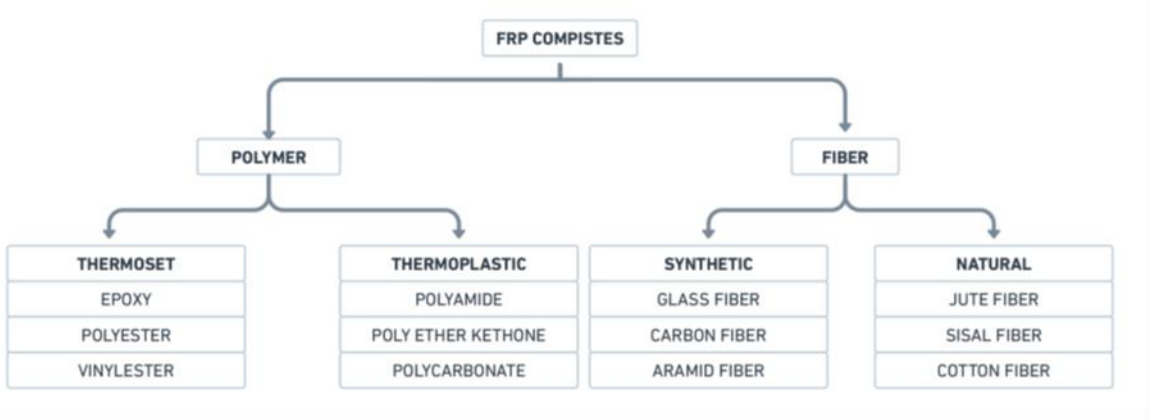

Figure 1.3. FRP composites [15]

1.4 Reinforcements

Among the reinforcement types illustrated in the diagrams before, fibers are among the most preferred due to their lightness, stiffness, and strength. [42] By adjusting the orientation and alignment of fibers within a composite, the mechanical properties of the material can be changed. This allows for the optimization of specific mechanical values in a desired direction. Additionally, in composites where fibers are homogeneously distributed within the matrix, uniform properties can be achieved in all directions. [16,71] Furthermore, one of the primary advantages of fibers is that their diameters are small relative to their grain sizes, which enhances their theoretical strength. This behavior is attributed to the size effect, wherein the probability of imperfections decreases as the size diminishes. Moreover, a high aspect ratio (length over diameter) facilitates a variety of packing methods. As a result, composites with different properties can be produced using diverse manufacturing techniques. [43,71,72] In this thesis, glass fiber was utilized as the reinforcement material.

1.5 Glass-Fibers

Glass fibers are among the earliest types of fibers used in commercial applications; therefore, their range of use is quite extensive. They are generally made from bulk glasses containing high proportions of silica and exhibit typical glass properties such as hardness, corrosion resistance, and inertness. These fibers are flexible, lightweight, and inexpensive. However, since their properties can vary based on chemical composition and process variables, glass fibers are further categorized into different types. The literature contains numerous studies, definitions, and explanations regarding these categories and glass fibers in general. [16,23,44,71,73,74]

Furthermore, comprehensive studies on other fiber types are also available in the literature. [14,16,19,20,25,27,28,42,43,46–51,72–84]

1.6 Matrix

Although fibers inherently exhibit excellent mechanical properties, they are not particularly resistant when subjected to stresses that cannot be uniformly distributed along their length. This weakness is mitigated by incorporating polymer matrices. The matrices aim to distribute the applied load, especially transverse stress, interlaminar shear stress, and bearing stress, to the reinforcement, namely the fibers. Additionally, certain mechanical properties of the composite are dominated by the matrix; examples include transverse stiffness and strength. The matrix also serves to protect the fibers from environmental conditions. Examples of such properties include the composite's temperature range, chemical resistance, abrasion resistance, and weathering capability. [42,71]

While fibers can reinforce every class of material, polymers are more widely preferred in the market for many applications due to their lightweight nature, low density, ability to interact with fibers at lower temperatures and pressures compared

to other material classes, and low cost. In addition to these features that facilitate manufacturing, polymers are also chosen because they provide protection against environmental factors and meet the desired interaction conditions with other materials. [42,71]

Polymers used as matrix materials can fundamentally be divided into two categories based on their molecular structure: thermosetting polymers and thermoplastic polymers.

Thermosetting resins, which have been employed the longest as matrices in composites, are materials that undergo a transformation in their molecular structure during the production of the composite material. This is because the long macromolecules constituting thermosetting resins possess reactive bonds that can be opened by a hardener, allowing them to form strong covalent side bonds with other molecules. Due to these properties, they show advanced characteristics in areas such as toughness and resistance, making them suitable for applications exposed to harsh environmental conditions. Examples of such applications include the aerospace, aviation, automotive, construction, and wind energy sectors, where they are used as adhesives, coatings, and insulation materials. [39,85–87]

Thermoplastic polymers are moldable materials at specific temperatures and solidify by cooling after shaping. The intramolecular forces holding the polymer chain weaken with increasing temperature, which, unlike thermosets, allows thermoplastics to be reshaped. Reshaping can be done through injection molding and other methods. At temperature ranges between the glass transition and melting temperature, it becomes possible to reshape these materials without losing their physical properties. Thus, they are much more advantageous than thermosets in terms of recyclability. Additionally, since they are less dense than thermosets, they become advantageous in terms of weight, and having higher toughness and being less brittle than thermosets are other advantages. [2,39,42,64,71,85–87] However, despite these advantages, factors such as their expensive production and some mechanical and thermal properties being lower than those of thermosets limit their

use. To better illustrate these differences, Grandi has prepared a table as follows. [71]

Table 1.1 Advantages and disadvantages of thermoset and thermoplastic materials

Material	Advantages	Disadvantages
Thermoset	More resistant to high temperatures.	Cannot be recycled
	Highly flexible design	Cannot be remolded or reshaped
	Thick to thin wall capabilities	Requires chemical reaction to set
	Excellent aesthetic appearance	
	High levels of dimensional stability	
	Cost-effective	
	Excellent resistance to solvents and corrosives	
	Fatigue strength	
Thermoplastic	Highly recyclable	Generally, more expensive than thermoset
	Aesthetically superior finishes	Can melt if heated
	High-impact resistance	High stress during flowing can damage reinforcements
	Remolding/reshaping capabilities	
	Chemical resistant.	

1.7 Sheet Molding Compound (SMC)

SMCs are composite structures with a thermoset matrix reinforced by fibers. While the fiber architecture can change depending on the application, glass fiber reinforcements are predominantly used due to their cost-effectiveness compared to other fibers and their inherent strength. These fibers generally range from 10 to 50 millimeters in length and constitute 15 to 50 percent of the composite's weight. These parameters are adjusted according to specific application requirements. [15,34,88]

Lightweight and thin-walled automotive parts in vehicles, such as molded components including insulation parts, door panels, and plastic seats, are often produced using sheet molding compounds (SMCs) to prevent a bulky appearance in terms of both weight and aesthetics. These wall thicknesses typically range between 1 and 3 millimeters. The primary production method is compression molding, which allows for the rapid fabrication of geometric shapes like ribs, inserts, and attachments. This technique not only requires less preparation time compared to other manufacturing methods but also offers a high degree of surface quality. In certain applications, production has also been observed using injection molding and roll forming techniques. [15,34,88,89]

Polyester is typically chosen as the thermoset resin because it is inexpensive and possesses properties that can be tailored to the application. Research involving other matrix types is also present in the literature. In addition to polyester, filler materials like calcium carbonate ($CaCO_3$) and additives that facilitate cross-linking and hardening are incorporated into the composite. Curing temperatures vary between 100 and 200 °C, depending on these additives and their chemical compositions. Furthermore, chemical additives that extend shelf life, enhance resistance to environmental conditions, or help maintain the desired physical form are added, varying according to the application. The exact compositions are dependent on the specific fields of use. [15,34,88]

The earliest examples of SMC materials appeared in the European and Japanese markets in the 1960s and shortly thereafter entered the U.S. market. Although the automotive industry has been the driving force behind the development of SMC materials, they have found applications across a wide range of sectors, from wind energy to marine industries. [15,33,34,88,90–97]

1.8 Bulk Molding Compound (BMC)

Bulk Molding Compounds (BMC), also known as Dough Molding Compounds (DMC), share many similarities with Sheet Molding Compounds (SMC) and are utilized in similar industrial sectors. BMCs are composed of thermoset resin and incorporate similar mineral fillers, colorants, and additives as those used in SMCs. Notably, the weight percentage of mineral fillers is higher in BMCs compared to SMCs. While polyester remains the most commonly used matrix in BMCs, and despite the existence of varieties without fiber reinforcement, the most prevalent type of fiber used is glass fiber. [15,36,42,88]

Glass fibers in BMCs are dispersed within the compound in three-dimensional random orientations. Although the terms DMC and BMC are used interchangeably, the distinction between them lies in fiber lengths: fiber lengths in DMC range between 6 and 10 mm, whereas in BMCs they are generally between 4 and 6 mm. Unlike the fibers in SMCs, these randomly oriented fibers in BMCs are not aligned in specific directions, which reduces the force values in desired directions specific to the application. [36,42]

In summary, while SMCs possess more parameters that can be tuned according to the application, BMCs lack this adaptability. Due to their short fibers, BMCs exhibit lower mechanical properties. SMCs are employed in structural applications requiring higher strength and rigidity and are used for components with large surface areas. In contrast, BMCs are utilized in applications with more modest requirements, such as non-functional closures and surface parts, and in components with smaller surface

areas. Additionally, their lower cost and simpler molding process make BMCs a preferred choice for basic applications. [15,36,37,42,88]

1.9 Motivation and Objective

As explained in previous sections, circular economy practices and sustainable production have become highly important in the automotive sector, as in many other industries. Most companies' main goals include establishing a sustainable business model that ensures a livable and clean environment and avoids future economic sanctions. The primary motivation of this thesis is to contribute to work aligned with these goals.

Another factor supporting this motivation is that the company TürkTraktör does not have any product-level recycling in place, nor does it use any parts derived from recycled or reused materials. Therefore, the main aim of this study is to select a frequently used component of a tractor, recycle it, and then determine a reuse route for the materials obtained from this recycling, ultimately producing at least one product to be used on the tractor. In doing so, it will support global and local targets, initiate a recycling journey for a product from scratch, and serve as a pioneering effort.

A thermoset composite material, which is more challenging to recycle than commonly recycled metals and plastics, has been chosen to achieve this aim. This thermoset composite, specifically a glass fiber-reinforced polyester-based sheet molding compound (SMC) used in exterior parts like hoods and fenders, is challenging to recycle. It is often disposed of in landfills or incinerated or incorporated as a low-quality filler after mechanical recycling. This difficulty in recycling makes it an attractive material to study. Moreover, since the amount of SMC waste is high, the attractiveness of recycling increases.

Although thermoset recycling has been studied in the literature for a considerable time, implementing recycling processes tailored to specific in-house needs becomes

a valuable form of know-how once it reaches the industrial scale. Ultimately, possessing a recycling process optimized for the particular material used in one's production processes or products confers significant economic and technological value by offering a competitive edge. Especially when considering current and upcoming sustainability regulations, such know-how gains strategic importance and thus is generally not shared.

For these reasons, an in-house method that diverges from the literature by accommodating a company's unique needs represents both a novel application and a source of strategic advantage. Therefore, in this thesis, an approach is proposed that builds upon existing studies in the literature, followed by optimization of a recycling route specific to the material in question. This optimization establishes a novel method, distinguishing this work from existing research.

In this study, the recycling processes are divided into three phases. First, experiments were conducted at the laboratory-scale. In these experiments, the thermal decomposition behavior of the material was understood, and suitable thermal recycling methods were tested. After the chosen thermal recycling methods, the obtained glass fibers and solid products were characterized. Then, recycled bulk molding compound (BMC) was produced using these fibers and solid products, and mechanical tests were performed to assess their behavior. Based on the characterization analyses and mechanical tests, pyrolysis was selected as the most suitable recycling method. Various cleaning methods were then applied to the fibers obtained from the pyrolysis process, and their results and necessity were discussed. Finally, the produced composites underwent visual examinations and paintability tests to understand their potential use.

In the next phase, the pilot-scale recycling process was examined. Before mass production, a scale-up process was conducted, and prototype part was produced. In contrast to the laboratory-scale, a system was installed at the pilot-scale to collect liquid products by condensing some of the volatile gases produced during pyrolysis. This increased the percentage of recycled material obtained. Increasing the recycling

percentage makes the part's recycling process more advantageous for circular economy and sustainable production. Considering this advantage, the pilot-scale pyrolysis process parameters were adjusted to increase the liquid product yield (wt%) without compromising the quality of the output of glass fibers and solid products. The products obtained from this process were subjected to the same characterization analyses, mechanical tests, and BMC composite production processes. As a result of these tests and analyses, the percentage of recycled materials to be used in the recycled BMC was determined, and a tractor part was produced.

In the final phase, the produced tractor component underwent performance testing. Computer simulations and physical tests were performed to evaluate the vehicle's feasibility.

At the end of these stages, a part of the vehicle that previously did not contain any recycled components was produced using recycled materials. Furthermore, another product derived from the recycling process was also used on the tractor. This way, a valuable product usage loop was created for the circular economy and sustainable production objectives, benefiting environmental and economic regulatory considerations.

The recycling process experience and methods developed in this study will serve as a foundation for subsequent work and represent an investment in the future. Consequently, the outcomes of this project are not limited to the physically obtained recycled products but also include the long-term value they will generate.

CHAPTER 2

LITERATURE REVIEW

In this chapter, a literature review has been conducted on studies that will form the basis for the recycling work undertaken in this study and similar research. First, the recycling methods of thermoset composites are briefly explained. Then, exemplary applications of the selected method and the parameters used in these applications are presented. Finally, the characterization studies conducted before and after recycling are addressed.

2.1 Recycling Methods

Since the material examined in this thesis is a thermoset composite, specifically Sheet Molding Compound (SMC), this section provides a brief overview of recycling methods for thermoset materials. The study conducted in this thesis focuses on pyrolysis as one of the thermal recycling methods. Additionally, other recycling methods and their outcomes are briefly discussed.

2.2 Mechanical Recycling

Mechanical recycling is a technique that fundamentally involves reducing the size of composite waste to a level suitable for to use as reinforcement in other composites. A substantial body of research available in this field. [98,99]

Research in this field has predominantly concentrated on composites reinforced with carbon fibers and glass fibers. This technique initiates with the waste material

entering a primary crushing process, during which the sizes of the pieces are reduced to between 50 and 100 millimeters. Components within the composite, such as metal parts, are separated at this stage. Subsequently, the primary size reduction process begins, wherein the material is further reduced to approximately 10 millimeters using a hammer mill or high-speed mill. Following size reduction, the classification phase commences. During this stage, particles are separated according to their sizes, typically employing cyclones and sieves. Smaller particles at this point consist of powder fragments rich in filler materials, while the larger ones are high aspect ratio fragments composed of fiber materials. [100]

2.3 Chemical Recycling

The polymer matrix is degraded under controlled temperature and pressure conditions using certain chemicals and solvents in chemical recycling techniques. This process enables the recovery of fiber reinforcements and allows the degraded matrix to be to produce of fuels or novel polymers. [15,98] Compared to thermal and physical methods, this technique is the most suitable for separating and recovering fibers from the polymer matrix without causing damage. The method performed with solvents is called solvolysis, and when water is used as the solvent, the process is known as hydrolysis.

During the degradation of the polymer matrix, various chemicals and solvents are utilized to achieve partial depolymerization of the polymer matrix, converting the polymer into mono-oligomers. Although this process yields successful results for fiber recovery, the solvents and chemicals used are environmentally hazardous. Consequently, its adaptation on a commercial scale is currently limited and not preferred. [2,15,98,101]

2.4 Thermal Recycling

In this section, a brief overview of the thermal processes most commonly found in the literature and industry, specifically incineration and fluidized bed methods, will be presented. This will be followed by a detailed discussion of the pyrolysis method, which will be used in this thesis study.

Thermal processes are frequently employed in converting fiber-reinforced polymers (FRPs). After the thermal recycling process, the polymers within the composite can be separated for reuse in other materials or recycled back into the same material. The fundamental principle in thermal processes is that heat energy breaks down the polymer chains that form the matrix, destroying the cross-linked structure. This polymer matrix degradation yields solid, liquid, and gaseous products. These methods aim to recover the potential energy and reusable materials. In these processes, the waste material is also reduced in size to make it suitable for processing. [2]

In the fluidized bed method, pieces reduced to approximately 25 mm are fed into a reactor containing a sand bed and pre-conditioned hot air. Subsequently, a high-temperature (450–550°C) gas is introduced into the system. This gas breaks down the polymers and transports the contained fiber materials and fillers to a structure called a cyclone. This enables the recovery of large quantities of fibers. However, the polymer matrix cannot be recovered in this method because it decomposes into solid and gaseous forms within the sand bed. It is an effective method solely for recovering fibers. [2,98]

In the incineration method, a high-temperature burning process takes place. Although small amounts of fiber recovery are possible with this method, the mechanical properties of the fibers deteriorate, rendering them usable only in downgraded applications. This method is generally used when landfill options are not feasible. Due to its environmental hazards, it is not a preferred method for sustainability. [15] Moreover, the resin becomes the only combustible material

providing maximum energy when it comes to composites like SMC, which have a high percentage of non-organic fillers and fiberglass. Additionally, substances like calcium carbonate ($CaCO_3$) undergo decay at high temperatures, absorbing energy during their chemical transformations. [98,101]

In summary, the fluidized bed method's inability to obtain liquid byproducts, the incineration method's primary environmental hazards, which make it disadvantageous for sustainability, and its subsequent weakness in material recovery are the reasons why these methods are not preferred for SMC recycling in this thesis.

2.4.1 Pyrolysis

Pyrolysis is one of the thermal treatments applied to recover significant quantities and longer lengths of fibers from FRP composites. In recycling composite materials, pyrolysis emerges as a highly advantageous option because it offers the potential for all products to be recycled and reused. Although similar to the fluidized bed method, the pyrolysis process occurs in an inert environment. [2,21] Conducting this process in an oxygen-free and inert atmosphere prevents combustion, making it less hazardous in terms of air pollution. [15]

While the polymeric materials within the composite decompose to form oil and gas products, it is possible to recover the fibers with minimal degradation for reuse when the pyrolysis process is carried out under controlled conditions. Moreover, studies in the literature have shown that the hydrocarbon products resulting from this process can be used as viable fuels and can be processed to produce new plastic products. Additionally, the fact that the resulting gas contains hydrogen, methane, and other hydrocarbons, along with possessing sufficient calorific value, enables energy recovery or even allows the pyrolysis process to become self-sufficient through feedback. [21]

Consequently, volatile compounds are produced alongside solid by-products. These include non-condensable gases and liquids formed from condensable gases that

condense after the pyrolysis process. [2] The nature of these resulting products depends on numerous parameters, ranging from the processing temperature to the type of thermoset resin (chemical properties). Various characterization methods are employed to analyze these products. [21]

The pyrolysis process fundamentally proceeds as follows. The waste material is placed into a combustion chamber or reactor. Before this step, the waste material undergoes size reduction according to the reactor's dimensions. [33,88,92] Subsequently, an inert gas is introduced into the reactor to expel oxygen, converting the environment into an inert atmosphere, known as purging. After purging, the system is conditioned to reach the desired temperature. [2] The elevation to the target temperature is conducted at predetermined heating rates. Once the target temperature is reached, it is maintained for a specified duration. [33,90,102,103] During this period, a steady flow of inert gas continues to be supplied to the reactor. This gas flow sweeps gaseous and liquid by-products from the material and through the reactor toward the condenser, where they are collected. After the desired holding time at the target temperature has elapsed, the pyrolysis process is terminated by stopping the heating, and the system is allowed to cool to ambient temperature without changing the inert conditions. Once the system has cooled, the solid products are collected. [2]

In this process, parameters such as heating rate, target temperature, and the volumetric rate of inert gas are adjusted for each composite to achieve optimal conditions based on the desired outputs. This tuning is facilitated by characterizing the composite using methods such as thermogravimetric analysis (TGA) and differential scanning calorimetry (DSC). These techniques provide insights into decomposition temperatures and the extent of carbonization. [21]

Studies have also been conducted on post-pyrolysis processes. After the pyrolysis of FRPs, the solid residues contain fibers with char (pyrolytic carbon) on their surfaces. [104] To remove this char from the fibers, additional pyrolysis or thermal treatment in an oxidative environment, namely oxidation, has been performed. [102,104]

Table 2.1 GFRP pyrolysis studies from the literature

Composite	Temperature (°C)	Heating Rate (°C/min)	Duration (min)	Atmosphere	Product Yields (wt%)			Recycle Work	Ref
					Solid	Liquid	Gas		
GF/calcium carbonate and Zinc, MgO and organic fillers and additives/polyester-styrene resin (SMC)	300	15	30	N2	82.6	9.7	7.7	Recycled fibers used to produce a BMC	[33,90]
	400	15	30	N2	75.2	14.5	10		
	500	15	30	N2	74.9	14.2	11		
	600	15	30	N2	73.9	14.9	11		
	700	15	30	N2	72.6	13.5	14		
CF/ polybenzoxazines resin	350	5	60	N2	83.6	14	0.7	Rescued carbon fibers' steam activation researched.	[104]
	400	5	60	N2	75.2	21.6	1.3		
	450	5	60	N2	74.4	22	1.5		
	500	5	60	N2	72.6	23.6	2		
	700	5	60	N2	70	24.6	3.8		
GF/calcium carbonate/polyester-styrene resin	450	5	90	N2	54.7	39.6	5.8	DMC produced with recycled fibers	[102]
Ground SMC / Extracted with acetone	500	27	120	Air	_	12.3	_	Fibers and fillers used for another composite applications	[105]
	500	27	120	N2	_	8.73	_		
Ground SMC / Unextracted with acetone	400	27	120	N2	_	11.74	_		
	400	27	120	Air	_	18.3	_		
GF/calcium carbonate and aluminum trihydrate fillers/polyester-styrene resin	350	10	60	N2	82.9	14.5	2.6	New utilization pathways for the resulting products have been discussed	[106]
	400	10	60	N2	52.6	41.2	6.2		
	450	10	60	N2	48.7	45	6.3		
	500	10	60	N2	45.8	45.7	8.5		
	650	10	60	N2	46.6	47	6.4		
	800	10	60	N2	38.2	47.4	14		
GF/silane binder/polyester resin	550	10	60	N2	30	59.4	11		

Additionally, efforts have been made to remove this char by manipulating pyrolysis parameters such as temperature and processing time. [2]

2.5 Characterization Analyses

Thermal analysis is the primary approach for measuring the weight or volume fractions of the constituents in fiber-reinforced polymer (FRP) composites. The weight ratio of fibers and polymers can be determined through thermal degradation or thermogravimetric analysis (TGA). TGA is a technique that provides highly precise weight change measurements as a function of temperature and/or time. It can be performed in air or inert gas atmospheres (e.g., nitrogen). [15,71] Modern TGA devices are often equipped with the capability to record DTA (Differential Thermal Analysis) signals simultaneously. The DTA signal can reveal thermal effects such as melting, crystallization, or glass transition, which do not involve a change in mass, in addition to events associated with weight loss. [107]

Another method frequently used for the thermal analysis of polymers is Differential Scanning Calorimetry (DSC). It is a thermo-analytical technique used to measure the difference in heat absorption or release required to increase the temperature of a sample relative to a reference material. This method allows for the examining endothermic and exothermic transitions occurring in the sample as a function of temperature. By observing these transitions, fundamental information such as transformation temperatures associated with phenomena like glass transition (Tg), melting (Tm), and crystallization (Tc) can be determined. [108]

Fourier Transform Infrared (FTIR) analysis is used to identify organic, inorganic, and polymeric materials by utilizing infrared light to scan samples. Changes in the absorption bands' characteristic pattern clearly indicate material composition alterations. FTIR is beneficial for identifying and characterizing unknown materials, detecting contaminants within a material, finding additives, and identifying

degradation and oxidation. In this study, FTIR will be employed alongside TGA analysis whenever possible. [109]

The TGA results for SMC composites identify char decomposition above and after 500°C and $CaCO_3$ decomposition (into CaO and CO_2) after approximately 700°C. This decomposition prevents the solid products from being reused in composite production because CaO acts as a thickening agent, disrupting the viscosity values of the paste. The SMC part to be used in this study will also be subjected to TGA and DSC analyses. Although similar trends are expected to be observed, differences are anticipated because of additional materials used in the automotive industry, such as paint, UV protection agents, and flame retardants. Based on these differences, the pyrolysis temperature will be determined to increase the yield of the desired product. [33,90,92]

Gas Chromatography-Mass Spectrometry (GC-MS) is a powerful technique for separating, quantifying, and identifying volatile compounds from pyrolyzed fiber-reinforced polymer (FRP) composites. This method is particularly beneficial for thermoset FRP composites due to their insoluble and infusible structures. Consequently, samples are pyrolyzed at high temperatures, and after decomposition, the volatile particles are analyzed using GC-MS. [15]

The GC-MS analysis results for the pyrolysis of SMC indicate that the liquid products primarily consist of aromatic hydrocarbons and oxygenated compounds such as carboxylic acids, esters, and ketones, resulting from the decomposition of the polymer matrix. The oil-like liquids obtained between 400°C and 700°C are rich in C5–C21 hydrocarbons. Approximately 40% fall within the petroleum boiling point range, while the remaining portion corresponds to aromatic compounds. Therefore, after mild processing, they have the potential for to be used as fuels. Below the threshold of 300°C, the pyrolysis process is incomplete, forming wax-like products. These products may subsequently cause fouling effects that make continuous processing impossible. Furthermore, as the temperature increases, more

stable aromatic hydrocarbons are produced; thus, operating at higher temperatures not only enhances the potential of the liquid products but also facilitates the process. [94,106]

In diffraction analysis, X-ray diffraction (XRD) is a method used to obtain detailed information about the crystal structure and chemical composition of a sample without causing permanent damage. When applied to the analysis of composites and the products resulting from pyrolysis, it provides insights into the types of fibers and the contents of solid by-products. If the sample is a mixture, as is the case with solid by-products after pyrolysis, we can determine what has decomposed and what remains by individually characterizing the elements within the mixture. The degree of crystallinity, deviations from the ideal composition of specific elements, and structural conditions can also be derived from data analysis. [109] The interaction between the X-ray beam and atomic planes leads to partial transmission of the beam, while the remainder is absorbed, refracted, scattered, and diffracted by the sample. X-rays are diffracted differently by each element, depending on their atomic arrangement and the types of atoms present. For example, when examining the XRD results of glass fiber-based FRP composites, a broad peak at (2θ) 20–30° can be observed. This peak originates from the presence of the d_{101} crystallographic plane of amorphous silica in the glass fiber. [109]

Scanning Electron Microscopy (SEM) scans the surface of a sample using a focused electron beam, enabling the acquisition of images with resolutions ranging from 1 to 5 nanometers. When this electron beam interacts with the specimen surface, it generates backscattered and secondary electrons, as well as X-rays. The secondary electrons are utilized for image formation. At the same time, the X-rays are analyzed using Energy Dispersive X-ray Spectroscopy (EDX) to provide information on the elemental composition and surface mapping of the sample. [109]

For instance, SEM-EDX analysis of glass fiber can detect its chemical composition, including elements such as oxygen (O), sodium (Na), magnesium (Mg), calcium

(Ca), silicon (Si), and zirconium (Zr). By examining the elemental ratios and formulas, the type of fiber, can be confirmed. In this study, SEM will be employed to investigate the surface quality and diameters of the fibers. EDX will be used where XRF is not employed. [15]

These methods have been collectively employed for the characterization of polymers and composites. [110] In this study, they will also be utilized in combination to obtain as detailed information as possible regarding the products formed through the processes and their potential applications.

CHAPTER 3

METHODS AND MATERIALS

In this thesis, the recycling and reuse of SMC composite material, collected as production or process waste or as scrap parts that have completed their service life on tractors, is investigated by employing pyrolysis, one of the thermal recycling methods. This study is composed of three main parts: laboratory-scale recycling processes, pilot-scale recycling processes, and performance testing of produced tractor components with recycled composite.

In the first stage, laboratory-scale recycling processes, the objective is to determine whether pyrolysis is the correct recycling route and conduct feasibility studies for producing composites from the products obtained through this method. To ensure accurate decisions on the process parameters, the thermal decomposition behavior of the waste material was examined using TG-DTA-DTG. Then, process parameters were determined based on this behavior and the related literature.

Alongside pyrolysis, oxidation and pyrolysis followed by oxidation were also tested, and comparative analyses were presented.

For these comparisons, Scanning Electron Microscopy analyses were conducted to inspect surface morphology to understand whether glass fibers were damaged and how effectively they could be separated from the polymer matrix. Then, X-ray diffraction (XRD) and X-ray fluorescence (XRF) analyses were conducted to understand the chemical composition of the solid products (solid residue) other than glass fibers and their effects on reuse. Lastly, tensile, flexural, impact, and hardness tests were conducted to understand the mechanical behavior of BMC composites produced using the solid residues and glass fibers obtained from these three different processes.

In addition, cleaning studies were carried out on the fibers obtained after the pyrolysis process. Mechanical, water-based, and acid-cleaning methods were tried and evaluated. Moreover, painting and serigraphy trials were conducted on the produced BMC composite materials, and the potential for their use on vehicles was investigated.

At this stage, only the solid products and their results could be examined within the capacity of the laboratory-scale equipment, as gaseous and liquid products were released through the exhaust and could not be captured.

The second stage, the pilot-scale recycling process, aims to scale up the pyrolysis process selected in the laboratory stage. Therefore, allow to produce larger quantities of recycled products and serve as a connection between the small-scale laboratory experiments and the full-scale industrial or serial production, which helped to refine the process.

Compared to the previous laboratory-scale stage, the sample sizes used in this phase are larger, allowing more recycled products to be produced. These dimensions will be explained in detail in later parts of this study. In addition, even though the furnace used in the pyrolysis process at this stage may seem similar to the one used at the laboratory-scale simply in terms of size, the laboratory-scale furnace has only about a 10 cm (approximately) effective heating zone. This means it can maintain the target temperature uniformly only in that limited zone, preventing the use of larger samples. However, the pilot-scale furnace can maintain a steady target temperature throughout almost its entire tube length, allowing samples to be placed along the entire tube length. In this way, the amount of solid material obtained from a single run is almost tripled.

Furthermore, since the pilot-scale represents a preliminary preparation for mass production, it was carried out under the supply and process discipline conditions similar to a series production environment. As a result, preparation times before and after the experiments and the intervals between different batches have been shortened. Unlike the laboratory-scale process, a dedicated system was established

solely for this recycling operation, reducing the likelihood of errors and ensuring the system's stable and continuous operation. In addition, since the system has a condenser feature, it offers the opportunity to condense and collect condensable volatile products. These matters can be used to distinguish the pilot-scale from the laboratory-scale. Detailed process flow schematics and equipment details are provided in subsequent parts of this section.

In the recycling system established at this stage, condensable volatile products can be captured and converted into liquid products. Although the primary objective of this thesis is to recycle and reuse the valuable glass fiber and other filler materials, the opportunity to contribute to the targets of circular economy and sustainable production and the potential to obtain and utilize a valuable raw material led to the decision to collect liquid products as well.

To maximize the recovery of these liquid products, the process parameters were modified using the TG-DTA-DTG results from the first stage and the related literature to achieve the optimal benefit from both solid and liquid products.

Following the implementation of this new process, SEM was used again to observe the extent to which glass fibers and solid products were affected, and both the glass fiber surfaces, and the solid residues were examined with EDX to determine their compositions. Moreover, solid residues were subjected to ash analysis for a detailed composition analysis. Then, to identify the ideal ratio by weight (wt%) for blending these recycled glass fibers and solid products with BMC dough, BMC composites containing 5%, 10%, and 15% (wt%) recycled materials were produced and subjected to mechanical tests. At the end of this process, the ideal composition was determined.

Meanwhile, the liquid products obtained from this process were collected, and their visual properties were described. GC-MS and bomb calorimeter analyses were carried out to understand their composition and potential.

In the third and final stage, after determining the parameters in the previous stages and producing BMC composites based on these parameters, the tractor component manufactured from the recycled materials was first simulated in a computer environment, and its physical performance was subsequently evaluated through a physical tractor bump test.

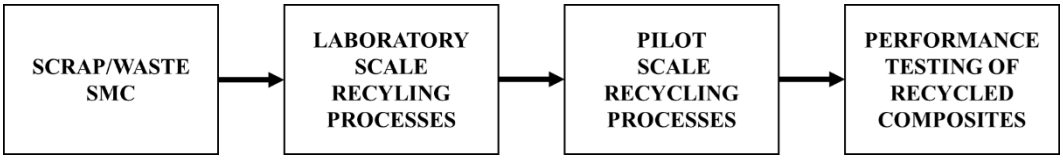

Figure 3.1. Thesis structure schematic

3.1 Laboratory Scale Recycling Processes

3.1.1 Determination of Process Parameters

Thermogravimetric and differential thermal/thermogravimetric analysis (TG-DTA-DTG) was conducted to understand the thermal decomposition behavior and determine the material composition percentages of the virgin SMC sample. The sample was sent for testing directly from the production facility at the stage before painting. The tests were performed at the ITS Caleb Brett Marine Survey SA Istanbul Laboratory. The analysis was carried out using a SEIKO TG-DTA 7200 instrument in accordance with the ISO 11358 standard for the thermogravimetric analysis of polymers. The sample weighed 10.619 mg. The analysis program was as follows: initially, the specimen was heated from 30°C to 800°C at a rate of 10°C per minute in a nitrogen (N_2) atmosphere; subsequently, from 800°C to 1000°C, it was heated at the same rate in an oxygen (O_2) atmosphere.

3.1.2 Laboratory Scale Recycling Methods

3.1.2.1 Sample Preparations

The laboratory and pilot-scale samples were taken from real-life body parts used in production. These samples are SMC, whose composition includes approximately 15–25 %wt. Fiberglass (25–30 mm long), 45–55%wt. $CaCO_3$ filler, and about 30%wt. Organic material. The precise formulation of these parts cannot be disclosed for proprietary reasons. Nonetheless, characterization analyses at both scales will be conducted to understand their composition further.

Parts taken from a body panel used in R&D studies and later scrapped were cut into different sizes to prepare them for experiments. In the initial phase, the samples were prepared by increasing their size and number based on observations of experimental results. Initially, the experiments started with small samples cut into squares of approximately 1×1 cm to observe whether complete pyrolysis occurred. Subsequently, the process continued with pieces cut to approximately 2×10 cm and 3x12 cm in size. When larger samples than 3x12 cm were used, it was observed that certain parts of the samples remained outside the effective heating zone and, therefore, did not reach the target temperature, resulting in incomplete pyrolysis. Therefore, experiments were conducted with a smaller but more significant number of samples. The samples were placed in porcelain combustion crucibles and inserted into the horizontal tube furnace.

The samples for pyrolysis followed by oxidation (PO) were prepared similarly to pyrolysis samples. However, no small-scale samples were prepared for the parts to be directly exposed to oxidation since the muffle furnace, whose properties will be explained later, has a larger capacity than the horizontal tube furnace used for pyrolysis, and its sample placement area is more suitable. Figure 3.3 provides a visual representation of the oxidation samples.

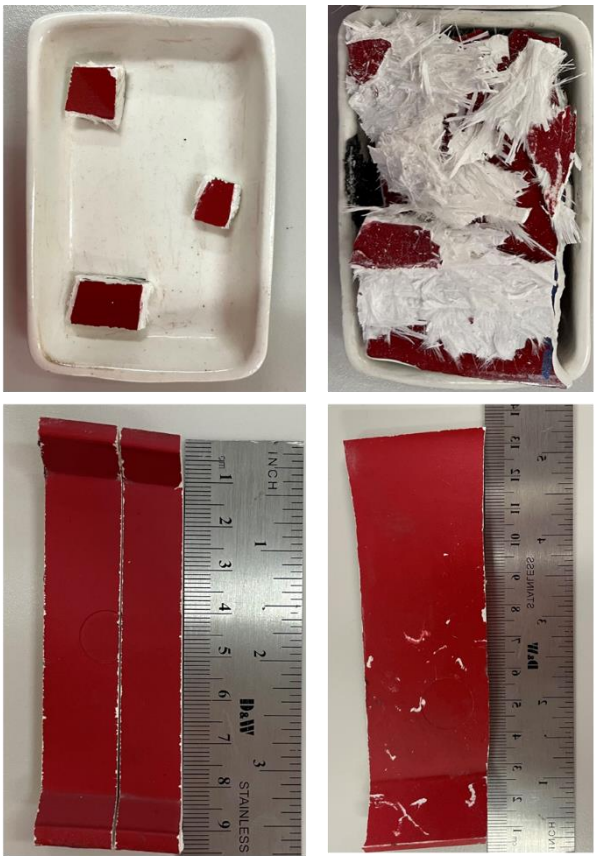

Figure 3.2. Samples in different sizes and numbers for laboratory-scale pyrolysis and PO processes

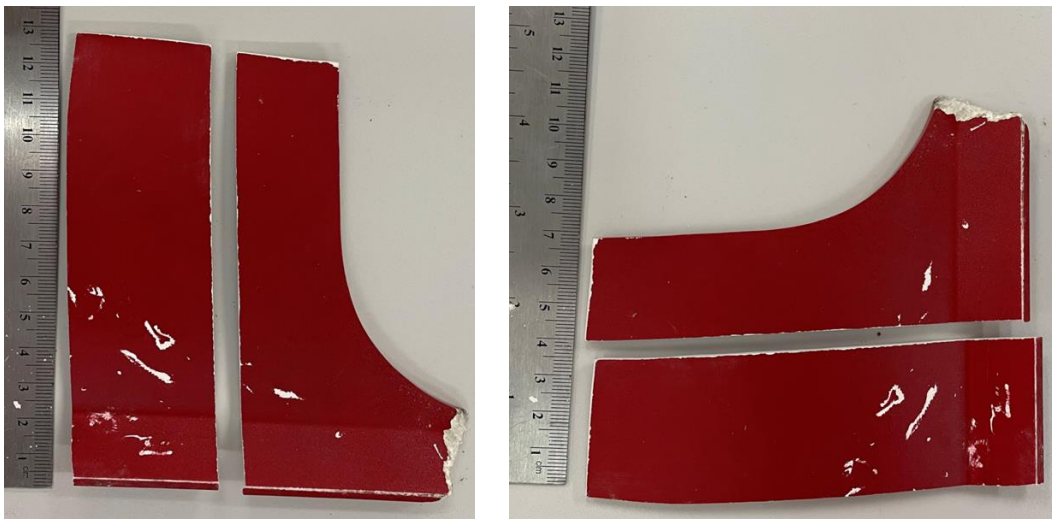

Figure 3.3. Samples used in laboratory-scale oxidation processes

3.1.2.2 Laboratory Scale Recycling Processes

The pyrolysis, oxidation, and PO experiments for the laboratory-scale recycling processes were conducted at the Middle East Technical University Clean Combustion Technologies Laboratory (METU-CCTL).

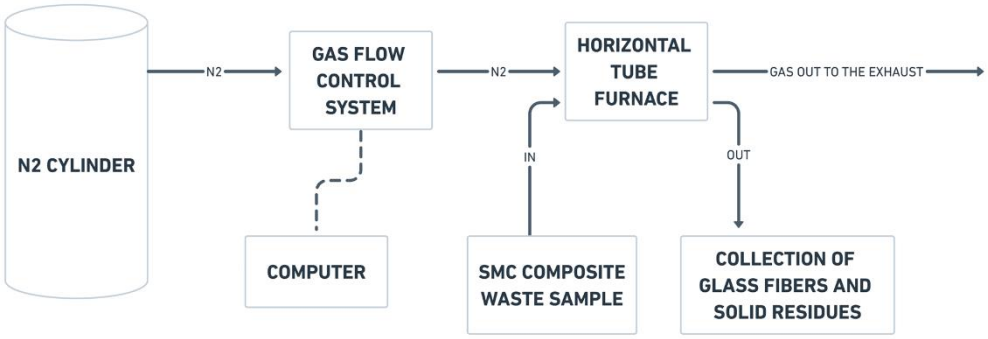

Figure 3.4. Laboratory scale pyrolysis experiment setup schematic

For the pyrolysis experiments, a PROTHERM PTF Series horizontal tubular furnace was utilized (Figure 3.5). PTF series tube furnaces are versatile heating devices designed for laboratory experimentation; operating at temperatures between 1100°C and 1600°C, these furnaces employ wire and silicon carbide (SiC) heating elements. In particular, SiC rods aligned parallel to the working tube help ensure consistent temperature uniformity and facilitate straightforward element replacement. The experimental procedure for pyrolysis was developed based on De Marco's methodology. [33,90,92,94,95] The target temperature of 500°C was reached at a heating rate of 15°C/min in an environment conditioned with nitrogen gas at a flow rate of 10 L/min. After maintaining the target temperature for 50 minutes, the system was allowed to cool to room temperature.

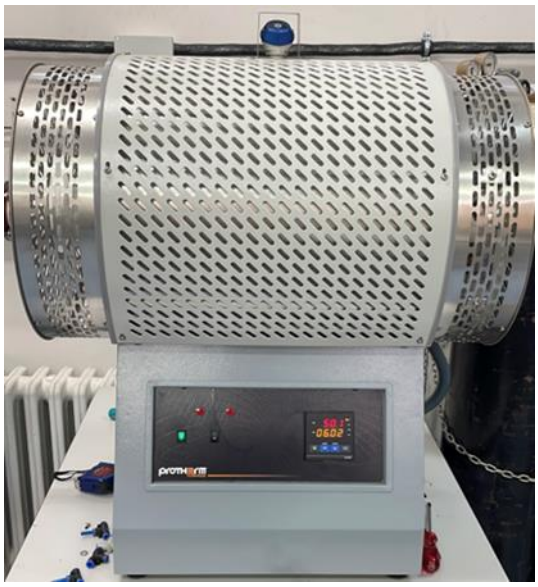

Figure 3.5. PROTHERM PTF Series horizontal tubular furnace (HTC) at CCTL

Figure 3.6. PROTHERM PLF Series muffle furnace at CCTL

For the oxidation process, a PROTHERM PLF Series muffle furnace was employed (Figure 3.6). PLF series furnaces are long-standing, reliable chamber furnaces that are widely used in laboratories and adaptable to various insulation options. These furnaces operate within a standard temperature range of 1400°C to 1600°C and incorporate front-loading for convenient access and double-skin construction to ensure cooler external surfaces. The target temperature of 500°C was reached at a

heating rate of 10°C/min, and after holding at this temperature for 50 minutes, the furnace was allowed to cool to room temperature.

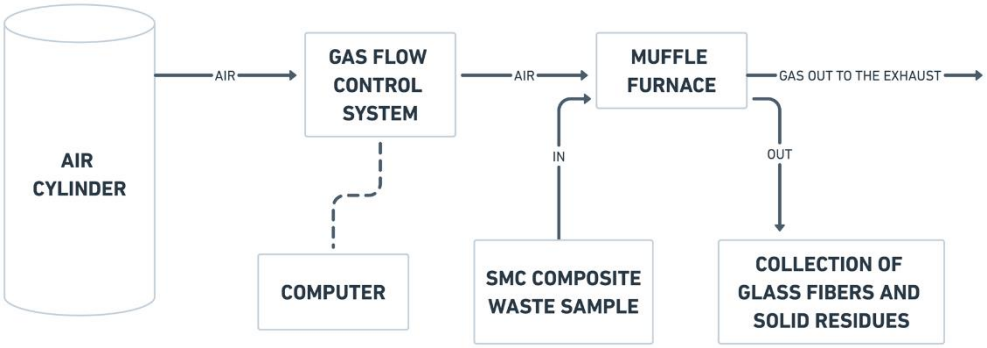

Figure 3.7. Laboratory scale oxidation experiment setup schematic

For the method involving pyrolysis followed by oxidation (PO), the experimental procedure was as follows: the target temperature of 500°C was reached at a heating rate of 15°C/min in an environment conditioned with nitrogen gas at a flow rate of 10 L/min. After maintaining the target temperature for 50 minutes, the system was allowed to cool to room temperature. Subsequently, as described above, oxidation was performed.

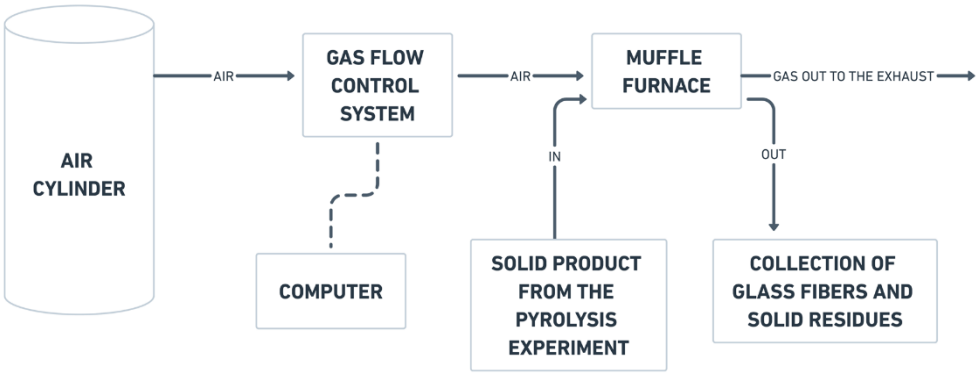

Figure 3.8. Laboratory scale PO experiment setup schematic

Because no devices or installed systems were used to trap volatile gases at the outlets of the furnaces used in the laboratory-scale recycling processes, only the solid yields could be determined in the experiments and recycling studies conducted here.

3.1.2.3 Surface Morphology Analyses

After the laboratory-scale recycling processes, scanning electron microscopy was employed to examine the surface morphology of the glass fibers obtained from pyrolysis, oxidation, and PO processes. In these examinations, attention was given to assessing the amount of solid residue remaining on the fiber surfaces, determining whether matrix separation had occurred, checking for any significant deformities or crack initiation on the surfaces, and identifying the presence of fractured or broken structures in randomly selected areas. Moreover, fiber diameters were examined, and average diameter values were calculated with standard deviations with a 95% confidence level. This analysis was conducted at METU MERLAB using a Phillips FEI QUANTA 400F Field Emission Scanning Electron Microscope (FE-SEM). The samples were coated with gold and palladium to ensure electrical conductivity. Imaging was performed at randomly selected points at various magnifications.

3.1.2.4 Chemical Composition Analyses

The chemical compositions of the solid products obtained after the laboratory-scale processes were examined using X-ray diffraction and X-ray fluorescence analyses. The term "solid products" refers to the materials remaining after the removal of glass fibers.

First, the solid products from laboratory-scale pyrolysis, oxidation and PO were subjected to X-ray diffraction analysis (XRD), and their existing crystal structures were interpreted and then, X-ray fluorescence (XRF) data were incorporated into the evaluation, allowing for a more detailed analysis and a clearer understanding of their chemical compositions. In these examinations, the primary focus was determining the current state of calcium carbonate ($CaCO_3$).

XRD measurements were performed using a MiniFlex 300/600 diffractometer equipped with a D/teX Ultra2 detector. The X-ray source was operated at a voltage of 40 kV and a current of 15 mA. Data acquisition was performed in a $\theta/2\theta$

configuration with a scanning range of 3° to 60° (2θ) using a step width of 0.02° and a scanning rate of 5.00° per minute. The goniometer used was an ASC-8 with the divergence and receiver slits set to 1.25° and open, respectively. No filters or monochromators were used during the measurement. Peaks were identified using the second derivative method, and profile fitting was performed automatically by applying a split pseudo-Voigt function for peak refinement. The setup provided high precision in the analysis of the crystal structure of the sample, allowing reliable interpretation of diffraction intensities and interplanar spacings. This analysis was conducted at METU MERLAB, XRDL.

For the XRF analysis, samples were dried overnight at 105°C and prepared as pellets without adding additives. Depending on the sample size, they were placed into 10 mm and 20 mm sample holders appropriate for their dimensions. The analyses were conducted semi-quantitatively in oxide form within the Fluorine-Uranium range. Analyses were done using a Rigaku X-ray fluorescence (XRF) spectrometer in EZS003XSV Bulk mode. The analyses were performed at METU MERLAB, KAL.

3.1.2.5 Recycled BMC Production from Laboratory Scale Recycling Products

After the laboratory-scale recycling processes, the obtained solid products and fibers were added to the original BMC paste mixture in specific percentages to produce new composites. The recycled materials were added in place of the $CaCO_3$ filler material, as performed by De Marco and Torres. [33,90] The percentage distributions of the pyrolysis, oxidation, and PO samples obtained from the first phase, as well as the percentage distributions of other materials used in composite production, are provided in Table 3.1. In this phase, since the quantities of products obtained from the laboratory-scale were low in mass, they were mixed in small proportions and compared with each other. Additionally, to compare with the performance of the standard BMC, control sample BMC-ST was produced, and to explore the case where glass fiber is added in place of the removed $CaCO_3$, control sample BMC-C

was also produced. Samples BMC-P, BMC-O, and BMC-PO represent the composite samples produced by laboratory-scale pyrolysis, oxidation, and PO.

Table 3.1 Recycled BMC compositions from the laboratory-scale processes

Composition (wt%)	**BMC-ST**	**BMC-C**	**BMC-P**	**BMC-O**	**BMC-PO**
Mediumflatic Polyester Resin	30.00	30.00	30.00	30.00	30.00
Other Components	5.00	5.00	5.00	5.00	5.00
Filler $CaCO_3$	50.00	49.25	49.25	49.25	49.25
Fiber Glass	15.00	15+0.75	15.00	15.00	15.00
Recycled Fiber	-	-			
Pyrolysis			0.75		
Oxidation				0.75	
PO					0.75

Figure 3.9. Dough mixer used in composite production. a) Z-type blades, b) Dough before mixing

The composites were manufactured from dough to final product with in-house using machines developed at CTP Composite. The BMC mixer, equipped with Z-type blades (Figure 3.9), processes the compound. The slurry is transferred into the mixing chamber, and the blades are activated. Subsequently, glass fibers are added

to the mixing chamber. The blade rotation speed is fixed at 23 RPM, and the mixing process is carried out for 4 minutes inward and 4 minutes outward, aiming to achieve a homogeneous distribution.

3.1.2.6 Mechanical Behavior Tests

Several tests were conducted to understand the mechanical behavior and properties of the recycled BMC composites produced using the solid products and glass fibers obtained from the laboratory-scale processes. In these tests, the composites' tensile, flexural, and hardness properties were examined, and their impact response was also evaluated. The samples prepared for tensile and flexural tests can be seen in Figure 3.10.

A tensile test assesses the material's ability to withstand forces that attempt to separate it by measuring tensile strength, elongation, and tensile modulus. [111,112] Composite samples were placed in a testing machine where a controlled force was applied, and the resulting deformation was recorded. From these recordings, tensile strength and modulus were calculated. The tensile test was performed using the Zwick/Roel Z050 Tensile Tester at CTP Composite. The tests were conducted in accordance with DIN EN ISO 178. The sample dimensions were 10x80x4 mm, and the test speed was 2 mm/min.

Flexural testing measures a material's resistance to bending forces. [111,112] The three-point bending method was used to test recycled composite samples. The primary measurement parameters in these tests were flexural strength and modulus. The flexural tests were carried out using the Zwick/Roel Z010 Flexural Tester at CTP Composite. These tests followed the DIN EN ISO 527-4 standard. The sample dimensions were 25x250x4 mm, and the test speed was 5 mm/min.

The Charpy impact test measures the energy absorbed by a material at the moment of the fracture, providing insight into its toughness. [111,112] A pendulum hammer

struck a notched specimen, and the energy required for fracture was recorded. The impact test was conducted using the Zwick/Roel Pendulum Impact Tester at CTP Composite. The tests adhered to the DIN EN ISO 179 standard. The sample dimensions were 10x80x4 mm, and the test velocity was 3.85 m/s.

The Barcol Hardness test measures the hardness of rigid materials, including plastics, reinforced composites, and metals. It evaluates the material's response and resistance to indentation, providing insights into its mechanical properties, surface quality, and wear resistance. [111] The hardness test was performed using the BCQ Barcol Hardness Tester 934-1 at CTP Composite. The tests were conducted according to the TS EN ISO 59 standard. The sample dimensions were 300x300x4 mm.

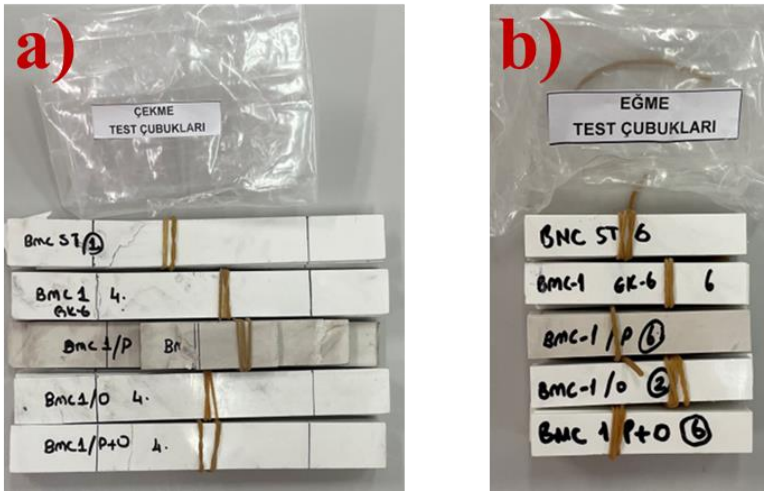

Figure 3.10. Mechanical test samples. a) For tensile tests b) For flexural tests

3.1.3 Surface Appearance and Paintability Tests

Visual examinations and paintability tests were conducted on the bulk molding compound (BMC) composite plates produced using glass fibers and solid products obtained from laboratory-scale recycling processes. Initially, the unpainted colors and surface quality of the composites produced were examined. Following this, their performance under smooth and textured paint applications was tested. Then, serigraphy trials were conducted on these composites to test their printability.

3.1.4 Glass Fiber Cleaning Methods

A portion of the fibers and solid products obtained after pyrolysis was placed into glass test tubes filled with water, while another portion was placed into glass test tubes containing one molar hydrochloric acid (HCl), and the tubes were sealed. After being manually shaken for approximately one minute, they were left to rest for 24 hours. In addition to this process, products placed into test tubes containing 250 mL of water were subjected to centrifugation using a BIOBASE TH-16 high-speed centrifuge at 6,000 RPM for 25 minutes. These samples were then examined using an optical microscope. Then, the samples were removed and analyzed under an optical microscope to assess the amount of solid residues on their surfaces. Additionally, mechanical cleaning was performed using a natural fiber/nylon brush and dissection forceps, and these samples were examined under the optical microscope in the same manner.

Figure 3.11. Optic microscope and computer for imaging at CCTL

For optical microscope imaging, a Nikon SMZ745T stereoscopic microscope with a 3.35–300x magnification, a 0.67–5x zoom range, and a 7.5:1 zoom ratio was used at CCTL.

3.2 Pilot-Scale Recycling Processes

3.2.1 Determination of Process Parameters

As in the laboratory-scale recycling processes, TG-DTA-DTG analyses and literature findings were reviewed.

In this phase, a TGA analysis was conducted again. The difference between this analysis and the laboratory-scale one is that, while the laboratory-scale sample was an unpainted piece without other surface protectants taken from the sample production line, this time, a sample taken from waste after direct use was analyzed. These analyses were performed at TÜBİTAK BUTAL.

The device used for the analysis was the TA Instruments SDT Q600 V20.9 Build 20. The analysis was conducted in a nitrogen atmosphere at a heating rate of 20 °C/min up to 800 °C with a flow rate of 100 ml/min and between 800 and 1000 °C in an oxygen atmosphere at the same flow rate.

Based on this information, research was conducted to prevent the degradation of the remaining filler materials and to avoid undesirable properties during re-use. At the same time, efforts were made to maximize the liquid yield. The decisions were made accordingly.

3.2.2 Pilot-Scale Recycling Process Method: Pyrolysis

During the pyrolysis experiments conducted at ICARBON, the samples were prepared for the scale-up processes by being cut into dimensions of approximately

10 × 20 cm. A notable aspect of these experiments was the direct insertion of the samples into the furnace, a key part of the experimental procedure.

Figure 3.12. Pilot-scale pyrolysis sample

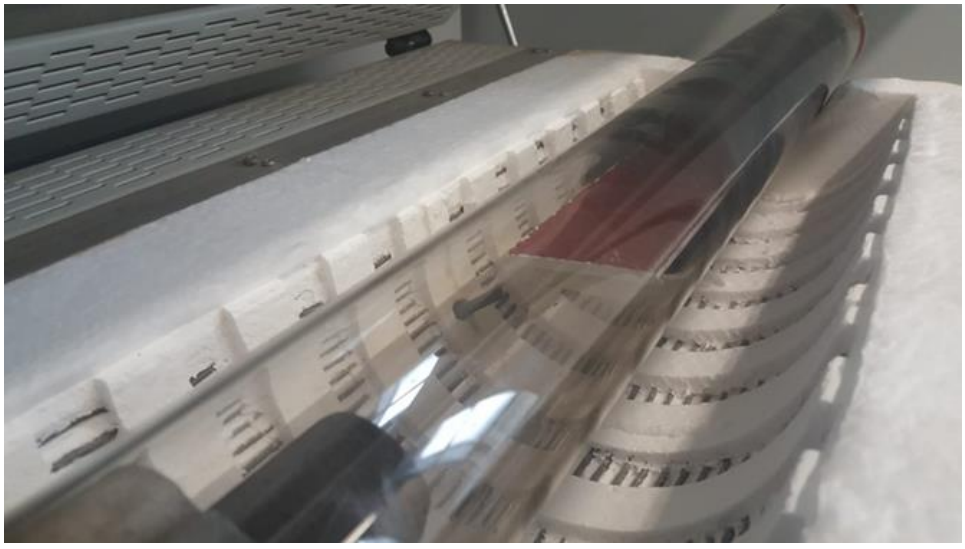

Figure 3.13. Placement of a directly inserted sample into the furnace

The experiments were conducted at the I-CARBON facilities using a PROTHERM ASP 11/70/500 model furnace, which has a maximum temperature of 1100°C, a maximum operating temperature of 1050°C, and a power rating of 1.8 kW. In these

experiments, in an environment conditioned with nitrogen gas at a flow rate of 10 L/min, the initial target temperature of 400°C was reached at a heating rate of 10°C/min and held for 10 minutes. Subsequently, the temperature was increased to a second target of 600°C at a heating rate of 5°C/min and maintained for 60 minutes. The aim of reaching 600°C was to avoid attaining the decomposition temperature of $CaCO_3$ while maximizing the liquid yield as much as possible. [21,33,90,102]

While the difference in sample size is one change from the previous laboratory-scale system in the pilot-scale pyrolysis process, the main difference is the installation of a condenser unit after the furnace. With this condenser system, gas capture and condensation are possible, thus the collection of liquid products.

As shown in the schematic diagram in Figure 3.14 and subsequently illustrated by the actual system photograph in Figure 3.15, the volatile, condensable products released during pyrolysis are passed through the condenser system, where they can be trapped and converted into liquid form. This approach makes it possible to recycle a higher percentage (by weight) of the material, moving closer to the goals of a circular economy and sustainable production. In doing so, the system produces a more desirable outcome that aligns with the overarching motivation of this thesis, which centers on the recycling process.

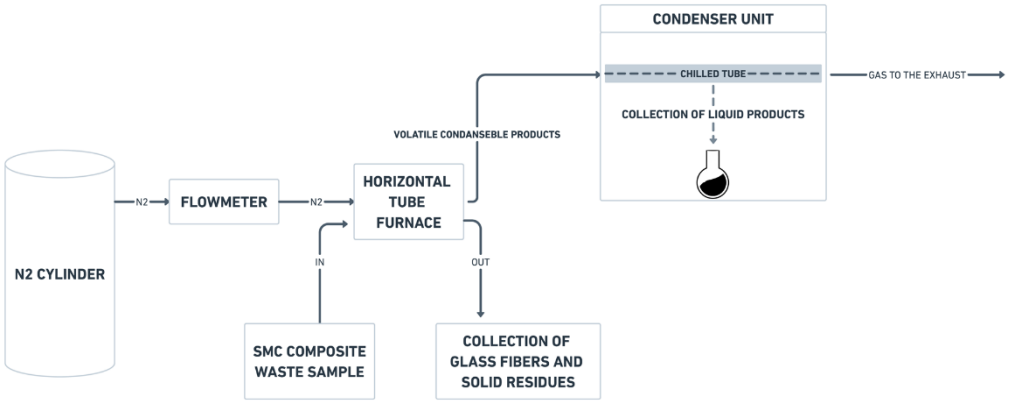

Figure 3.14. Pilot-scale pyrolysis system schematic

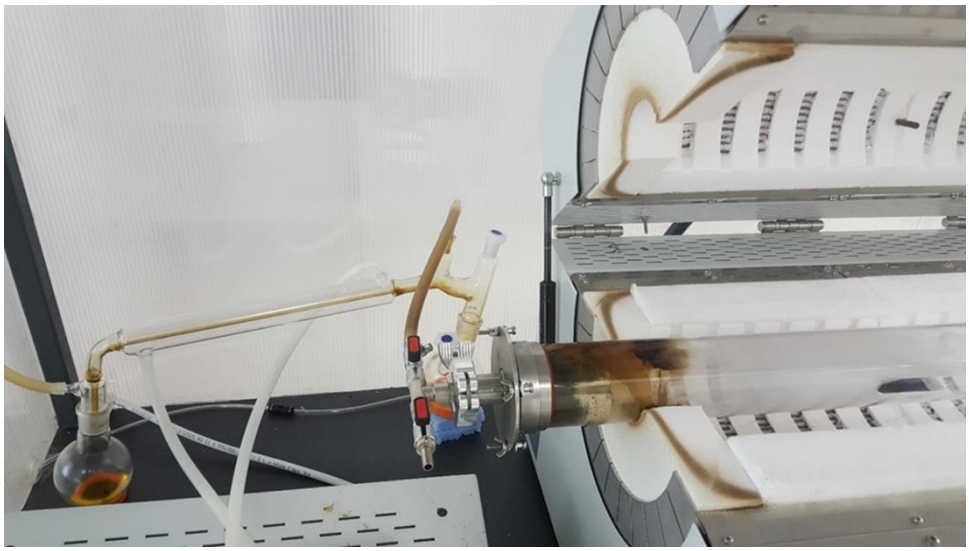

Figure 3.15. Condenser unit of the pilot-scale pyrolysis system

3.2.3 Surface Morphology and Chemical Composition Analyses

As in the laboratory-scale processes, the surfaces of the glass fibers obtained after the pilot-scale process were examined using scanning electron microscopy for any deformation, surface irregularities, or crack formation. In addition, the amount of residue on the fiber surfaces was assessed. Unlike at the laboratory-scale, the solid residues produced in this stage were also imaged with scanning electron microscopy to determine their contents visually.

Unlike in the laboratory-scale work, energy dispersive X-ray analysis was used alongside scanning electron microscopy to understand the composition of both the material remaining on the fiber surfaces and the solid residues. This allowed the chemical compositions to be examined. The SEM-EDX analyses were performed at TÜBİTAK-BUTAL using a VEGA3 TESCAN device. Before imaging, the submitted samples were coated with gold.

In addition to the EDX imaging, the solid residues obtained after the process were separated from the glass fibers as much as possible and subjected to ash analysis. In this way, the inferences drawn from the EDX analysis were supported by the ash analysis, which was also conducted at TÜBİTAK BUTAL. Differential scanning calorimetry, Fourier-transform infrared spectroscopy, and composition determination analyses were conducted for ash analysis. This enabled the identification of the percentage distribution of the elements observed in energy-dispersive X-ray analysis within the ash. A HITACHI DSC 200 was employed for differential scanning calorimetry, and JASCO FT/IR-4700 Attenuated Total Reflectance (ATR) devices were utilized for Fourier-transform infrared spectroscopy.

Additionally, the glass fiber composition determination was performed in accordance with the TS EN ISO 1172:2023, Method B standard which can be referred as burn-off or calcination test. This test maintains the samples at the target temperature until all combustible products have burned and exited the environment. A target temperature of 600°C was selected. This temperature is unsuitable for fillers that decompose below the calcination temperature. However, since this study's primary and focal filler is calcium carbonate, which is expected to decompose above 800 °C , this test was considered appropriate. As a result of this test, the proportions of glass fibers and fillers in the resulting products will be determined.

3.2.4 Composite Production

After the pyrolysis processes, composites were produced using the same method as in the laboratory. However, this time, the composite composition percentages were prepared according to the ratios provided in Table 3.2.

In these BMC productions, control groups were established. The samples named BMC-ST2, BMC-C1, BMC-C2, and BMC-C3 represent, respectively, virgin BMC, BMC with 0.75% virgin fiber added in place of $CaCO_3$, 5% virgin fiber added in

place of $CaCO_3$, 5% $CaCO_3$ added in place of virgin fiber to allow comparison with samples obtained from the previous experiment, and BMCs with 5% (BMC-P5), 10% (BMC-P10), and 15% (BMC-P15) recycled material added while removing $CaCO_3$ in the same proportions.

Table 3.2 Recycled BMC compositions produced by using the pilot-scale pyrolysis products and control sample compositions

Composition(wt%)	**BMC-ST2**	**BMC-C1**	**BMC-C2**	**BMC-C3**	**BMC-P5**	**BMC-P10**	**BMC-P15**
Mediumflatic Polyester Resin	30.00	30.00	30.00	30.00	30.00	30.00	30.00
Other Components	5.00	5.00	5.00	5.00	5.00	5.00	5.00
Filler $CaCO_3$	50.00	49.25	45.00	55.00	45.00	40.00	35.00
Fiber Glass	15.00	15.75	20.00	10.00	15.00	15.00	15.00
Recycled Fiber	-	-	-	-	5.00	10.00	15.00

3.2.5 Mechanical Behavior Tests of Produced Recycle BMC Composites from Pilot-Scale Pyrolysis Process

The same methods used at the laboratory-scale were also applied to the BMC composites produced from the products obtained through the pilot-scale pyrolysis process. These tests were conducted at the CTP Composite company using the same equipment and protocols to determine the most suitable mixing percentage.

3.2.6 Liquid Products Characterization

After the pyrolysis process, characterization procedures were carried out to understand the resulting liquids' possible applications and energy potential. As a result, it was possible to briefly assess what type of fuel they could be used as or which production processes they could serve as raw materials. A more detailed

interpretation of these aspects lies beyond the scope of this thesis and would require more extensive investigation.

To determine the potential applications of these liquids and their energy capacity, a bomb calorimeter analysis to obtain GCV value, was performed. In addition, gas chromatography-mass spectrometry (GC-MS) analysis was conducted to understand the chemical composition of the products. The bomb calorimeter analysis was carried out at TÜBİTAK BUTAL in accordance with ASTM 240 D standards. The GC/MS analysis was likewise carried out at TÜBİTAK MAM in accordance with the same standard.

3.3 Performance Testing of Recycled Tractor Component

In line with the recycling method determined at the laboratory-scale and the recycled material composition percentage established at the pilot-scale, a prototype tractor component was produced at CTP Composite. To investigate its feasibility for use in tractor production, this prototype component was subjected to a series of performance analyses and tests. The reasons for selecting this specific tractor component are explained in the Results section. In this section, the analyses and tests that were performed are described.

3.3.1 MBD Based Flex Body Analysis and Simulation (MBD-FBAS)

The MBD-FBAS method is used to examine the behavior of flexible components in engineering systems. This analysis simulates and evaluates the behavior of parts with the potential to undergo large deformations, accounting for real physical effects such as loads, vibrations, and deformations. [113] It represents the simulation-based equivalent of the bump test described in this section. Conducting this analysis is one of the requirements for newly designed parts before their implementation in tractor production. The analysis was performed within TürkTraktör using ALTAIR Hypermesh, OptiStruct, and MotionSolve software.

The three-dimensional geometry model obtained from the design teams was cleaned and organized appropriately for analysis. Since the part has variable thickness and is less than 10 mm, a mesh structure was created using the mid-surface technique to generate a surface at the center of the geometry's thickness. The mesh was generated with 77800 elements and an average thickness value of 3 mm. After this stage, aset points were assigned to the model, and the model was transferred to the MotionView program for bump simulation/analysis. By defining connection joints at the assigned aset points, the bump analysis was conducted under test conditions developed in-house from previous projects. The values obtained from the MotionView program were examined in the HyperView program for post-processing.

3.3.2 Tractor Bump Test

The tractor bump test is a mechanical testing method conducted in a simulated field environment to evaluate the tractor's mechanical durability, suspension performance, and structural integrity. The main goal of this test is to understand the behavior of components, particularly the cabin, body, and exterior trim parts, under cyclic dynamic stress. Real-world stresses are mimicked by driving the tractor on a road with bumps at regular intervals. This test ensures that the tractor parts meet performance standards and optimize its design and functionality. [114] This is the critical test for the part selected for recycling that must pass beyond its material mechanical properties. Once approved in this test, the component can be deemed suitable for production use. This test was conducted within TürkTraktör.

CHAPTER 4

RESULTS AND DISCUSSION

This chapter presents the results of the studies conducted using the methods described in the previous chapter.

Initially, the solid products resulting from the laboratory-scale processes were examined, characterized, and subjected to cleaning studies. Subsequently, the glass fibers and solid products obtained from these processes were added in specific proportions to virgin BMC paste, replacing $CaCO_3$ fillers, and BMC composites were produced using this paste. The mechanical properties of these produced composites were then tested. Additionally, the composites underwent a series of painting and serigraphy tests to evaluate their usage potential, and no issues were encountered. As a result of this phase, pyrolysis was selected as the ideal recycling method, and it was decided that cleaning processes were unnecessary due to the inefficiency of such methods and the disadvantages of adding this step when scaling up to an industrial level.

The next stage, the pilot-scale process, was conducted as a scale-up process following the laboratory scale prior to mass production. In this process, the sample sizes used increased. The amount of solid product, which was approximately 20 to 30 grams at the laboratory scale, increased up to 100 grams at this stage, resulting in approximately a threefold increase in solid product per run compared to the previous phase. Additionally, because the established system was used exclusively for this process and supply management similar to mass production was ensured, the preparation time before the process and the processing time after were reduced, resulting in a faster process flow. The solid products obtained from the pilot-scale pyrolysis were characterized. Recycled materials at 5%, 10%, and 15% (wt%) were added to virgin BMC paste, replacing $CaCO_3$ in the same proportions, and BMC

composites were produced and subjected to mechanical tests. As a result of these tests, it was determined that a mixture at 10% was optimal. Additionally, the liquid products obtained at this stage were collected and characterized, and potential application areas were discussed.

In the final stage, performance testing, the mechanical properties of the BMC composites created with an 10% composition were defined on a 3D model developed in a computer environment. Computer-aided engineering (CAE) simulation and analysis were conducted, and the composites received application approval. Subsequently, this part was produced with the determined composite mixture and subjected to physical testing on a tractor, where it also passed the tests successfully.

At the end of these stages, a part of the vehicle that previously did not contain any recycled components was produced using recycled materials. Furthermore, another part produced from materials obtained through this recycling process was also used on the tractor. This created a valuable product usage loop for circular economy and sustainable production. Consequently, this established a profitable process in terms of both environmental and economic regulations.

4.1 Laboratory Scale Recycling Process

4.1.1 Determination of Process Parameters

The TG-DTA-DTG results of the unpainted SMC sample taken from the production line are presented in Figure 4.1 and Figure 4.2. In these graphs, the blue line represents the thermogravimetric analysis (TG) data, showing the weight loss (%) of the material as a function of temperature. The right-hand side y-axis labeled "TG (%)" corresponds to this decomposition percentage.

The red line illustrates the derivative thermogravimetry (DTG) data, highlighting the rate of weight loss (%/min). The peaks observed in the DTG curve indicate the

temperature ranges where decomposition occurs and how rapidly it proceeds. The left-hand side y-axis labeled "DTG (%/min)" corresponds to this rate.

The curve marked in green represents the differential thermal analysis (DTA) data, showing the energy released or absorbed during the thermal events mentioned, such as decomposition or phase transitions. The left-hand side y-axis labeled "DTA (µV)" corresponds to this line.

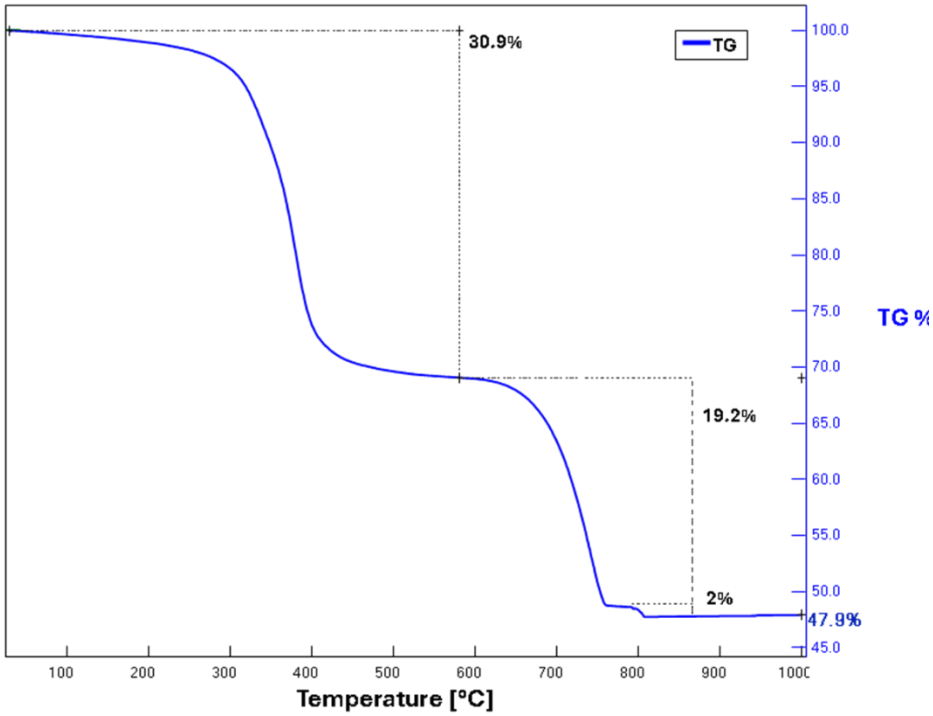

Figure 4.1. TG analysis result of the SMC sample from production line

Table 4.1 presents the characteristic features of these decompositions, namely the decomposition temperature (Td), peak temperature (Tp), and the end of decomposition temperature (Ted). These decompositions occur in three stages: two main stages and one minor stage.

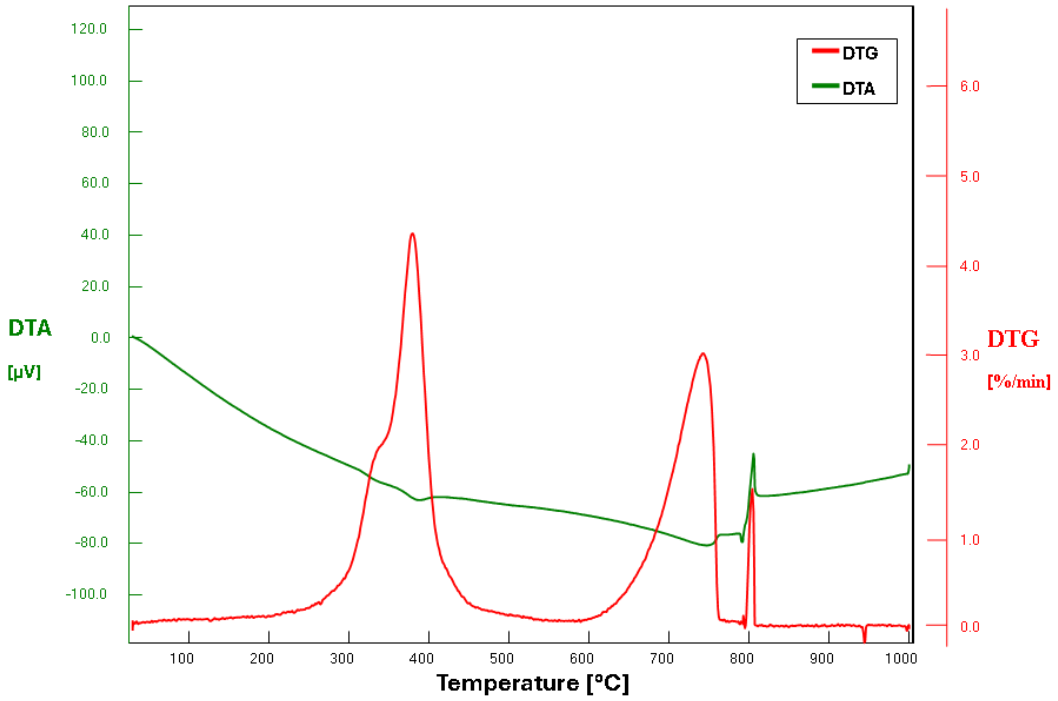

Figure 4.2. DTA-DTG analysis results of the SMC sample from production line

When explaining these decompositions, it is noted that the first two stages occur in a nitrogen (N_2) environment, resulting in thermal decomposition. After 800°C, oxygen (O_2) is introduced, and the third stage becomes a combustion event. The 30.9% weight loss observed in the first phase corresponds to volatile matter, plasticizers, monomers, and polymers. The total weight loss of 21.2% in the second and third phases represents the loss of combustible material. The remaining 47.9% corresponds to the solid residue, which includes fiberglass, ash, and inorganic and thermally stable materials.

Table 4.1 Decomposition rates and characteristic temperatures of the SMC sample from the production line

	Decomp. (%)	**T_d (°C)**	**T_p (°C)**	**T_{ed} (°C)**
First Stage	30.9	210	340	400
Second Stage	~19.2	600	650	750
Third Stage	~2	790	805	810

Based on this TG and DTA-DTG curves and studies in the literature [21,33,90,92–95,102,115], the temperatures for the laboratory-scale experiments were determined. It was concluded that a temperature above 400°C is necessary for complete pyrolysis, while staying below 600°C is important to avoid the risk of losing materials like $CaCO_3$, which are beneficial for subsequent use. Considering the studies in the literature, a target temperature of 500°C was selected.[33,90]

4.1.2 Selecting the Ideal Recycling Process

To recover fibers for recycling, understand and compare the ease of post-process cleaning and separation procedures, and assess the degree of degradation of the products, different recycling methods were tested. Since a condenser unit was not available at the laboratory-scale, all condensable and non-condensable gases were directly vented out of the system through the exhaust. Consequently, the gas and liquid yields could not be determined in this part of the study. The solid yields are presented in Table 4.2.

4.1.2.1 Pyrolysis

It was observed that the pieces obtained after pyrolysis exhibited a charcoal-like structure (Figure 4.4). By applying gentle pressure using hands, brushes, or tweezers, the fibers could be separated from other solid residues. Additionally, without exerting excessive force, fiber bundles could be extracted from the matrix using forceps (Figure 4.3). However, these bundles were observed to remain almost adherent to some solid residues within themselves. The dust accompanying the fibers was black and could be removed using a brush. To understand the composition of these solid products, samples were taken for XRD and XRF analyses. SEM imaging was conducted to examine the surfaces and diameters of the fibers obtained. The

solid yield resulting from the pyrolysis experiments was $74.5 \pm 1.2\%$, which is consistent with values reported in the literature. [33,90,92,95]

Figure 4.3. Extracted fibers after laboratory-scale pyrolysis

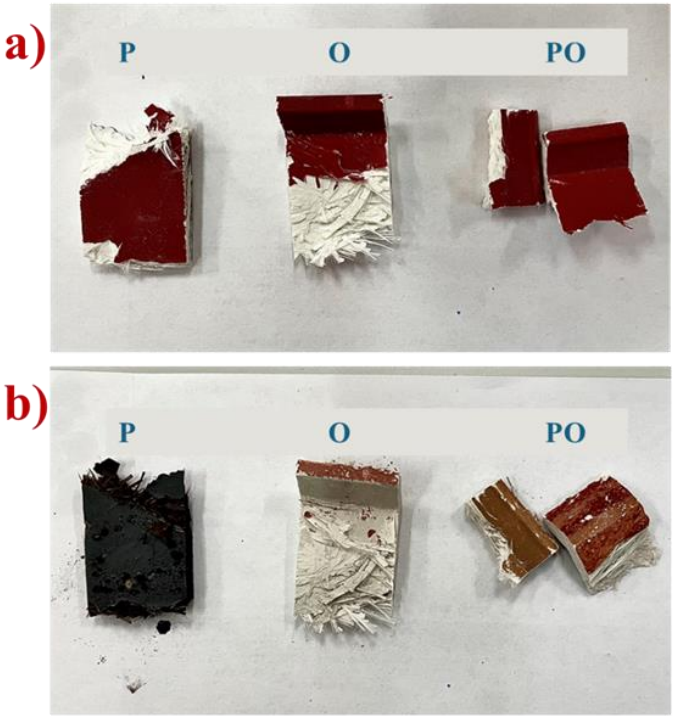

Figure 4.4. Left to right: Pyrolysis, Oxidation, PO. a) before processes, b) after processes

4.1.2.2 Oxidation

As shown in Figure 4.4, the pieces obtained after oxidation appeared white in color, contrasting with the pyrolysis results. It was more clearly observed that the red paint layer on the part was not fully decomposed. In the pyrolysis process, whether the paint decomposed was not easily visible due to the charcoal-like color of the resulting product.

The solid yield was lower compared to pyrolysis. This difference is thought to be due to the oxidative environment causing the polyester undergoing combustion to leave very little or no char, converting into CO_2 and H_2O, and minor decomposition of $CaCO_3$ occurring. [21]

Similar to pyrolysis, it was observed that fibers could be separated from solid residues by applying gentle pressure. The fibers emerged in bundles, and although there were solid residues present (fewer than the pyrolysis), these residues are believed to be mainly $CaCO_3$. [21,33,90,92,102,116] Samples from these white, powdery solid residues were taken for characterization analyses using XRF and XRD. SEM imaging was performed to examine the surfaces and diameters of the fibers.

4.1.2.3 Pyrolysis Followed by Oxidation

As seen in Figure 4.4, the products obtained after the pyrolysis followed by oxidation, from now on can be called as PO, process resembled those from the oxidation samples in appearance. Similar to the oxidation results, it was observed that the red paint layer was not fully decomposed. This indicates that the paint layer was not completely decomposed in the pyrolysis process either. This may be due to the paint layer and final coating containing UV-resistant, flame retardant, and similar chemicals.

The solid yield showed very minimal differences compared to oxidation. This was expected since the temperature and environment were the same, and the slight variation is thought to be due to the processing time.

Table 4.2 Solid yields (%) of laboratory-scale recycling processes

	Pyrolysis	**Oxidation**	**PO**
Solid Yield (%)	74.5 ± 1.2%	68.8 ±1.8	68.4 ±1.7

4.1.2.4 Surface Morphology of the Glass Fibers after Recycling Processes

In this section, the surface morphology of glass fibers obtained after each laboratory-scale process was imaged and analyzed using SEM. The primary focus of these examinations included determining whether any distinct structural degradation had occurred on the fiber surfaces, comparing the post-process fiber diameters, assessing the extent of residual material remaining on the fiber surfaces, and evaluating the frequency of broken fibers observed in randomly selected bundle images. Interpretations were then made based on these findings.

For the imaging process, sequential magnifications corresponding to 1 mm, 200 μm, 100 μm, 20 μm, and 10 μm were utilized. Finally, an image captured at the 100 μm scale, where fiber diameters were observed and measured, was presented for more detailed assessment.

The products obtained after laboratory-scale pyrolysis were examined using SEM. At 1 mm scale (Figure 4.5), residues were observed to remain around and on the surfaces of the fibers. Although clumped probable carbon products and fillers like $CaCO_3$ had been separated from the fibers, they were still abundant. Moreover, no cracks, broken parts, or deformed shapes were observed. At 200 μm scale (Figure 4.5), solid products clumped on the fibers could be seen. No noticeable fractures or irregularities were observed. Similar results were found at 100 μm scale (Figure 4.6).

At 20 µm, solid residues were seen to adhere to the fiber surfaces, with minor deformations affecting the surface geometry observed in some areas.

At 10 µm scale (Figure 4.7), no crack formation or major surface damage was observed. Only minor surface deformations and some solid residues adhering to the surface, as seen at 20 µm, were detected.

When fiber diameters were measured at ten points in a randomly selected, an average value of 13.6 µm was obtained. The following points should be noted for the fiber diameter results. When measuring fiber diameters, parameters such as fiber orientation, surface residues, and instrument settings must be considered, meaning the measurement values should not be viewed as definitive. However, given that the measured values are close to 13 µm and that standard E-glass fibers in the industry also have a diameter of approximately 13 µm, it can be inferred that the diameters remain similar to their original state.

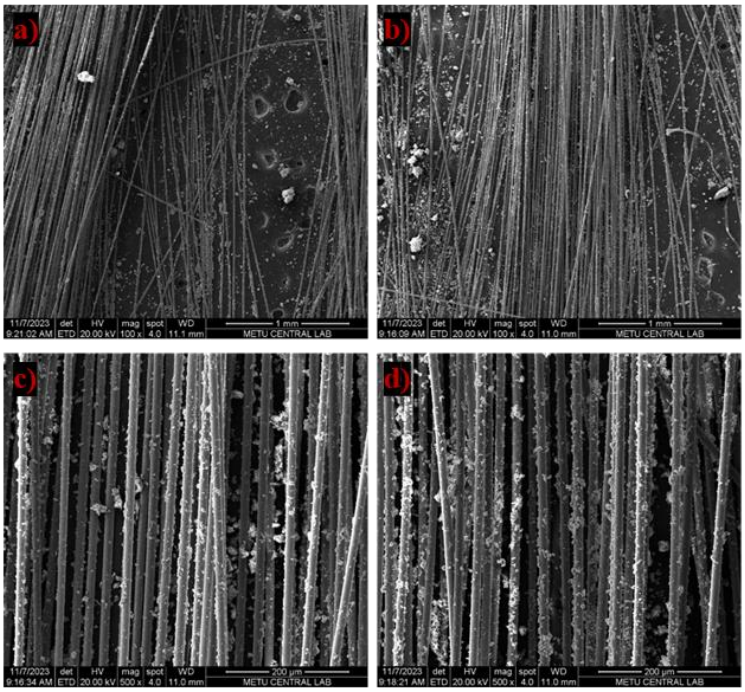

Figure 4.5. SEM images of laboratory-scale pyrolysis samples, a) 1mm, b) 1mm, c) 200 µm, d) 200 µm

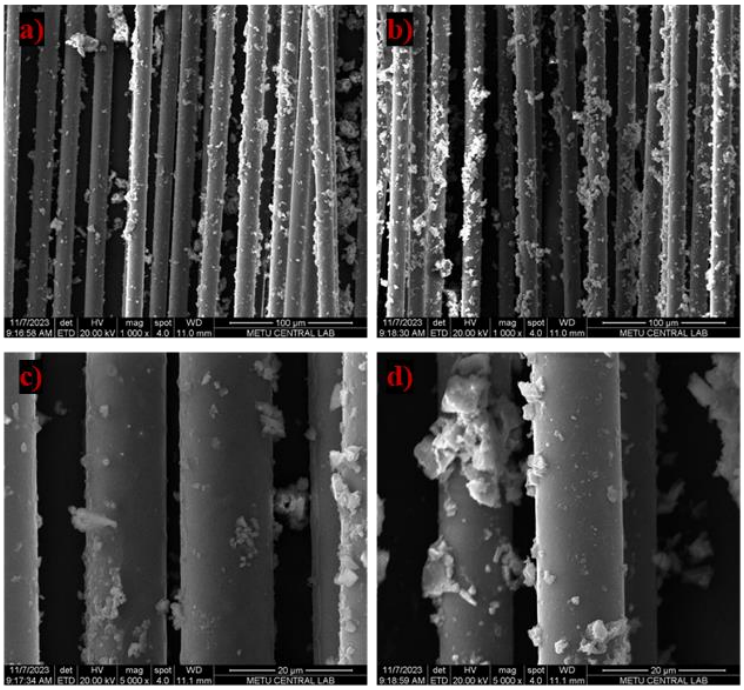

Figure 4.6. SEM images of laboratory-scale pyrolysis samples a) 100 µm b) 100 µm, c) 20 µm, d) 20 µm

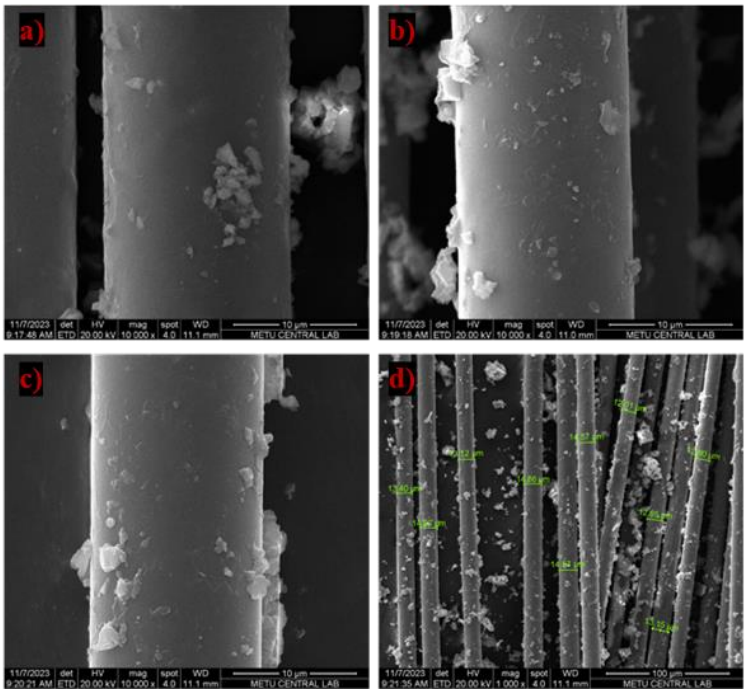

Figure 4.7. SEM images of laboratory-scale pyrolysis samples a) 10 µm, b) 10 µm, c) 10 µm and d) fiber diameters at 100 µm

Upon examining the laboratory-scale oxidation results, at 1 mm scale, less solid residue and cleaner fiber surfaces were observed compared to the pyrolysis results. However, broken fiber structures were detected. At 200 µm scale, cleaner surfaces than those observed after pyrolysis were evident. The background appearance of residues had also diminished, and no clumped solid residues were present. Similar observations were made at 100 µm and 20 µm scales. At 10 µm scale, although fewer than in pyrolysis, solid residues were still present on the surface. Unlike the pyrolysis sample, much fewer minor surface deformations were observed on the fibers subjected to oxidation. This suggests that the minor deformation observed on the pyrolysis surface resulted from combustible products that could be decomposed and removed through oxidation.

When fiber diameters were measured at ten points in a randomly selected, an average value of 13.8 µm was obtained.

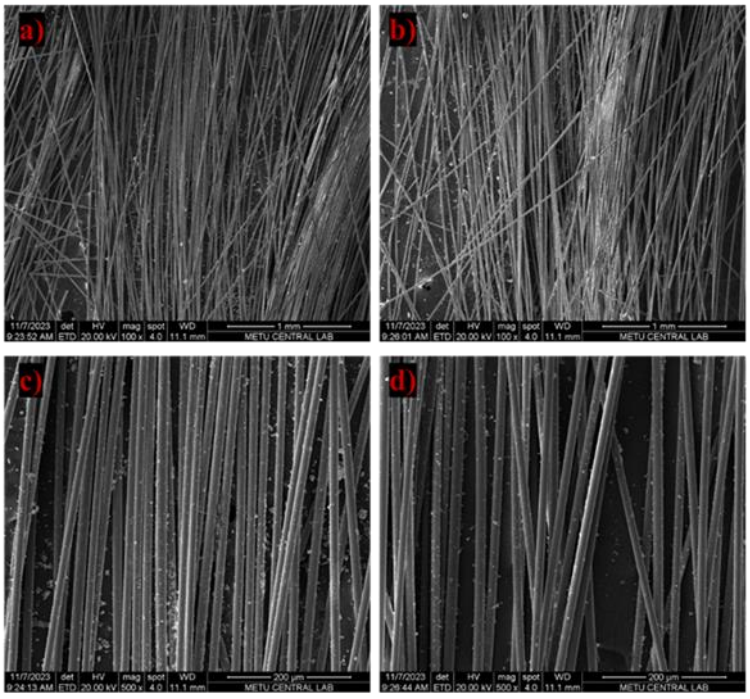

Figure 4.8. SEM images of laboratory-scale oxidation samples, a) 1mm, b) 1mm, c) 200 µm, d) 200 µm

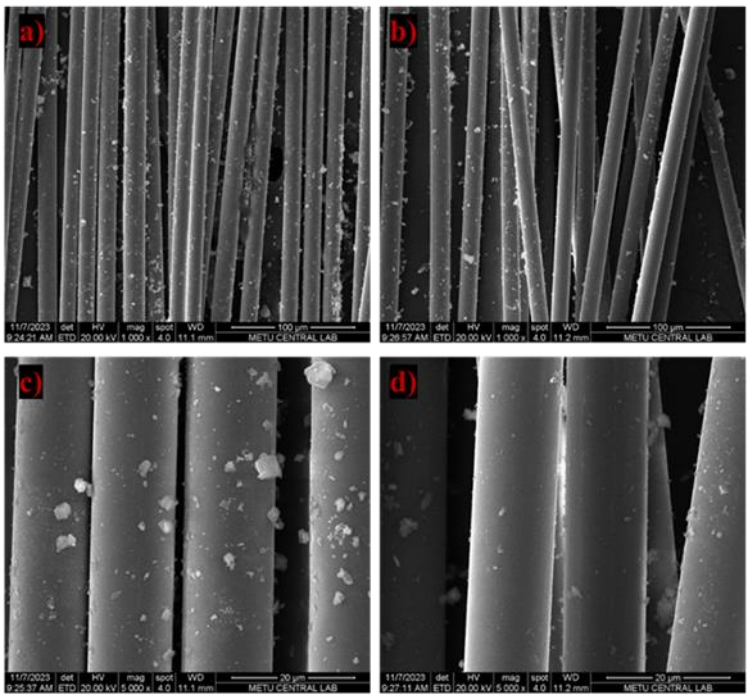

Figure 4.9. SEM images of laboratory-scale oxidation samples a) 100 µm b) 100 µm, c) 20 µm, d) 20 µm

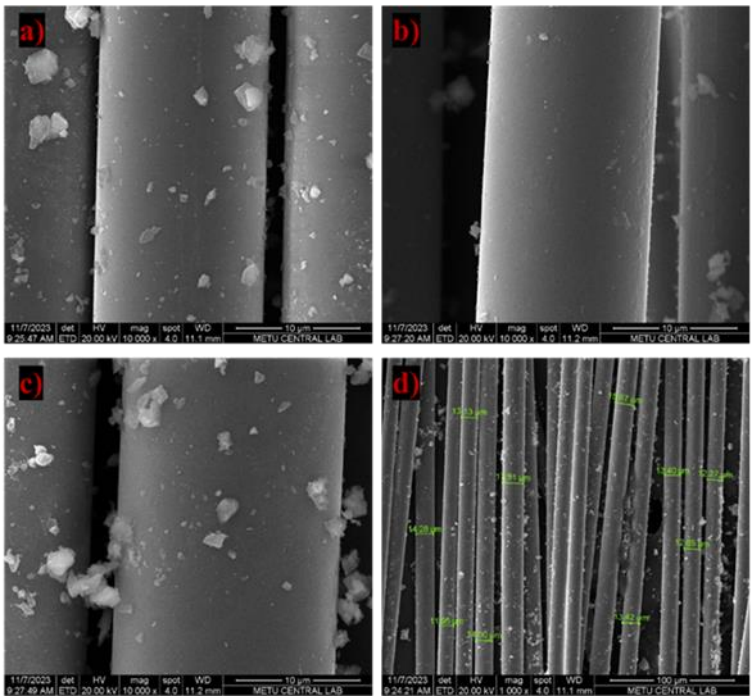

Figure 4.10. SEM images of laboratory-scale oxidation samples a) 10 µm, b) 10 µm, c) 10 µm and d) fiber diameters at 100 µm

Examining the results of the pyrolysis followed by oxidation (PO) process at laboratory-scale, broken and fractured fiber structures were encountered at 1 mm scale. This process exhibited the least amount of solid residue. At 200 µm scale, broken fiber images were again observed. The surfaces and background appeared cleaner compared to other processes. Similar to the oxidation sample, there was no appearance of clumped solid residues. Therefore, it was concluded that the clumped solid appearance consisted of combustible products that could be eliminated through the oxidation method. Similar results were observed at 100 µm and 20 µm scales. Likewise, the 10 µm images resembled the oxidation results.

When fiber diameters were measured at fourteen points in a randomly selected, an average value of 13.8 µm was obtained.

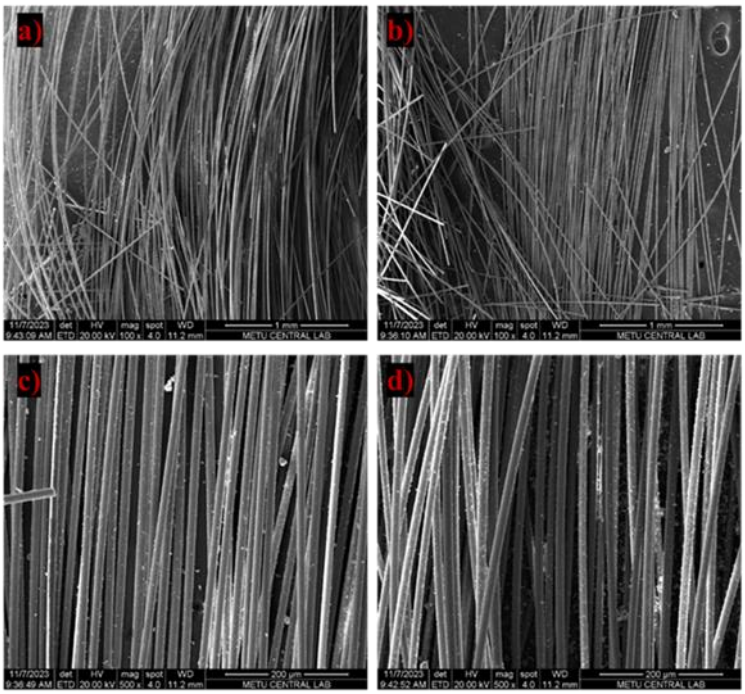

Figure 4.11. SEM images of laboratory-scale PO samples, a) 1mm, b) 1mm, c) 200 µm, d) 200 µm

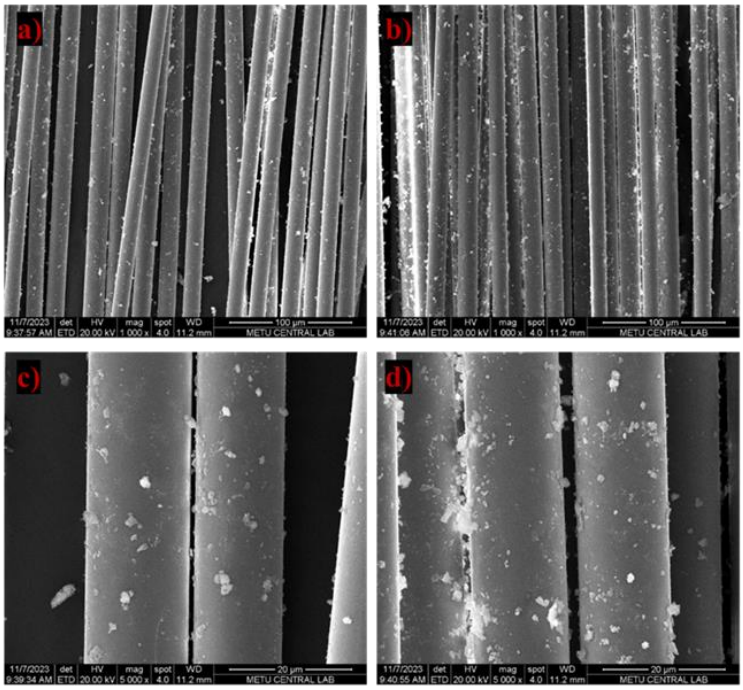

Figure 4.12. SEM images of laboratory-scale PO samples a) 100 µm b) 100 µm, c) 20 µm, d) 20 µm

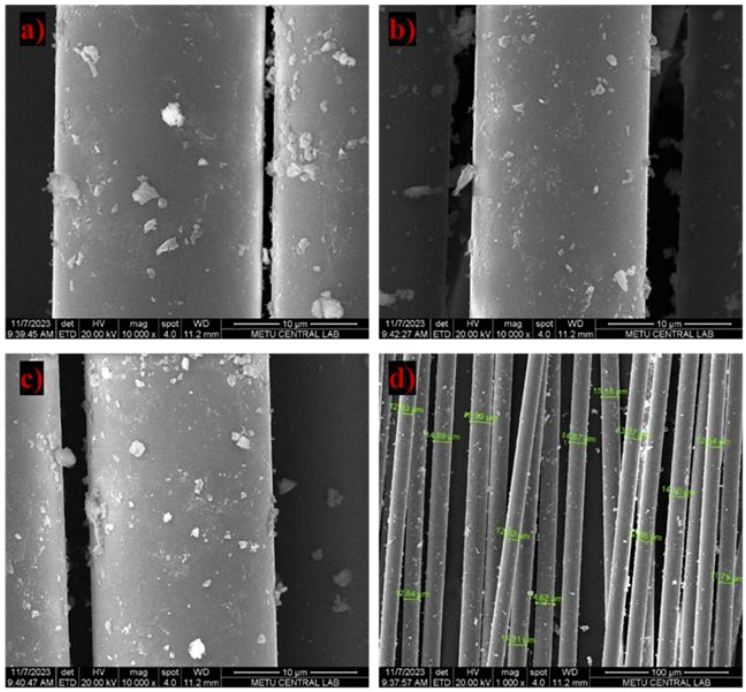

Figure 4.13. SEM images of laboratory-scale PO samples a) 10 µm, b) 10 µm, c) 10 µm and d) fiber diameters at 100 µm

In summary, at laboratory-scale, when the fibers obtained from pyrolysis were examined, more solid residues were observed compared to the other processes. No major deformations affecting surface quality were detected, and no cracks or broken fibers were observed. In the oxidation and PO processes, combustible products present on the surfaces of the pyrolysis products were removed from the fiber surfaces. Unlike in pyrolysis, broken fibers were observed. More broken fibers were noted in the PO process compared to oxidation. There was no significant difference in fiber diameters among the processes. Despite the fiber diameters being remarkably similar, the variation in the number of broken fibers is thought to be due to oxidation making the fibers more brittle. The higher incidence of broken fibers in the PO process compared to oxidation is believed to be an effect resulting from the longer processing time. In applications involving the reuse of fibers, the pyrolysis method is particularly advantageous as it not only preserves the integrity and strength of the fibers but also enables the residues surrounding them to be reutilized in other composite products.

4.1.2.5 Composition of Solid Residues After from Laboratory Scale Processes

In this section, the chemical compositions of the solid products obtained after the laboratory-scale processes were examined using X-ray diffraction and X-ray fluorescence analyses. The similarities and differences among the processes in terms of chemical composition were then discussed. The term "solid products" refers to the materials remaining after removing glass fibers. However, due to mechanical cleaning, residual glass fibers can be found within these solid products.

First, the solid products were subjected to X-ray diffraction analysis (XRD), and their existing crystal structures were interpreted. This step incorporated X-ray fluorescence (XRF) data into the evaluation, allowing for a more detailed analysis and a clearer understanding of their chemical compositions. In these examinations, the primary focus was determining the current state of calcium carbonate ($CaCO_3$).

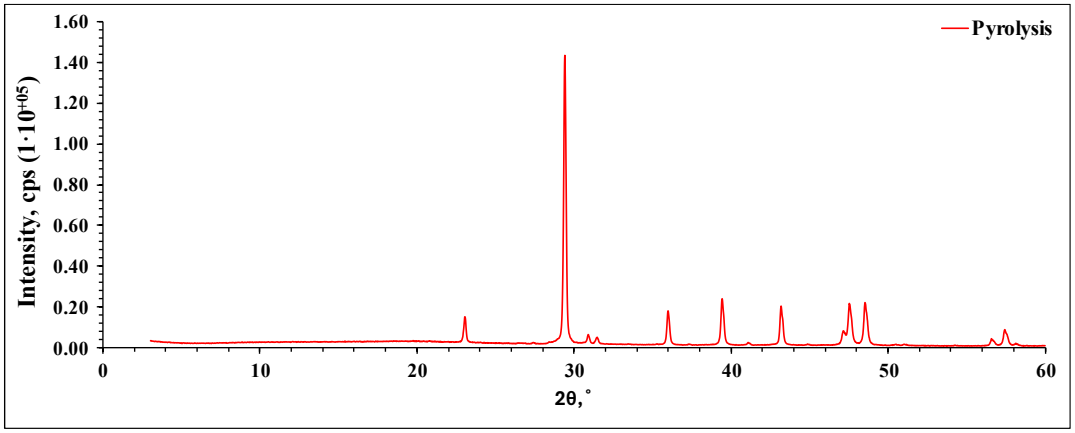

Figure 4.14. XRD- Measured profile view of laboratory-scale pyrolysis residue

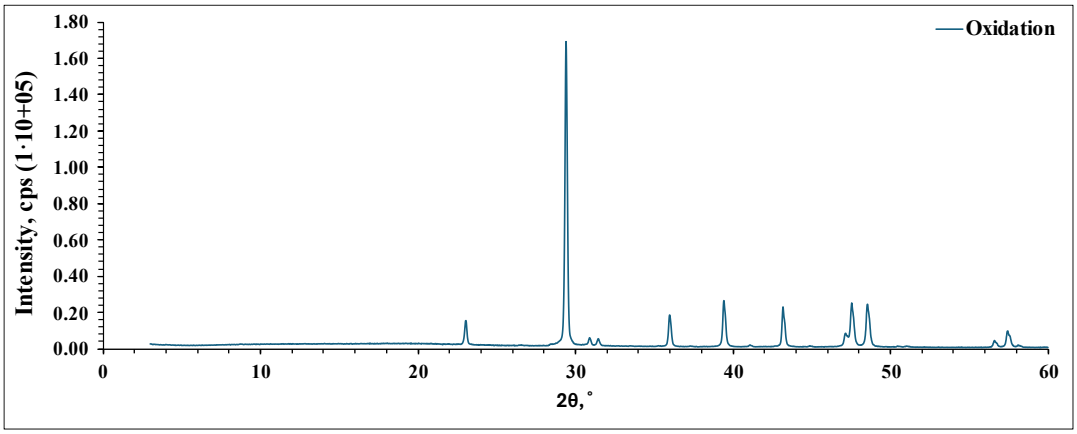

Figure 4.15. XRD- Measured profile view of laboratory-scale oxidation residue

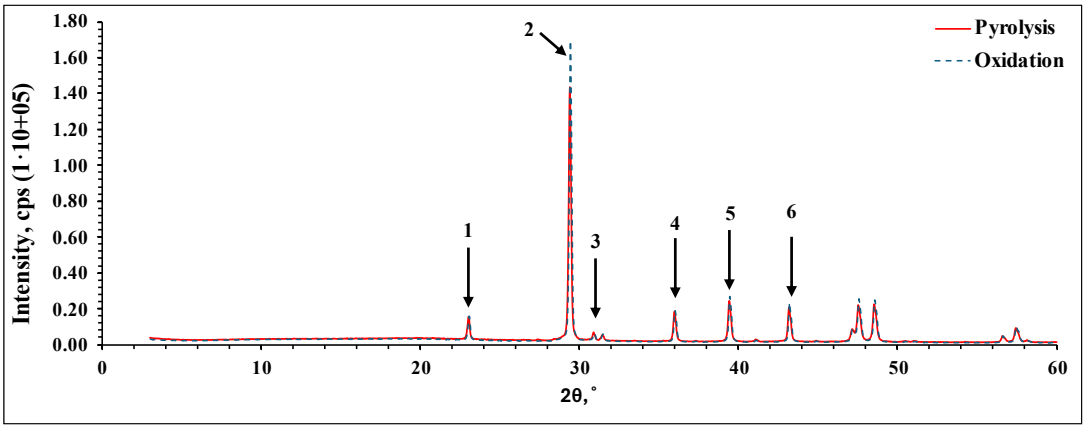

Figure 4.16. Comparison of XRD measured profile view of residues of pyrolysis and oxidation at laboratory-scale

Table 4.3 XRD Peaks with corresponding phases

Peak No.	2θ (°)	Phase	(Int. I., cps°) Pyrolysis	(Int. I., cps°) Oxidation
1	23.03°	Quartz (SiO_2)	1758	1812
2	29.39°	Calcite ($CaCO_3$)	20619	23605
3	30.88°	Calcite ($CaCO_3$)	646	713
4	39.41	Calcite ($CaCO_3$)	4034	4264
5	35.97°	Calcium Oxide (CaO)	2695	2737
6	43.17°	Calcium Oxide (CaO)	3366	3584

The XRD analysis of the solid products obtained from pyrolysis and oxidation at laboratory-scale demonstrated differences in the composition and chemical transitions of the filler materials. Upon examining the results of both processes, peaks were observed at 29.39°, 23.03°, and 30.88° on the 2θ axis. These peaks indicate that $CaCO_3$ is dominantly present in both samples. Additionally, in the oxidation graph (Figure 4.15), a small peak is observed at 8.72°, which is absent in the pyrolysis graph (Figure 4.14). This may be attributed to the formation of a new crystalline phase, potentially calcium hydroxide or other oxidation-related compounds. Furthermore, the oxidation sample exhibits sharper peaks compared to the pyrolysis sample, which could be a result of exposure to oxygen during the process.

When the same products were analyzed via XRF, significant differences were observed. The pyrolysis sample contained 74.9 wt.% calcium oxide (CaO), whereas the oxidation sample contained 90.8 wt.%. This suggests that in the pyrolysis sample, the decomposition of $CaCO_3$ is either absent or partial, while during oxidation, the oxidative effect accelerates the decomposition, resulting in higher levels of CaO.

Table 4.4 XRF – SQX Calculation result for laboratory-scale pyrolysis residue

No.	Component	Result (wt.%)
1	CaO	74.90
2	SiO_2	14.70
3	Al_2O_3	4.40
4	TiO_2	1.84
5	MgO	1.79
6	Fe_2O_3	0.82
7	ZnO	0.47
8	CuO	0.46
9	SrO	0.24
10	SO_3	0.15
11	P_2O_5	0.11
12	K_2O	0.11

The effect of oxidation is also evident in other components. After pyrolysis, the silicate (SiO_2) and alumina (Al_2O_3) contents were measured at 14.7 wt.% and 4.4 wt.%, respectively. After oxidation, these values decreased to 2.64 wt.% and 0.906 wt.%, respectively. This suggests preferential oxidation of silicates or reactions leading to the formation of undetectable phases. Trace elements such as Fe_2O_3, ZnO, and BaO were identified in the solid residues of both processes, likely originating from the initial formulation of the SMC. In summary, while both processes yield similar overall compositions, the key difference lies in the decomposition of $CaCO_3$. The pyrolysis method, with its lower decomposition of $CaCO_3$, emerges as a better option for applications such as the formation of BMC composites, where the retention of $CaCO_3$ is advantageous. [33]

Table 4.5 XRF – SQX Calculation result for laboratory-scale oxidation residue

No.	Component	Result (wt.%)
1	CaO	90.80
2	SiO_2	2.64
3	MgO	2.08
4	TiO_2	1.87
5	Al_2O_3	0.91
6	BaO	0.55
7	Fe_2O_3	0.50
8	ZnO	0.30
9	SrO	0.10
10	P_2O_5	0.10
11	SO_3	0.10
12	Cl	0.04
13	K_2O	0.02

4.1.2.6 Evaluation of Post-Recycling Glass Fiber Cleaning

In this section, the cleaning of the fibers was examined. By "fiber cleaning," we refer to the effort to remove any residual solid products from the fiber surfaces and the surrounding medium. The findings obtained here were used to determine whether this removal process was successful.

Fibers obtained from the pyrolysis sample, which were mechanically cleaned using forceps and a brush, both individually and in bundles, were subjected to cleaning with water and acid, and the results were examined under an optical microscope. The magnified image of the part from which the fibers were taken is also provided in Figure 4.17.

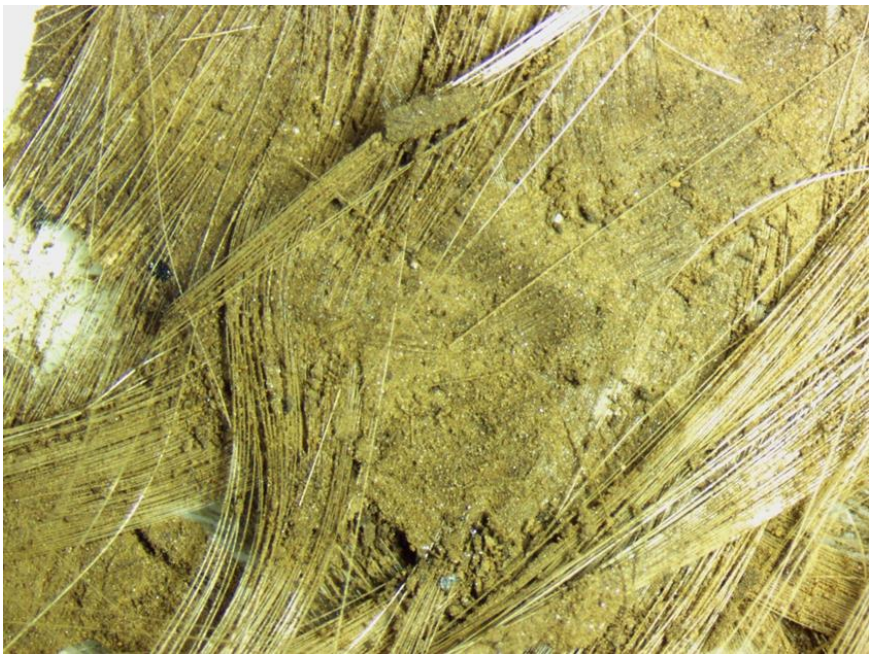

Figure 4.17. Part of a solid residue that fiber bundles were taken under optical microscope

Figure 4.18. Images of water cleaned fibers under optical microscope

In the bundled samples cleaned with water, a significant amount of solid residue was observed. Additionally, as the magnification increased during the imaging of the bundles, the residues on the fibers became more apparent. When individual fibers were examined, it was similarly observed that there was a substantial amount of residue on the fibers. The imaging results can be seen in Figure 4.18.

When examining the bundles from the samples cleaned with acid, a similar appearance to that of water cleaning was observed, indicating that solid residues were abundantly present. Although some individual fibers displayed cleaner images compared to water cleaning, these observations were sporadic. Other individual fibers showed results similar to those cleaned with water (Figure 4.19).

When looking at samples that were only mechanically cleaned, it was observed that they did not exhibit a significantly different appearance compared to the samples cleaned with water or acid (Figure 4.20).

Figure 4.19. Images of acid cleaned fibers under optical microscope

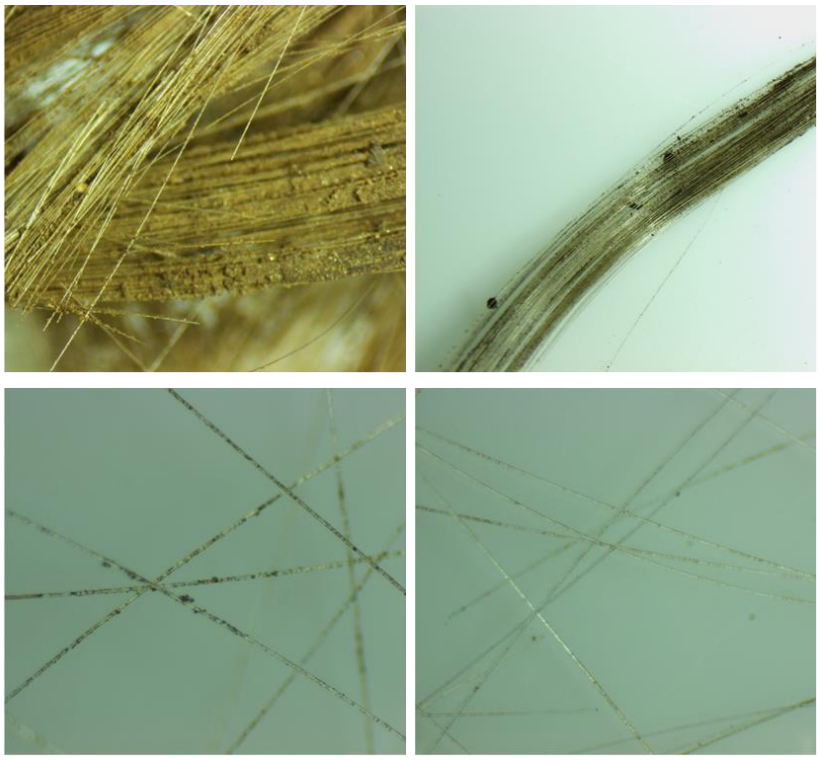

Figure 4.20. Images of mechanically cleaned fibers under optical microscope

Based on these observations, no clear benefit was found in cleaning with water or acid. Additionally, it should not be overlooked that the solid products being removed could be beneficial for reuse. Furthermore, considering that these methods would introduce extra cost and processing complexity when scaled up to an industrial level, their implementation appears unnecessary.

It has been deemed sufficient for the product after pyrolysis to undergo mechanical processing to the extent that it can be reintroduced into the composite paste and dispersed homogeneously.

4.1.2.7 Mechanical Behavior of Recycled BMC Composites Produced from Laboratory Scale Recycling Processes

In this section, bulk molding compound (BMC) composites were produced using the glass fibers and solid products obtained from the laboratory-scale recycling

processes, together with the mixture ratios described in the previous chapter. Specimens taken from these composites were then subjected to mechanical tests, including tensile, flexural, impact, and hardness tests, to evaluate their performance.

These tests were conducted at CTP Composite under the standards mentioned in previous chapters, and the company provided the results. Multiple measurements were taken to determine the final measurement results, and the standard deviation was reported at a 95% confidence level. However, the stress-strain curve data are unavailable; if desired, more detailed investigations can be carried out in future studies.

When comparing the tensile strength values, it was observed that the sample named BMC-C, which had virgin fiber added, provided the best value. The next best-performing sample was the one where fibers and filler materials recycled using the pyrolysis method were used. In other words, the sample produced with products recycled via pyrolysis exhibited even better tensile properties than the BMC-ST sample. Additionally, as expected from the characterization analyses, the worst performance was observed in the PO sample. In terms of tensile strength, the pyrolysis sample demonstrated better properties than the other recycled samples.

Looking at the tensile modulus, it was found that the recycled samples were better than the control sample in terms of modulus. Only the PO sample performed worse than the BMC-ST; apart from that, all recycling methods surpassed the BMC-ST sample in modulus value. According to this result, adding recycled fibers and filler materials makes the material less brittle compared to virgin $CaCO_3$. Conversely, adding virgin fiber made it more brittle.

When flexural strengths were examined, it was observed that the recycling methods or adding extra virgin fiber deteriorated the composite's flexural properties. The same results were seen for flexural modulus, with one exception: the PO sample had a slightly higher degree than the oxidation sample, but the difference was too small to be considered significant.

In examining impact strengths, the BMC-ST provided the best result, while the control sample and the pyrolysis sample yielded almost the same result, followed by the oxidation and PO samples. This suggests that adding material in a way that changes the composition negatively affects impact strength, but it does not lead to a dramatic change. The same situation applies to hardness values as in the impact tests.

Table 4.6 Mechanical testing results of produced BMC samples

	BMC-ST	**BMC-C**	**BMC-P**	**BMC-O**	**BMC-PO**
Tensile Strength (MN/m²)	25 ± 1	26 ± 2	25 ± 3	23 ± 3	22 ± 2
Tensile Modulus (GN/m²)	72 ± 1	70 ± 6	75 ± 3	72 ± 2	71 ± 1
Flexural Strength (MN/m²)	67 ± 4	63 ± 1	58 ± 5	39 ± 4	36 ± 5
Flexural Modulus (GN/m²)	81 ± 3	78 ± 2	75 ± 2	66 ± 2	67 ± 3
Unnotched Charpy Impact Strength (kJ/m²)	23 ± 1	21 ± 0	21 ± 2	19 ± 2	20 ± 1
Barcol Hardness	60 ± 1	58 ± 2	58 ± 3	54 ± 1	52 ± 1

In conclusion, the samples produced by recycling methods do not show dramatic differences compared to the BMC-ST. However, the low proportion of recycled material may have influenced this outcome. Therefore, experiments in subsequent stages were carried out with higher mixing ratios. Based on the results of this test and the characterization analyses, it can be observed that converting the material using only the pyrolysis method yields more successful results compared to other recycling methods.

Additionally, considering environmental factors, as can be seen from the XRF results, the gas products resulting from the oxidation method have the potential to be harmful to the environment. Furthermore, the effects of this method on carbon transformation and the environment have been discussed in previous sections. Therefore, only the pyrolysis method was chosen as the recycling method.

4.1.3 Surface Appearance and Paintability of BMCs from Laboratory Scale Recycling Products

In this section, visual examinations and paintability tests were conducted on the bulk molding compound (BMC) composite plate produced using glass fibers and solid products obtained from the laboratory-scale recycling processes. These tests will have a direct impact on the potential usability of recycled materials in commercial applications. Therefore, observing these properties is important.

Initially, the unpainted colors and surface quality of the produced composites were examined. Following this, their performance under smooth and textured paint applications was tested. Finally, screen printing trials were carried out on these composites to understand their performance in this context.

Figure 4.21. Recycled BMC composite plates. a) Pyrolysis, b) Oxidation, c) PO, d) All together

When examining the surfaces of these unpainted samples, it was noted that the composites produced with oxidation and PO products were light-colored, close to white. In contrast, the composite produced with pyrolysis products had a dappled-gray appearance with darker spots on a brownish white base color. These composite samples, produced using industrial techniques and equipment, can be seen in Figure 4.21.

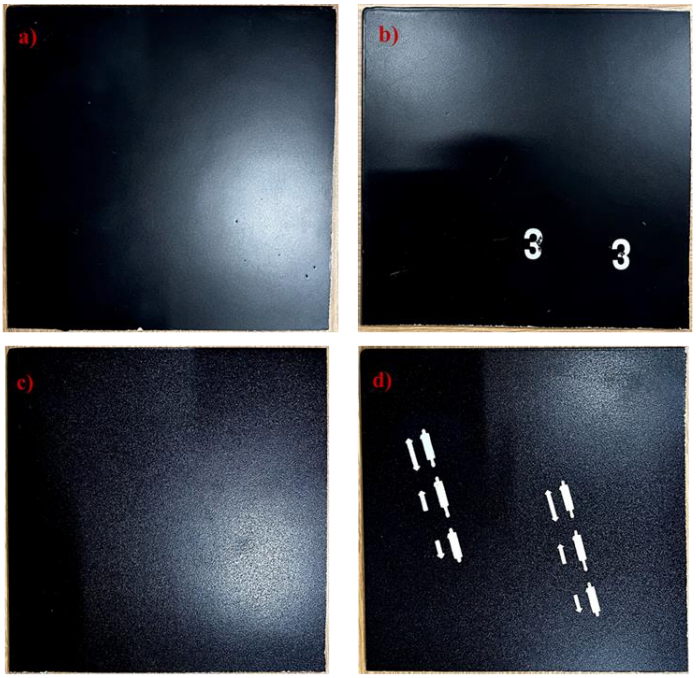

Figure 4.22. Paint and serigraphy samples. a) smooth, painted b) smooth, painted and with serigraphy, c) rough, painted, d) rough, painted and with serigraphy

Subsequently, painting and serigraphy tests, which are important for usability in different product groups and applications, were conducted on these samples. In these tests, the parts were painted using combinations rough, and smooth finishes.

Serigraphy trials were performed on both the smoothly painted part and the unpainted part to test the visual usage limits of the composites. As a result of these tests, it was observed that the parts could be easily painted and that serigraphy could be applied on them, whether they were painted or unpainted. Therefore, no issues are expected regarding visual product integrity and marketing criteria. The appearances

of the samples after the painting and serigraphy tests, can be seen in Figure 4.22 and Figure 4.23.

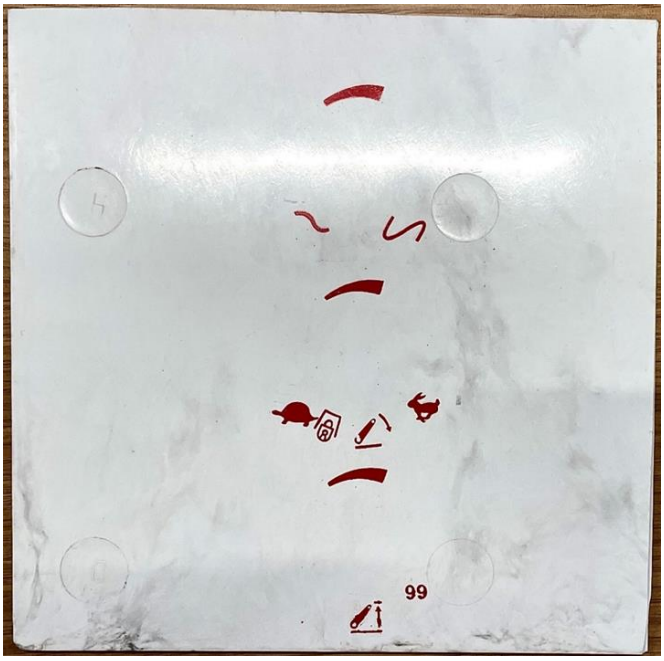

Figure 4.23. The non-painted sample tile with serigraphy

4.2 Pilot-Scale Recycling Processes

In the first stage of this thesis, the appropriate recycling process was identified, and the necessity of subsequent cleaning methods was determined. Following the selection of pyrolysis as the recycling method at the laboratory-scale, pilot-scale pyrolysis experiments were conducted. Unlike the laboratory setup, the pilot-scale system is capable of condensing some of the volatile gases produced during pyrolysis, thus allowing the recovery of liquid products. These liquid products generally consist of mixtures of organic compounds, commonly referred to as oils [94]. After suitable treatment, they can be used in fuel mixtures or serve as raw materials for producing other plastic materials [21,94,95,115,117]. Additionally, the flammable nature of the gases generated by pyrolysis, and their potential to supply a

portion of the energy required for the process, indicates promising prospects for more sustainable production practices. [90,92,95]

Based on these considerations, the pyrolysis parameters were revised.

Guided by the TG-DTA-DTG data presented in both in this and previous section and the literature, [33,90,94,95] a temperature of 600°C was selected to increase the liquid yield while preventing the decomposition of calcium carbonate. During the experiments, as the temperature approached the 500–600°C range, the emitted gases changed color from orange, suggesting residual organic compounds, to white smoke. This color change was considered an indicator of complete pyrolysis.

This section examines the results of the pilot-scale pyrolysis. After evaluating the appearance and yield of the products, scanning electron microscopy will be used to analyze the surface morphology of the glass fibers, and energy dispersive X-ray analysis will provide insights into the residues on their surfaces. The composition of the solid residue will be discussed using energy dispersive X-ray analysis and ash analysis results. Subsequently, mechanical tests will be conducted on bulk molding compound composites produced with different proportions of these fibers and solid products to determine the optimal mixing ratio. In addition, characterization and gross calorific value analyses of the liquid products obtained at the pilot-scale will be presented, and their potential application areas will be considered.

4.2.1 Pilot-Scale Process Sample Thermal Decomposition Behavior

The TGA results of the waste/scrap material used in the pilot process, which has reached the end of its service life, were very similar to the TG-DTA results obtained at the laboratory scale. Paint and surface coatings do not significantly affect the shape of the TGA curve, meaning they do not alter the thermal decomposition behavior. Based on these analysis results, when the target temperature of the process was chosen as 600 °C, which is the second decomposition initiation point, it was

concluded that the liquid yield could be maximized without causing the decomposition of $CaCO_3$. Characteristic temperatures can be seen in Table 4.7.

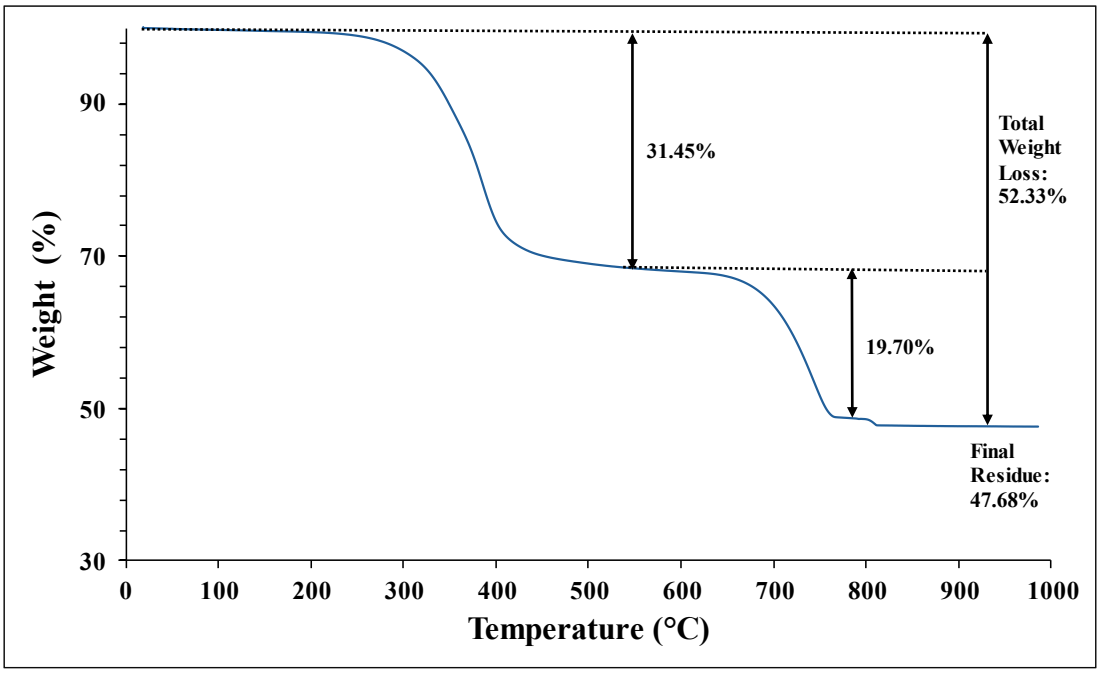

Figure 4.24. TGA thermogram of the pilot-scale process sample

Table 4.7 Decomposition rates and characteristic temperatures of the pilot-scale process sample

	Decomp. (%)	**T_d (°C)**	**T_p (°C)**	**T_{ed} (°C)**
First Stage	31.5	200	340	405
Second Stage	19.7	600	700	750
Third Stage	1.2	790	805	810

4.2.2 Pilot-Scale Pyrolysis Results

The solid product resulting from this process retains its geometric shape as it was before the treatment, similar to the first phase, and can be easily disassembled through gentle mechanical cleaning, allowing fibers to be readily separated. Images of the material before and after the process are provided in Figure 4.25.

At this stage, when a gentle mechanical process was applied to the obtained products, they dispersed easily, and the fibers could be extracted from them (Figure 4.26). In the previous section, it was determined that the material remaining on the fibers did not have a harmful effect on the production of new BMC composites. Therefore, no cleaning was performed. Instead, to ensure that the compound produced from these materials would mix more easily and uniformly, the fibers and solid products were separated as much as possible and then stored together. In this way, the loss of recycled materials was minimized and mixing within the composite compound was made easier.

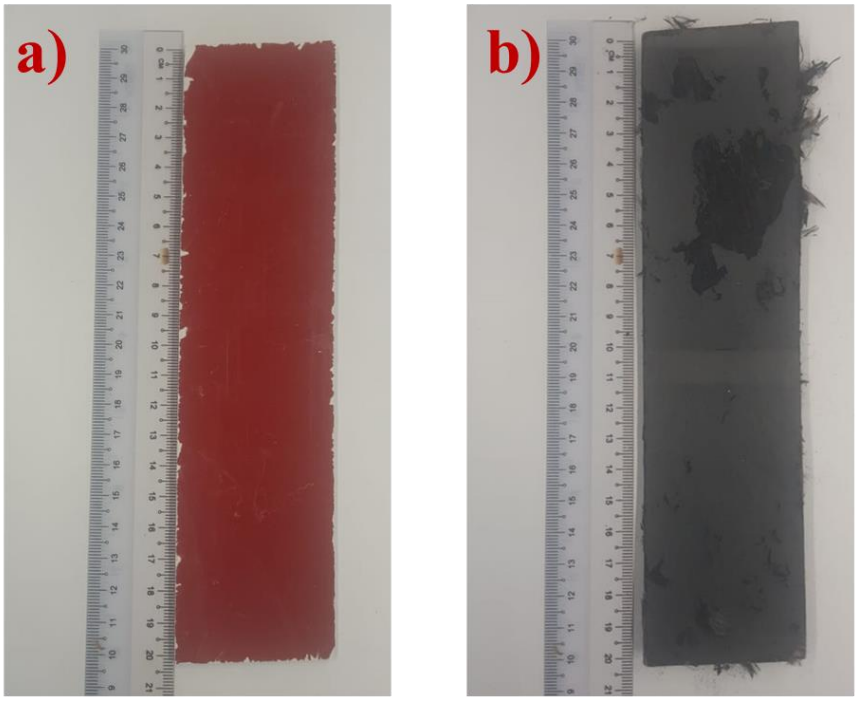

Figure 4.25. Pilot-scale pyrolysis sample. a) before, b) after the process

Figure 4.26. Separation of fibers after the pyrolysis process

The glass fibers and solid samples obtained from this process were set aside for surface and characterization analyses.

In addition, the product yields obtained after the pilot-scale pyrolysis process are presented in Table 4.8.

Table 4.8 Product yields of pilot-scale pyrolysis

Process	**Solid Yield (%)**	**Liquid Yield (%)**	**Gas Yield (%)**
Pyrolysis	64.5 ± 0.5	16.3 ± 0.4	19.3 ± 0.7

4.2.3 Surface Morphology of Glass Fibers After Pilot-Scale Recycling Process

After the pilot-scale pyrolysis process, the glass fibers were imaged with a 100 μm scale-bar using scanning electron microscopy (Figure 4.27). In these images, compared to the laboratory-scale process, less residue was observed on the glass fiber surfaces. This is believed to be due to the higher temperature and longer processing time. However, some residue still remains. Thus, unlike the laboratory-scale oxidation examples, a relatively clean surface was not achieved. No cracks or

noticeable surface deformities were observed, indicating that the fibers did not suffer significant visible damage.

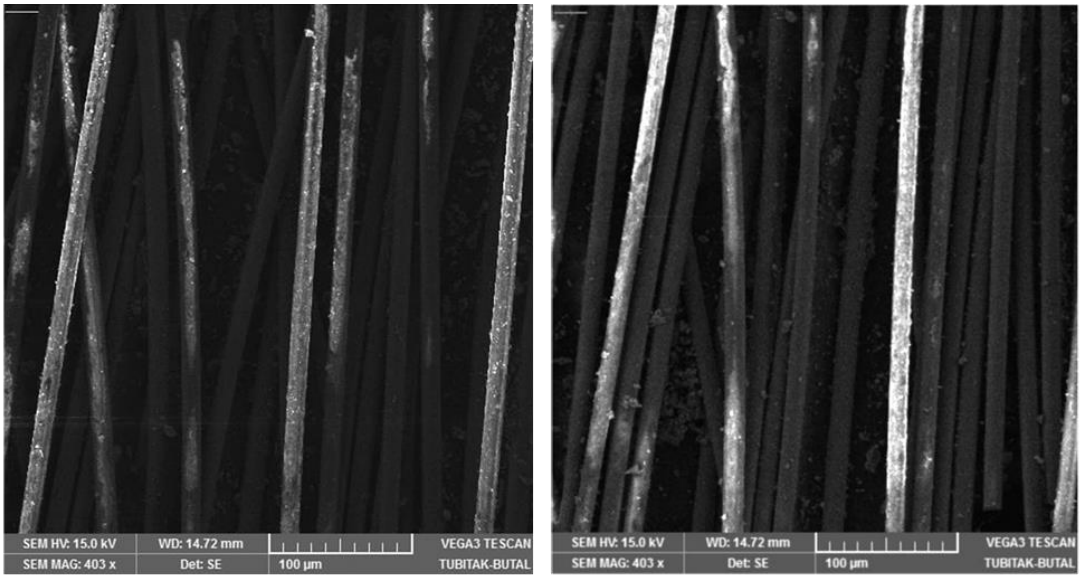

Figure 4.27. SEM images of pilot-scale pyrolysis samples at 100 µm

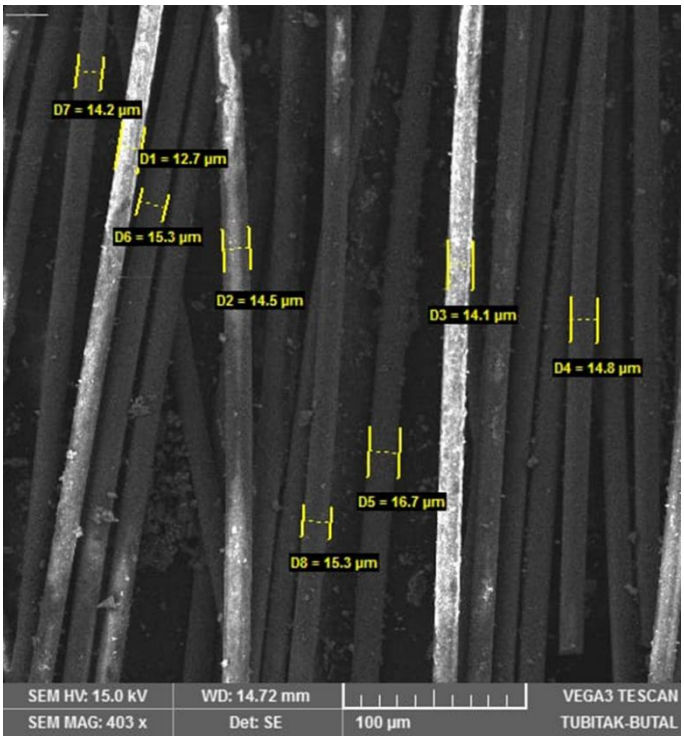

Figure 4.28. Fiber diameters of glass fibers after pilot-scale pyrolysis at 100 µm

In addition, as shown in Figure 4.28, eight fiber diameter measurements were performed, resulting in an average diameter of 14 μm. Although this is slightly higher than the values found for the three processes at the laboratory-scale, it does not suggest that the pilot-scale process is more damaging to the fiber diameters than the previous three processes.

The solid residues separated from the glass fibers by mechanical cleaning were also imaged at a 200 μm scale. Based on previous laboratory-scale chemical composition analyses, it was anticipated that these residues would contain glass fiber fragments. As shown in Figure 4.29, glass fiber fragments measuring approximately 400–450 μm in length were identified among the solid residues. Thus, choosing not to use these solid residues would also mean forfeiting a portion of the glass fibers. This demonstrates the importance of refraining from further cleaning operations on the fibers and of reusing the solid residues in the production of new BMC composites, thereby promoting more effective utilization of the recovered materials.

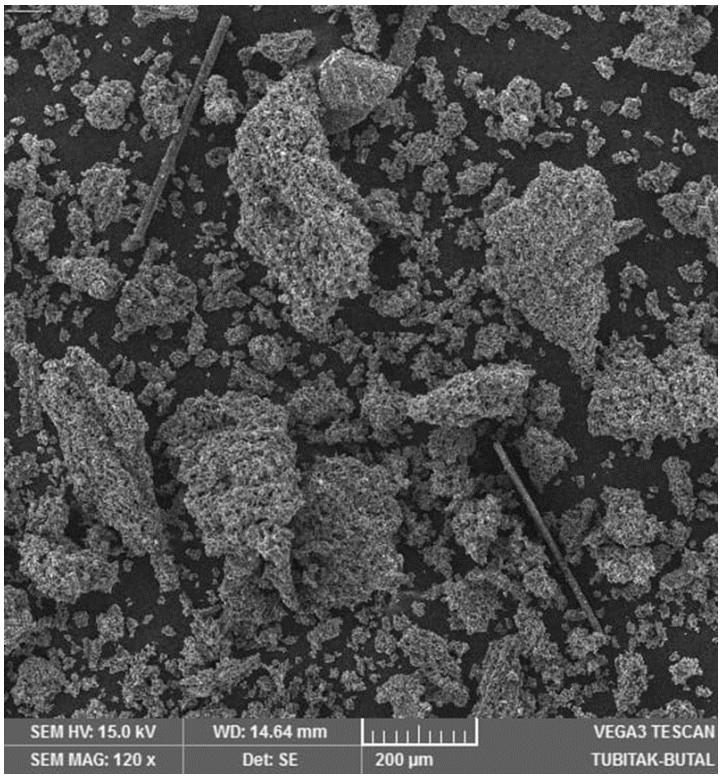

Figure 4.29. SEM image of solid residues after pilot-scale pyrolysis at 200 μm

4.2.4 Composition of Solid Residues After Pilot-Scale Pyrolysis Process

During the imaging of fibers subjected to pilot-scale pyrolysis, energy dispersive X-ray analysis (EDX) data were also collected. The results of this analysis are shown in Figure 4.30. High concentrations of Si, O, and Ca were detected at the points analyzed on the fiber surfaces. These findings are similar to those from the laboratory-scale processes, which confirms the presence of glass fibers. Carbon was also detected on the fibers, However, because graphene papers were used during sample preparation for the analysis, it would not be appropriate to draw conclusions about the carbon content.

In addition, elements such as Al and Br were observed on the fibers, and Mg, and Ti were detected in the solid residues. These are likely derived from other filler materials originally present in the SMC composite. The solid residues were also examined by EDX (Figure 4.31). Consistent high levels of Ca and O confirm the presence of calcium-rich residues.

The FTIR spectrum (Figure 4.32) showed the calcium carbonate ($CaCO_3$) in the residue dominantly, as indicated by characteristic transmittance peaks between 1400 - 1500 cm^{-1} and 700 - 900 cm^{-1}, specifically at 1415 cm^{-1} and 873 cm^{-1}. [118]

Broad absorption in the 1000–1100 cm^{-1} range showed the presence of silicate phases, therefore, the contribution of glass fiber components to the residue. [119]

The absence of peaks in the 2800–3000 cm^{-1} range, which shows the C–H stretching in organic compounds, highlights the decomposition of the polymer matrix, leaving no significant organic residues. [120]

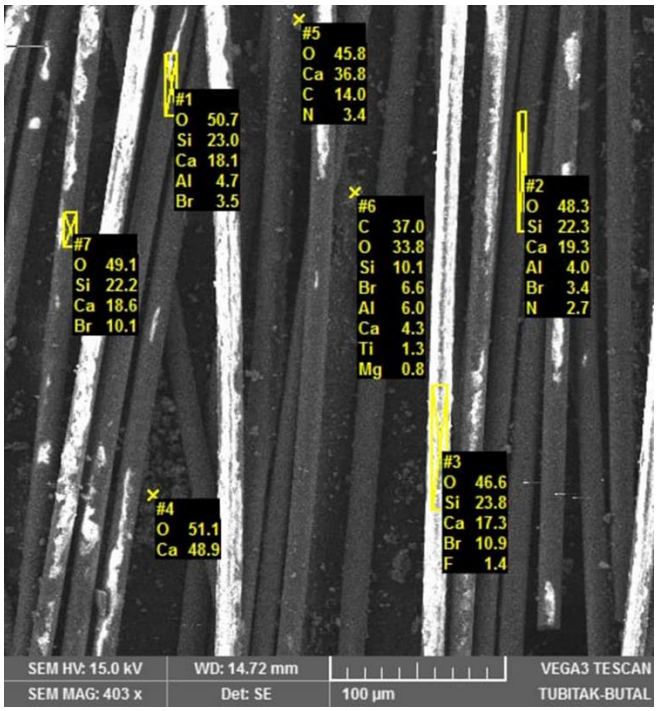

Figure 4.30. SEM-EDX image of glass fibers after pilot-scale pyrolysis at 100 µm

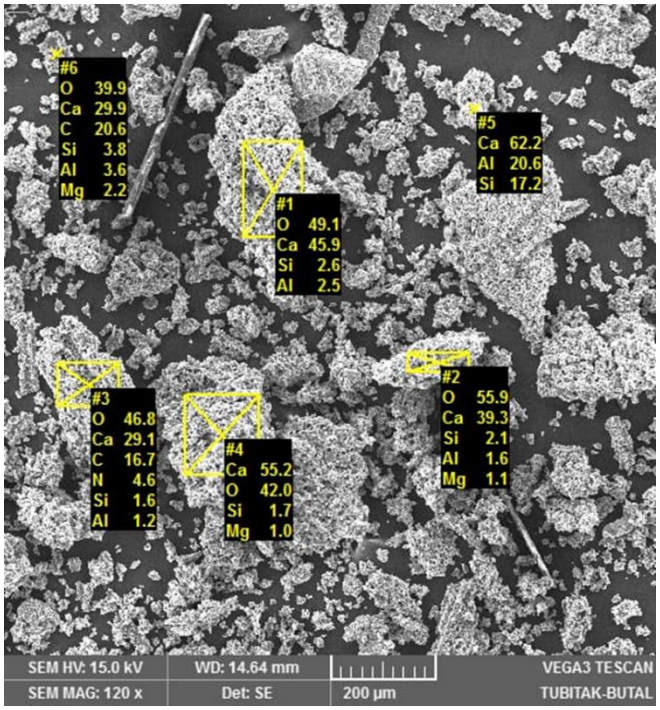

Figure 4.31. SEM-EDX image of solid residues after pilot-scale pyrolysis at 100 µm

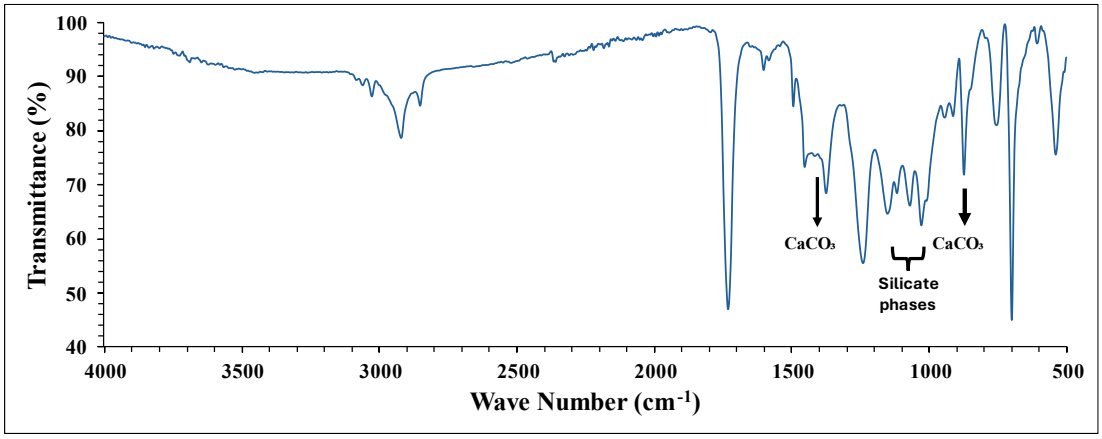

Figure 4.32. FTIR Spectrum for solid residue obtained after pilot-scale pyrolysis

Upon examination of the DSC results, two minor endothermic events were observed at 53.5 °C and 76.0 °C. These transitions are thought to result from adsorbed moisture or trace residual volatiles. The absence of other endothermic or exothermic peaks indicates that the remaining materials are stable within this temperature range and do not undergo any phase changes. Consequently, no significant response was observed in the remaining samples besides these minor losses.

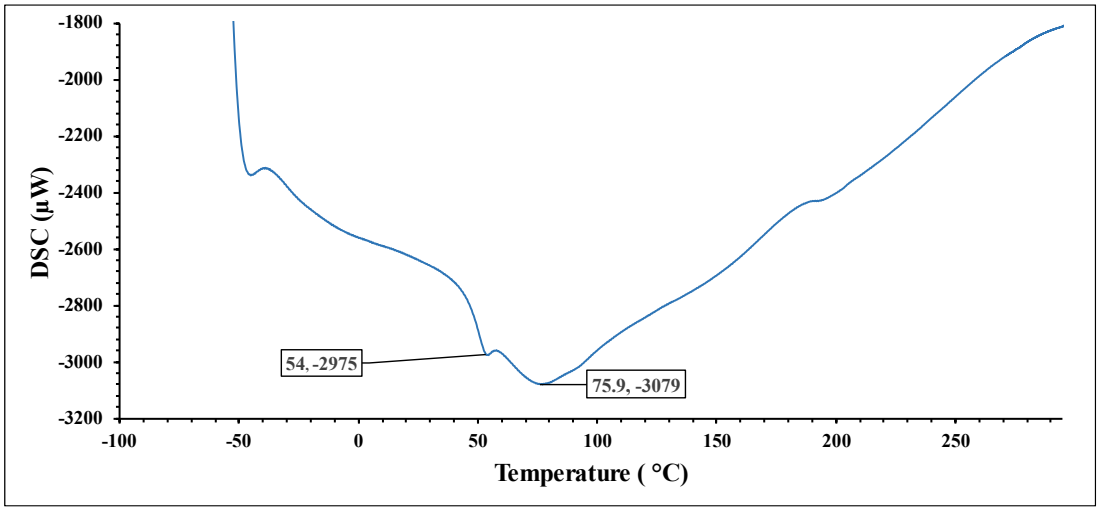

Figure 4.33. DSC Thermogram for solid residue obtained after pilot-scale pyrolysis

The burn-off or calcination test is used to determine the composition of glass fiber and inorganic fillers after burning all combustible products. Table 4.9 shows the remaining yield of the materials (wt% total weight before the test).

Table 4.9 Yields of glass fiber and mineral-fillers after burn-off tests

	Glass Fiber	**Mineral - Fillers**
Yield (% wt to mass before the test)	27.80 ± 0.45	39.40 ± 0.26

These results demonstrate that filler materials present in both the fibers and the solid residues remain similar to their original states used in composite production, and their presence is not expected to negatively affect the properties of new composites.

In addition, detailed analyses of the solid products, excluding the resulting glass fibers, were conducted. When the results of Energy Dispersive X-ray (EDX), Fourier-Transform Infrared Spectroscopy (FTIR), and Differential Scanning Calorimetry (DSC) analyses were interpreted together, it was concluded that there was no decomposition of calcium carbonate ($CaCO_3$). These results corroborate the findings from X-ray Fluorescence (XRF) and X-ray Diffraction (XRD) analyses conducted at the laboratory scale, where, due to the lower temperatures, $CaCO_3$ decomposition was expected to be minimal.

Thus, the process, theoretically limited to 600°C, increased the yield of liquid products while simultaneously preventing degradation in the solid products formed. The intended outcomes prior to the process were successfully achieved.

4.2.5 Mechanical Behavior of Recycled BMC Composites Produced from Pilot-Scale Recycling Process

After the pilot-scale pyrolysis process, recycled bulk molding compound (BMC) composites were produced using glass fibers and solid residues in specific compositions. These recycled BMC composites were subjected to mechanical tests.

Although the pyrolysis samples showed some degradation in their properties, no dramatic decreases were observed. These reductions and the mechanical

performance are believed to result from the weakening of the fibers due to the pyrolysis process. [33,90,92,115]

Even though the results were similar, the BMC-P10 composite produced with 10% recycled product demonstrated better performance than the others. Beyond 10%, the decline in mechanical properties was not solely due to the pyrolysis process. It was also attributed to the longer length of the added recycled fibers compared to the standard BMC fibers. [33] Typically, BMC doughs are produced with fibers ranging from 2 to 6 mm long, whereas the fibers resulting from the process (Figure 4.26) exceed nearly 30 mm. This increased length hinders fibers' homogeneous distribution and wetting during standard BMC preparation. It is believed that the high standard deviations in the results are also due to this factor. Additionally, extending the mixing times to mitigate this issue causes damage to the fibers, leading to further declines in mechanical properties. [33]

De Marco's study found the optimal result to be 6%. Still, it is believed that the differences in sample sizes and the glass fiber content in the produced composites influenced this outcome. [33]

Composites were compared by replacing 5% of the $CaCO_3$ filler material with 0.75% virgin fiber and 4.75% virgin $CaCO_3$ in BMC-C1, adding 5% virgin fiber in BMC-C2, adding 5% virgin $CaCO_3$ filler in BMC-C3, and adding 5% recycled product in BMC-P5. The comparisons revealed that reducing the glass fiber content by adding filler materials worsened the mechanical properties, whereas adding recycled products yielded better results than adding virgin fillers. The similar trend was observed in BMC-C1. Tensile strength test results were particularly distinguished in this regard.

When examining other mechanical properties, it was found that the composites produced by mixing control groups and products processed through pyrolysis did not differ dramatically. Only in flexural properties were superior results observed. However, considering the longer fiber lengths mentioned above and the high standard deviations in these tests, similar results to the original material are expected

to be obtained. Therefore, after being assessed according to their application areas, these recycled composites can potentially replace virgin BMC. Parts that do not require high mechanical strength, such as interior cabin and user-interface components, will be suitable for initial trials. The component to be selected in the next phase has been chosen with this understanding.

Table 4.10 Mechanical testing results of produced BMC samples in different composition

	BMC-ST2	**BMC-C1**	**BMC-C2**	**BMC-C3**	**BMC-P5**	**BMC-P10**	**BMC-P15**
Tensile Strength (MN/m²)	25 ± 2	25 ± 4	23 ± 4	18 ± 2	19 ± 2	19 ± 3	18 ± 2
Tensile Modulus (GN/m²)	72 ± 2	72 ± 2	76 ± 2	69 ± 1	72 ± 1	78 ± 2	77 ± 1
Flexural Strength (MN/m²)	67 ± 2	70 ± 5	67 ± 4	62 ± 2	67 ± 6	76 ± 6	65 ± 6
Flexural Modulus (GN/m²)	81 ± 3	81 ± 2	81 ± 2	75 ± 3	82 ± 4	91 ± 4	87 ± 5
Unnotched Charpy Impact Strength (kJ/m²)	23 ± 1	20 ± 3	21 ± 3	14 ± 1	18 ± 1	22 ± 2	19 ± 3
Barcol Hardness	65 ± 3	60 ± 2	63 ± 2	62 ± 1	66 ± 2	69 ± 3	66 ± 3

4.2.6 Liquid Products Obtained from Pilot-Scale Scale Recycling Process

The liquid products obtained from pilot-scale pyrolysis were first subjected to bomb calorimetry tests to measure their calorific value. These tests yielded a GCV (gross calorific value) of 8078 ± 182 kcal/kg, corresponding to 33.82 ± 0.76 MJ/kg. This

value aligns with findings in the literature, notably Torres [117], and is nearly identical to results reported by Cunliffe. [21]

Although this value appears low compared to other hydrocarbon fuels, it is sufficiently high to be considered a viable fuel. [21] Moreover, it closely approaches that of commercial No. 1 fuel oil (ASTM 240). [117] Given its calorific potential, one potential application involves reintroducing these liquids into the process, making it more self-sustaining. Alternatively, they could be employed in various heating applications, contributing to recycling efforts.

A GC/MS analysis was also performed on these liquid products to understand their composition better. According to studies in the literature, this liquid is a complex mixture of organic compounds containing 5 to 21 carbons, with molecular weights ranging from 86 to 324. It primarily consists of aromatic compounds and contains numerous oxygenated compounds, such as ketones, carboxylic acids, alkylbenzenes, among others. [21,94,117]

Table 4.11 GC/MS results for liquids obtained from pilot-scale pyrolysis process

Peak No.	Retention Time	Area (%)	Library/ID
1	2.77	3.85	Acetic Acid
2	2.96	3.41	Acetic Acid
3	4.93	3.87	Toluene
4	8.35	5.72	Ethylbenzene
5	9.7	19.35	Styrene
6	12.91	7.18	α-Methylstyrene-
7	14.71	3.44	1,2-Propanediol, Diacetate
8	15.82	3.09	Acetophenone
9	22.37	0.75	Naphthalene, 2-Methyl
10	27.43	6.22	Benzene, 1,1'-(1,3-Propanediyl)bis

The liquid products obtained from the pilot-scale pyrolysis were analyzed at TÜBİTAK MAM using GC/MS. During this analysis, the abundance peaks and their areas were compared against the same institution's library, enabling an estimation of the sample's composition and subsequent interpretation based on the matches obtained.

The results obtained are presented in Table 4.11. This table presents the significant area peaks. Appendix-A provides a complete list of all area peaks.

GC/MS analysis indicates that SMC material undergoes extensive breakdown into a range of pyrolysis products. The polyester-styrene matrix in SMC decomposes into various compounds, including aromatic hydrocarbons, organic acids, and anhydrides.

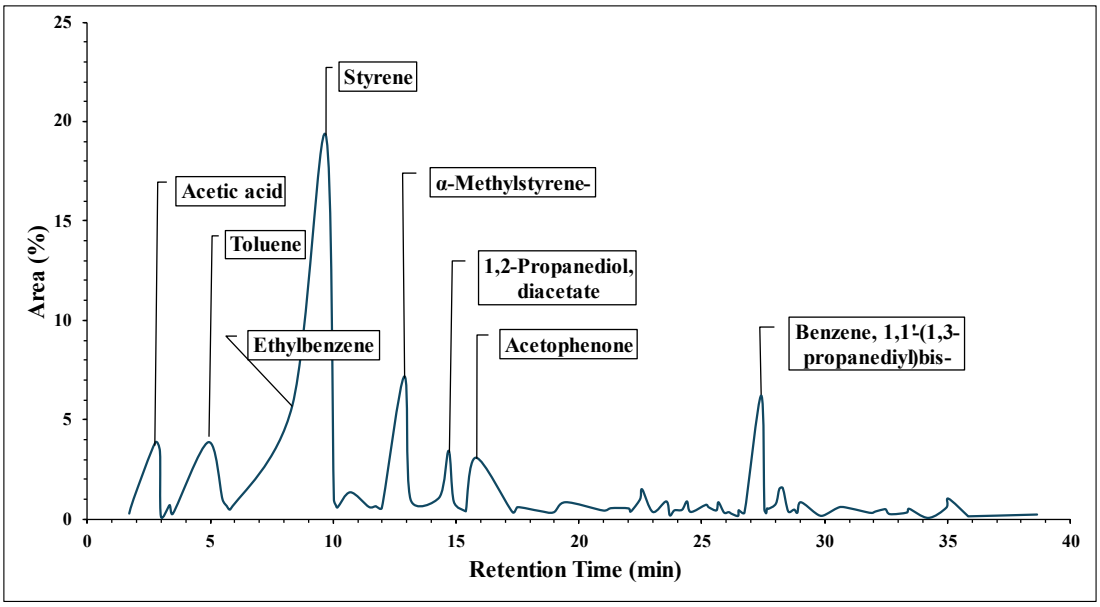

Figure 4.34. GC/MS area (%) peaks of liquid products

Upon reviewing the results, the most prominent finding is the dominance of styrene. This outcome aligns with the original composition of unsaturated polyester resins crosslinked with styrene monomers. The preservation of styrene in significant quantities suggests that controlled pyrolysis conditions can effectively depolymerize these resins while minimizing further degradation of the monomer.

The presence of aromatic hydrocarbons and high-molecular-weight products also indicates potential for use as chemical intermediates in industrial applications. Phthalic anhydride is believed to originate from polyester resin decomposition, offering prospects for new material production, such as alkyd resins, plasticizers, and coatings.

In summary, the products derived from SMC pyrolysis show potential for reuse. Process parameters can be adjusted and refined to meet specific application requirements, and if secondary treatments are employed after pyrolysis, the purity and economic viability of the resulting products may be enhanced.

4.2.7 Gaseous Products Obtained from Pilot-Scale Recycling Process

The gases produced in this thesis study were not analyzed. As mentioned in Chapter 2: Literature Review, the gases generated after this process mainly contain CO_2 and CO. [90] It can be said that these gases are produced both from the cracking of ester structures and, to a lesser extent, from the decomposition of $CaCO_3$ present in the filler materials. [92] De Marco's findings were also supported by Cunliffe's study, which revealed that the breakdown of hydroxyl groups, ether/ester bonds, and alkyl lining units is the leading cause of CO_X gases. [21]

The resulting gases' calorific value is low. However, they contain sufficient energy to sustain the process, and their utilization in this area would be logical. [92]

Considering these studies and their results, utilizing the resulting gases for system feedback would help reduce the process's energy consumption, thereby making the process more cost-effective and increasing the amount of recycled and subsequently used products obtained from the material. This would assist in achieving one of the objectives of this study, namely the circular economy.

4.3 Performance Testing of Produced Tractor Component from Recycled BMC

Considering the quantity and quality of the sample sent, and after discussions with the composite manufacturing company, a decision was made regarding the component to be produced with recycled material for use on the vehicle. As can be seen in Figure 4.35, the selected part is the rear hood service cover.

The reasons for choosing this part are that it is not very much large in terms of size, which can result to prototype production and tolerance problems; it is not a load-bearing component, so its mechanical strength requirements are low; and when used as a replacement for an SMC part, it offers advantages in terms of both cost and environmental sustainability.

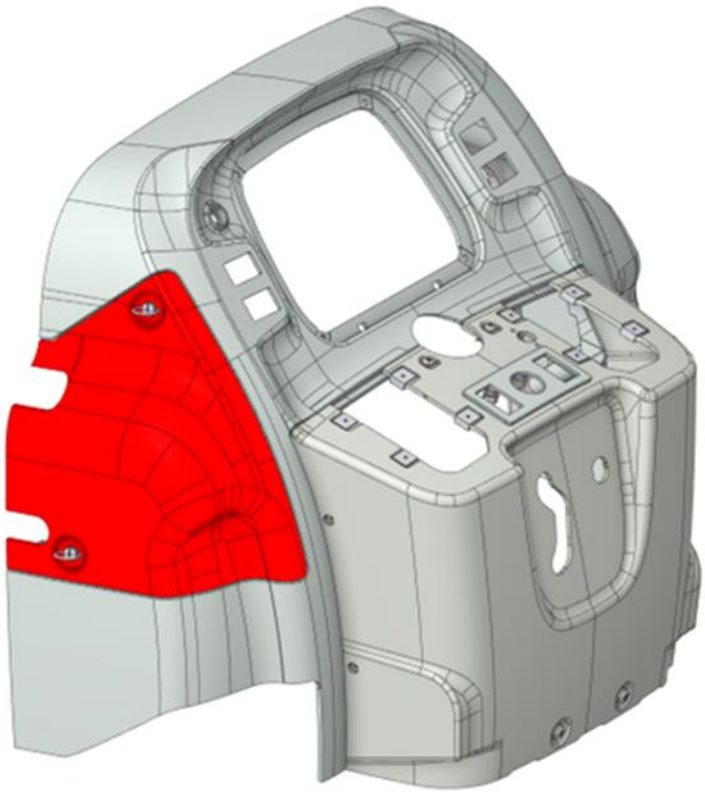

Figure 4.35. 3D geometry of the selected part (highlighted part with red coloring)

4.3.1 CAE Simulation and Analysis

Before being physically tested on the tractor, the produced tractor component was examined using computer-aided simulation and analysis programs.

A dynamic analysis was conducted during the evaluation, focusing on the type-step where stress values were the highest. The stress observed at this time step is shown in Figure 4.36. The stress in this area was approximately 10 MPa and was located around the connection points.

Since fatigue analysis for composite materials is an emerging field, the rule of thumb fatigue strength methodology was adopted for the evaluation. The peak stress observed did not exceed twice the material's tensile strength (which is approximately 20 MPa for BMC-P10), so this stage was evaluated positively.

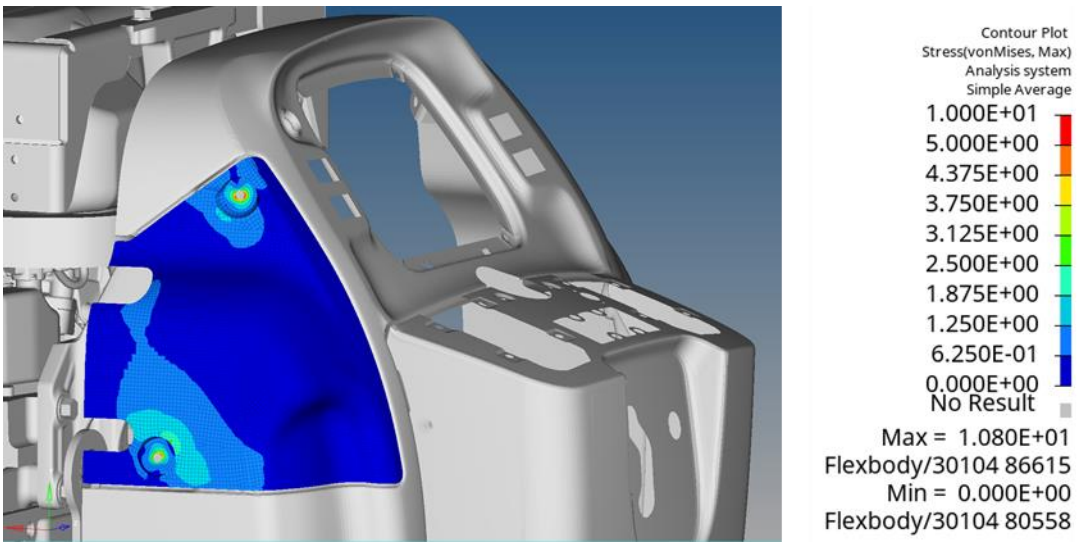

Figure 4.36. Simulation/Analysis result for the selected tractor part (Stress in MPa)

Additionally, a modal analysis and simulation were performed, and the results can be seen in Table 4.12. According to these results, the lowest mode was 39 Hz. One of the passing criteria for tractor parts is that, although not highly rigid, they are

expected to be above 10 Hz generally, except in exceptional cases. Based on this criterion, the part also received a successful result from this evaluation and was produced as a prototype for physical bump testing, where it also passed the test.

Table 4.12 Modal analysis result for the selected tractor part

Mode No	**Frequency (Hz)**	***Mode No***	**Frequency (Hz)**	***Mode No***	**Frequency (Hz)**	***Mode No***	**Frequency (Hz)**
1	39	***6***	118	***11***	196	***16***	331
2	46	***7***	124	***12***	226	***17***	341
3	74	***8***	143	***13***	257	***18***	349
4	89	***9***	157	***14***	274	***19***	365
5	96	***10***	171	***15***	309	***20***	380

4.3.2 Bump Test

The part, which was analyzed and simulated in a computer environment, was mounted on a prototype tractor after being manufactured by CTP Composite to enable physical fatigue tests and to observe its behavior during physical use. During this process, attention was paid to the fit of the part and whether there were any difficulties in mounting it. No difficulties were observed. Subsequently, the tractor connected to the bump test device underwent 40,000 cycles, initially with both wheels together for 20,000 cycles and then with the right and left wheels separately for 10,000 cycles each. Upon examination of the part after testing, no deformation, cracks, or breaks were observed. Thus, it was concluded that there were no issues with using the part in prototype tractors. Photos of the test and the part can be seen in Figure 4.37 and Figure 4.38.

Figure 4.37. Tractor component produced with recycled BMC. a) by itself, b) on the tractor

Figure 4.38. Tractor mounted on the bump test mechanism

CHAPTER 5

CONCLUSION

Plastics continue to permeate new areas of our daily lives with each passing day, and in parallel, composites are steadily gaining prominence across many industrial sectors. Their cost-effectiveness enables them to replace metals and ceramics in a wide range of applications, and the ability to tailor them for specific uses further enhances their appeal. Among these composites, thermoset composites are popular in sectors from automotive to aerospace, because of their superior mechanical properties and capacity for customization according to end-use requirements.

However, one significant drawback of thermoset composites is that, unlike thermoplastic composites, they cannot be reused or recycled. Although incineration and landfilling are viable waste management techniques, both have environmental hazards. They can also be mechanically ground for use as low-grade filler material, however this is not the best option because of material value loss. Regulations in the United States and Europe are increasing pressure on companies to be more diligent in this regard.

This study developed a process for recycling and reusing sheet molding compound (SMC), a thermoset composite commonly employed in the automotive sector. SMC materials are collected as scrap during tractor production or at the end of a tractor's service life. Thermal recycling methods involving pyrolysis, oxidation, and pyrolysis followed by oxidation were tested on a laboratory-scale. Alongside a literature review, TG-DTA-DTG analysis was conducted to understand the decomposition characteristics of the material and to determine suitable process parameters, identifying 500 °C as the optimal target temperature.

At this stage, only solid products, fiberglass, and other solid residues were collected and characterized using SEM, XRF, and XRD. Samples from each process were

incorporated into Bulk Molding Compound (BMC) paste by partially substituting $CaCO_3$, producing composite plates. These plates were subjected to mechanical tests and compared with both standard BMC and one another. Considering characterization results, mechanical tests, and literature data, pyrolysis was chosen as the primary method. Additionally, the plates underwent painting and serigraphy trials to evaluate surface-dependent applications and potential usage areas, demonstrating no issues and indicating that surface properties would not limit their applications.

Next, the fiberglass obtained from pyrolysis was subjected to mechanical, water-based, and hydrochloric acid cleaning and then examined via optical microscopy. However, this cleaning process was neither successful nor deemed essential, and ultimately, the decision was made to proceed without further cleaning.

A pilot-scale process was established in the second phase, creating a system between laboratory and serial production scales. This setup increased the amount of solid product obtained per run, allowed the collection of liquid products through a condenser, and accelerated throughput by adhering more closely to serial production protocols—mitigating supply and system delays. Because liquid products could now be collected, new process parameters were explored to enhance liquid yield. In determining these parameters, literature findings and TGA analyses were employed to examine decomposition behavior in the waste materials. The aim was to stay within the highest possible temperature (600°C) at which $CaCO_3$ does not decompose into CaO or CO_2. Moreover, after processing, observations revealed a shift from an orange-colored gas to a whiter smoke, suggesting the complete removal of organic compounds.

Following this stage, the resulting solid products were studied with SEM and characterized using EDX, FTIR, and DSC, confirming that $CaCO_3$ remained intact. These solids were then incorporated into BMC paste at 5%, 10%, and 15% by weight, replacing $CaCO_3$ in equal proportion. Mechanical tests indicated that the recycled BMC composites did not exhibit dramatically poorer performance than

virgin BMC, making them viable substitutes. Ten percent emerged as the optimal proportion, as going beyond this level hinders homogeneity, and extending mixing time to achieve homogeneity can damage the fibers, observations consistent with prior literature.

At this stage, the liquid products were analyzed by GC-MS and bomb calorimeter, revealing their potential as fuels or feedstock for other material production processes. Although gaseous products could not be collected, a literature review suggested they could be harnessed to power the ongoing process, thereby reducing operational costs.

Finally, using 10% of the glass fibers and solid products obtained from the pilot-scale pyrolysis process, a tractor component was fabricated from BMC composite and tested on an actual tractor. In addition to physical tests, CAE analysis and simulation were performed using the mechanical properties determined in earlier testing, confirming that the part was suitable for in-vehicle use. Consequently, this research demonstrates a recycling pathway for a thermoset material via pyrolysis, establishing means for reusing the resulting solid, liquid, and gaseous products. It completes the product loop, representing a crucial step toward a circular economy and sustainable production.

REFERENCES

[1] M. Geissdoerfer, P. Savaget, N.M.P. Bocken, E.J. Hultink, The Circular Economy – A new sustainability paradigm?, J Clean Prod 143 (2017) 757–768. https://doi.org/10.1016/j.jclepro.2016.12.048.

[2] C. Podara, S. Termine, M. Modestou, D. Semitekolos, C. Tsirogiannis, M. Karamitrou, A.F. Trompeta, T.K. Milickovic, C. Charitidis, Recent Trends of Recycling and Upcycling of Polymers and Composites: A Comprehensive Review, Recycling 9 (2024). https://doi.org/10.3390/recycling9030037.

[3] R. Geyer, J.R. Jambeck, K.L. Law, Production, use, and fate of all plastics ever made, Sci Adv 3 (2017). https://doi.org/10.1126/sciadv.1700782.

[4] Plastics – the fast Facts 2023, 2023. https://plasticseurope.org/knowledge-hub/plastics-the-fast-facts-2023/ (accessed November 23, 2024).

[5] C. of the E.U. European Parliament, Directive 2008/98/EC of the European Parliament and of the Council of 19 November 2008 on waste and repealing certain Directives (Text with EEA relevance), Official Journal of the European Union (2008).

[6] C. of the E.U. European Parliament, Directive 2000/53/EC of the European Parliament and of the Council of 18 September 2000 on end-of life vehicles - Commission Statements, Official Journal L 269 , 21/10/2000 P. 0034 - 0043 (2000).

[7] United States Congress, Resource Conservation and Recovery Act, (1976).

[8] TürkTraktör, TürkTraktör: Leader of the Market for 17 Years in a Row, (n.d.). https://www.turktraktor.com.tr/about-us/our-news/2024/turktraktor-leader-of-the-market-for-17-years-in-a-row (accessed November 24, 2024).

[9] TürkTraktör, Our Shareholders, (n.d.). https://www.turktraktor.com.tr/about-us/our-shareholders (accessed November 24, 2024).

[10] Koç Holding, Koç Holding Launches the “Carbon Transition Program” in Line with its Goal to Become Carbon Neutral by 2050, (2021). https://www.koc.com.tr/media-center/latest-news/2021/koc-holding-launches-carbon-transition-program (accessed November 24, 2024).

[11] CNH Industrial, CNH Sustainability Report 2023, 2024.

[12] TurkTraktor Sustainability Report 2023, 2024. https://www.turktraktor.com.tr/sustainability/sustainability-reports (accessed November 23, 2024).

[13] F.C. Campbell, Introduction to Composite Materials, in: Structural Composite Materials, ASM International, 2010: pp. 1–29. https://doi.org/10.31399/asm.tb.scm.t52870001.

[14] A.K. Sharma, R. Bhandari, A. Aherwar, R. Rimašauskienė, Matrix materials used in composites: A comprehensive study, Mater Today Proc 21 (2020) 1559–1562. https://doi.org/10.1016/j.matpr.2019.11.086.

[15] B. De, M. Bera, D. Bhattacharjee, B.C. Ray, S. Mukherjee, A comprehensive review on fiber-reinforced polymer composites: Raw materials to applications, recycling, and waste management, Prog Mater Sci 146 (2024). https://doi.org/10.1016/j.pmatsci.2024.101326.

[16] S. Erden, K. Ho, Fiber reinforced composites, in: Fiber Technology for Fiber-Reinforced Composites, Elsevier, 2017: pp. 51–79. https://doi.org/10.1016/B978-0-08-101871-2.00003-5.

[17] A. MIDOUN, H. BENAHMED, S. KHALDI, Contribution to the analysis of thermal behaviour of polymer composites: case of polyethylene/titanium diboride composites, Bulletin of Materials Science 47 (2024) 272. https://doi.org/10.1007/s12034-024-03361-7.

[18] F.W. Billmeyer, Textbook of Polymer Science, 3rd Edition, 3rd ed., 1984.

[19] M.A. Karim, M.Z. Abdullah, T. Ahmed, AN OVERVIEW: THE PROCESSING METHODS OF FIBER-REINFORCED POLYMERS (FRPS), INTERNATIONAL JOURNAL OF MECHANICAL ENGINEERING AND TECHNOLOGY (IJMET) 12 (2021). https://doi.org/10.34218/IJMET.12.2.2021.002.

[20] C.E. Bakis, L.C. Bank, V.L. Brown, E. Cosenza, J.F. Davalos, J.J. Lesko, A. Machida, S.H. Rizkalla, T.C. Triantafillou, Fiber-Reinforced Polymer Composites for Construction—State-of-the-Art Review, Journal of Composites for Construction 6 (2002) 73–87. https://doi.org/10.1061/(ASCE)1090-0268(2002)6:2(73).

[21] A.M. Cunliffe, N. Jones, P.T. Williams, Recycling of fibre-reinforced polymeric waste by pyrolysis: Thermo-gravimetric and bench-scale investigations, J Anal Appl Pyrolysis 70 (2003) 315–338. https://doi.org/10.1016/S0165-2370(02)00161-4.

[22] S. Karavida, A. Peponi, Wind Turbine Blade Waste Circularity Coupled with Urban Regeneration: A Conceptual Framework, Energies (Basel) 16 (2023) 1464. https://doi.org/10.3390/en16031464.

[23] T. Sathishkumar, S. Satheeshkumar, J. Naveen, Glass fiber-reinforced polymer composites – a review, Journal of Reinforced Plastics and Composites 33 (2014) 1258–1275. https://doi.org/10.1177/0731684414530790.

[24] D.K. Rajak, P.H. Wagh, E. Linul, Manufacturing Technologies of Carbon/Glass Fiber-Reinforced Polymer Composites and Their Properties: A Review, Polymers (Basel) 13 (2021) 3721. https://doi.org/10.3390/polym13213721.

[25] M. Altin Karataş, H. Gökkaya, A review on machinability of carbon fiber reinforced polymer (CFRP) and glass fiber reinforced polymer (GFRP)

composite materials, Defence Technology 14 (2018) 318–326. https://doi.org/10.1016/j.dt.2018.02.001.

[26] S. Gharde, B. Kandasubramanian, Mechanothermal and chemical recycling methodologies for the Fibre Reinforced Plastic (FRP), Environ Technol Innov 14 (2019). https://doi.org/10.1016/j.eti.2019.01.005.

[27] H. Zheng, X. Zeng, J. Zhang, H. Sun, The Application of Carbon Fiber Composites in Cryotank, in: Solidification, InTech, 2018. https://doi.org/10.5772/intechopen.73127.

[28] M.S. Islam, L.F. Benninger, G. Pearce, C.-H. Wang, Toughening carbon fibre composites at cryogenic temperatures using low-thermal expansion nanoparticles, Compos Part A Appl Sci Manuf 150 (2021) 106613. https://doi.org/10.1016/j.compositesa.2021.106613.

[29] Y. Qiu, H. Yang, L. Tong, L. Wang, Research Progress of Cryogenic Materials for Storage and Transportation of Liquid Hydrogen, Metals (Basel) 11 (2021) 1101. https://doi.org/10.3390/met11071101.

[30] W. Han, J. Zhou, Q. Shi, Research progress on enhancement mechanism and mechanical properties of FRP composites reinforced with graphene and carbon nanotubes, Alexandria Engineering Journal 64 (2023) 541–579. https://doi.org/10.1016/j.aej.2022.09.019.

[31] A.A. Rajhi, Mechanical Characterization of Hybrid Nano-Filled Glass/Epoxy Composites, Polymers (Basel) 14 (2022) 4852. https://doi.org/10.3390/polym14224852.

[32] L. Org´, P.J.J. Dumont, SHEET MOLDING COMPOUNDS, n.d.

[33] A. Torres, I. De Marco, B.M. Caballero, M.F. Laresgoiti, M.J. Chomón, G. Kondra, Recycling of the solid residue obtained from the pyrolysis of fiberglass polyester sheet molding compound, Advances in Polymer Technology 28 (2009) 141–149. https://doi.org/10.1002/adv.20150.

[34] L. Orgeas, P.J.J. Dumont, SHEET MOLDING COMPOUNDS, n.d.

[35] E. Moritzer, M. Scholle, The main factors influencing glass fiber length reduction in the processing of bulk molding compounds (BMC), in: 2024: p. 040003. https://doi.org/10.1063/5.0208080.

[36] D. Bryce, L. Yang, R. Moradi, J. Thomason, DEVELOPMENT OF BULK MOULDING COMPOUNDS AND EXTRUSION COMPOUNDING PROCESSES USING RECYCLED GLASS FIBRES, n.d.

[37] M.C. Faudree, Y. Nishi, A New Double-Step Process of Shortening Fibers without Change in Molding Equipment Followed by Electron Beam to Strengthen Short Glass Fiber Reinforced Polyester BMC, Materials 17 (2024) 2036. https://doi.org/10.3390/ma17092036.

[38] M. Ribeiro, A. Fiúza, A. Ferreira, M. Dinis, A. Meira Castro, J. Meixedo, M. Alvim, Recycling Approach towards Sustainability Advance of Composite Materials' Industry, Recycling 1 (2016) 178–193. https://doi.org/10.3390/recycling1010178.

[39] W. Post, A. Susa, R. Blaauw, K. Molenveld, R.J.I. Knoop, A Review on the Potential and Limitations of Recyclable Thermosets for Structural Applications, Polymer Reviews 60 (2020) 359–388. https://doi.org/10.1080/15583724.2019.1673406.

[40] E. Guzman Maldonado, N. Bigot, Y. Denis, N. Hamila, Thermomechanical modeling and experimental characterization of continuous fiber-reinforced thermoplastic composites at forming temperatures, in: Advanced Structural Textile Composites Forming, Elsevier, 2025: pp. 355–388. https://doi.org/10.1016/B978-0-443-21578-0.00015-9.

[41] M. Biron, Thermoplastic Composites, in: Thermoplastics and Thermoplastic Composites, Elsevier, 2018: pp. 821–882. https://doi.org/10.1016/B978-0-08-102501-7.00006-0.

[42] A.R. Bunsell, J. Renard, Fundamentals of Fibre Reinforced Composite Materials, CRC Press, 2005. https://doi.org/10.1201/9781420056969.

[43] A. Kumar, S. Dixit, S. Singh, S. Sreenivasa, P.S. Bains, R. Sharma, Recent developments in the mechanical properties and recycling of fiber-reinforced polymer composites, Polym Compos (2024). https://doi.org/10.1002/pc.29261.

[44] Q. Hu, Y. Feng, C. Fang, Y. Wang, L. Yang, Z. Xu, Y. Fu, Y. Chen, F. Ruan, X. Shi, Performance evaluation of glass fiber reinforced thermoplastic composites prepared via the co-wrapping method, Mater Lett 379 (2025) 137624. https://doi.org/10.1016/j.matlet.2024.137624.

[45] M. Hitesh Kumar, P. Mohandoss, L. Anjana, Investigation on tensile and creep behaviour of glass fiber reinforced polymer (GFRP) bars: A review, Mater Today Proc (2023). https://doi.org/10.1016/j.matpr.2023.04.656.

[46] V. Kumar, R. Bedi, M. Kumar, The fatigue of carbon fiber reinforced polymer composites – A review, Mater Today Proc (2024). https://doi.org/10.1016/j.matpr.2024.06.004.

[47] S. Sathees Kumar, B. Sridhar Babu, Ch.N. Chankravarthy, N. Prabhakar, Review on natural fiber polymer composites, Mater Today Proc 46 (2021) 777–782. https://doi.org/10.1016/j.matpr.2020.12.599.

[48] R.A. Reddy, K. Yoganandam, V. Mohanavel, Effect of chemical treatment on natural fiber for use in fiber reinforced composites – Review, Mater Today Proc 33 (2020) 2996–2999. https://doi.org/10.1016/j.matpr.2020.02.982.

[49] N. Saba, M. Jawaid, M.T.H. Sultan, An overview of mechanical and physical testing of composite materials, in: Mechanical and Physical Testing of Biocomposites, Fibre-Reinforced Composites and Hybrid Composites, Elsevier, 2019: pp. 1–12. https://doi.org/10.1016/B978-0-08-102292-4.00001-1.

[50] A. Ballo, T. Närhi, Biocompatibility of fiber-reinforced composites for dental applications, in: Biocompatibility of Dental Biomaterials, Elsevier, 2017: pp. 23–39. https://doi.org/10.1016/B978-0-08-100884-3.00003-5.

[51] P. Sai Shravan Kumar, K. Viswanath Allamraju, A Review Of Natural Fiber Composites [Jute, Sisal, Kenaf], Mater Today Proc 18 (2019) 2556–2562. https://doi.org/10.1016/j.matpr.2019.07.113.

[52] L. Wang, X. Gao, D. Wang, H. Shang, Y. Zhao, B. Zhang, Nickel-carbon composites toward supercapacitor and self-charging systems: A review, Fuel 381 (2025) 133639. https://doi.org/10.1016/j.fuel.2024.133639.

[53] M.R.H. Mazumder, P. Govindaraj, N. Salim, D. Antiohos, F.K. Fuss, N. Hameed, Digitalization of composite manufacturing using nanomaterials based piezoresistive sensors, Compos Part A Appl Sci Manuf 188 (2025) 108578. https://doi.org/10.1016/j.compositesa.2024.108578.

[54] R.A. Laghari, M. Jamil, A.A. Laghari, A.M. Khan, Material characteristics and machinability of metal matrix composite materials: A critical review on recent advances and future perspectives, Measurement 242 (2025) 115839. https://doi.org/10.1016/j.measurement.2024.115839.

[55] M. Ma, J. Chen, L. Dong, Y. Su, S. Tian, Y. Zhou, M. Li, Polyoxometalates and their composites for antimicrobial applications: Advances, mechanisms and future prospects, J Inorg Biochem 262 (2025) 112739. https://doi.org/10.1016/j.jinorgbio.2024.112739.

[56] Q. Huang, L. Sheng, T. Wu, L. Huang, J. Yan, M. Li, Z. Chen, H. Zhang, Research progress on the application of carbon-based composites in capacitive deionization technology, Desalination 593 (2025) 118197. https://doi.org/10.1016/j.desal.2024.118197.

[57] J. Li, T. Guan, Z. Zhang, Y.-T. Fu, F.-L. Guo, P. Huang, Z. Li, Y.-Q. Li, S.-Y. Fu, Orientation of discontinuous fillers in polymer composites:

modelling, characterization, control and applications, Prog Mater Sci 148 (2025) 101360. https://doi.org/10.1016/j.pmatsci.2024.101360.

[58] J.-W. Zha, F. Wang, B. Wan, Polymer composites with high thermal conductivity: Theory, simulation, structure and interfacial regulation, Prog Mater Sci 148 (2025) 101362. https://doi.org/10.1016/j.pmatsci.2024.101362.

[59] V. Palani, A. Swain, Nonlinear vibration analysis of composite and functionally graded material shell structures: A literature review from 2013 to 2023, Int J Non Linear Mech 168 (2025) 104939. https://doi.org/10.1016/j.ijnonlinmec.2024.104939.

[60] S.F. Nabavi, H. Dalir, A review on laser-assisted manufacturing process of thermoset composites: A review of fundamentals, processes, scientific modelling, challenges and prospective, Opt Laser Technol 181 (2025) 111713. https://doi.org/10.1016/j.optlastec.2024.111713.

[61] X. Feng, X. Yuan, J. Zhou, K. An, F. Zhu, X. Wei, Y. Huang, J. Zhang, L. Chen, J. Liu, C. Li, J. Wei, A review: CNT/diamond composites prepared via CVD and its potential applications, Mater Sci Semicond Process 186 (2025) 109008. https://doi.org/10.1016/j.mssp.2024.109008.

[62] H. Prashanth Palani Velayuda Shanmugasundram, E. Jayamani, K.H. Soon, Review: Classification, theories, and methodologies concerning bio-based polymer dielectric composites, Renewable and Sustainable Energy Reviews 209 (2025) 115026. https://doi.org/10.1016/j.rser.2024.115026.

[63] S. Olhan, B. Antil, B.K. Behera, Repair technologies for structural polymeric composites: An automotive perspective, Compos Struct 352 (2025) 118711. https://doi.org/10.1016/j.compstruct.2024.118711.

[64] A.H. Iswanto, S.H. Lee, M.H. Hussin, T.S. Hamidon, M. Hajibeygi, H. Manurung, N.N. Solihat, P.R. Nurcahyani, M.A.R. Lubis, P. Antov, V. Savov, L. Kristak, J. Kawalerczyk, L.M. Osvaldová, S. Farid, R.

Selvasembian, W. Fatriasari, A comprehensive review of lignin-reinforced lignocellulosic composites: Enhancing fire resistance and reducing formaldehyde emission, Int J Biol Macromol 283 (2024) 137714. https://doi.org/10.1016/j.ijbiomac.2024.137714.

[65] M. K B, N. Abu Talip Yusof, K. Sudhakar, N. Zainol, N. Hasan, M.S. Abdul Karim, Development of sustainable polymer-based dielectric composites from agricultural waste: A review, Heliyon 10 (2024) e39118. https://doi.org/10.1016/j.heliyon.2024.e39118.

[66] H. Prashanth Palani Velayuda Shanmugasundram, E. Jayamani, K.H. Soon, Review: Classification, theories, and methodologies concerning bio-based polymer dielectric composites, Renewable and Sustainable Energy Reviews 209 (2025) 115026. https://doi.org/10.1016/j.rser.2024.115026.

[67] N. Rasool, W.N. Baba, S. Rafiq, U. Mirza, S. Maqsood, Macro and nano level intervention of reinforcing agents for production of novel edible whey composite films and their applications in food systems: A review, Food Chem 437 (2024) 137715. https://doi.org/10.1016/j.foodchem.2023.137715.

[68] A. Gupta, N. Puri, Recent advances in hydrogen production using metal organic frameworks and their composites, Int J Hydrogen Energy 78 (2024) 303–324. https://doi.org/10.1016/j.ijhydene.2024.06.126.

[69] B.-J. Kim, C.-B. Oh, J.S. Won, H.I. Lee, M.Y. Lee, S.H. Kwon, S.G. Lee, H. Park, D.G. Seong, J. Jeong, J.C. Kim, Development of high-toughness aerospace composites through polyethersulfone composition optimization and mass production applicability evaluation, Compos Part A Appl Sci Manuf 189 (2025) 108590. https://doi.org/10.1016/j.compositesa.2024.108590.

[70] Y. Yang, R. Boom, B. Irion, D.-J. van Heerden, P. Kuiper, H. de Wit, Recycling of composite materials, Chemical Engineering and Processing:

Process Intensification 51 (2012) 53–68. https://doi.org/10.1016/j.cep.2011.09.007.

[71] L. Grandi, REMANUFACTURING OF END-OF-LIFE COMPOSITES FROM MECHANICALLY RECYCLED GLASS FIBRES AND A STYRENE-FREE POLYESTER, 2016.

[72] W.H. Dresher, The age of fibers, JOM 21 (1969) 17–26. https://doi.org/10.1007/BF03378781.

[73] Introduction to Composite Materials Design, Third Edition, CRC Press, 2017. https://doi.org/10.1201/9781315296494.

[74] S. Dong, P. Zhou, Z. Ning, X. Wu, C. Li, G. Xian, Durability of carbon- and glass-fiber reinforced thermoplastic polymer composites: A literature review, Journal of Building Engineering 98 (2024) 111055. https://doi.org/10.1016/j.jobe.2024.111055.

[75] R. Binali, L.R. Ribeiro da Silva, D.Y. Pimenov, M. Kuntoğlu, A.R. Machado, E. Linul, A review on progress trends of machining of Carbon Fiber Reinforced Plastics, Journal of Materials Research and Technology 33 (2024) 4332–4359. https://doi.org/10.1016/j.jmrt.2024.10.050.

[76] A.Ç. Kılınç, C. Durmuşkahya, M.Ö. Seydibeyoğlu, Natural fibers, in: Fiber Technology for Fiber-Reinforced Composites, Elsevier, 2017: pp. 209–235. https://doi.org/10.1016/B978-0-08-101871-2.00010-2.

[77] V. Acar, F. Cakir, E. Alyamaç, M.Ö. Seydibeyoğlu, Basalt fibers, in: Fiber Technology for Fiber-Reinforced Composites, Elsevier, 2017: pp. 169–185. https://doi.org/10.1016/B978-0-08-101871-2.00008-4.

[78] N. Horzum, N. Arik, Y.B. Truong, Nanofibers for fiber-reinforced composites, in: Fiber Technology for Fiber-Reinforced Composites, Elsevier, 2017: pp. 251–275. https://doi.org/10.1016/B978-0-08-101871-2.00012-6.

[79] E. Yalamaç, M. Sutcu, S.B. Basturk, Ceramic fibers, in: Fiber Technology for Fiber-Reinforced Composites, Elsevier, 2017: pp. 187–207. https://doi.org/10.1016/B978-0-08-101871-2.00009-6.

[80] V. Beachley, X. Wen, Effect of electrospinning parameters on the nanofiber diameter and length, Materials Science and Engineering: C 29 (2009) 663–668. https://doi.org/10.1016/j.msec.2008.10.037.

[81] R.S. Kumar, Textiles for industrial applications., CRC Press, 2014.

[82] P. Venkateshwar Reddy, R.V. Saikumar Reddy, J. Lakshmana Rao, D. Mohana Krishnudu, P. Rajendra Prasad, An overview on natural fiber reinforced composites for structural and non-structural applications, Mater Today Proc 45 (2021) 6210–6215. https://doi.org/10.1016/j.matpr.2020.10.523.

[83] L. Kerni, S. Singh, A. Patnaik, N. Kumar, A review on natural fiber reinforced composites, Mater Today Proc 28 (2020) 1616–1621. https://doi.org/10.1016/j.matpr.2020.04.851.

[84] S.J. Pickering, Recycling Thermoset Composite Materials, in: Wiley Encyclopedia of Composites, Wiley, 2012: pp. 1–17. https://doi.org/10.1002/9781118097298.weoc214.

[85] S. V. Kanhere, V. Bermudez, A.A. Ogale, Carbon and glass fiber reinforced thermoplastic matrix composites, in: Fiber Reinforced Composites, Elsevier, 2021: pp. 273–306. https://doi.org/10.1016/B978-0-12-821090-1.00007-7.

[86] W.S. Khan, E. Asmatulu, Md.N. Uddin, R. Asmatulu, Recycling and reusing of thermoplastic and thermoset composites, in: Recycling and Reusing of Engineering Materials, Elsevier, 2022: pp. 141–161. https://doi.org/10.1016/B978-0-12-822461-8.00001-2.

[87] L. Martinez, Thermoset and Thermoplastic Composites ... What's the Difference?, INSTRON (2024).

[88] R. DeRosa, E. Telfeyan, J.S. Mayes, Current state of recycling sheet molding compounds and related materials, Journal of Thermoplastic Composite Materials 18 (2005) 219–240. https://doi.org/10.1177/0892705705045006.

[89] T. Hirai, Roll forming of SMC and TMC, considering the resin-fibre interface, Compos Struct 32 (1995) 541–548. https://doi.org/10.1016/0263-8223(95)00042-9.

[90] I. De Marco, J.A. Legarreta, M.F. Laresgoiti, A. Torres, J.F. Cambra, M.J. Chomón, B. Caballero, K. Gondra, Recycling of the products obtained in the pyrolysis of fibre-glass polyester SMC, Journal of Chemical Technology and Biotechnology 69 (1997) 187–192. https://doi.org/10.1002/(SICI)1097-4660(199706)69:2<187::AID-JCTB710>3.0.CO;2-T.

[91] W. David Graham, Molded Recycled SMC Parts 4 0 0 C O M M O N W E A L T H D R I V E , W A R R E N D A L E , P A 1 5 0 9 6-0 0 0 1 U, 1992.

[92] I. De Marco, B. Caballero, A. Torres, M.F. Laresgoiti, M.J. Chomón, M.A. Cabrero, Recycling polymeric wastes by means of pyrolysis, Journal of Chemical Technology and Biotechnology 77 (2002) 817–824. https://doi.org/10.1002/jctb.636.

[93] I. de Marco, B.M. Caballero, M.A. Cabrero, M.F. Laresgoiti, A. Torres, M.J. Chomón, Recycling of automobile shredder residues by means of pyrolysis, J Anal Appl Pyrolysis 79 (2007) 403–408. https://doi.org/10.1016/j.jaap.2006.12.002.

[94] A. Torres, I. De Marco, B.M. Caballero, M.F. Laresgoiti, M.A. Cabrero, M. Jesú S Chomó, GC-MS analysis of the liquid products obtained in the pyrolysis of fibre-glass polyester sheet moulding compound, 2000. www.elsevier.com/locate/jaap.

[95] A. Torres, I. De Marco, B.M. Caballero, M.F. Laresgoiti, J.A. Legarreta, M.A. Cabrero, A. González, M.J. Chomón, K. Gondra, Recycling by

pyrolysis of thermoset composites: characteristics of the liquid and gaseous fuels obtained, n.d. www.elsevier.com/locate/fuel.

[96] V. Austermann, J. Neuhaus, D. Schneider, R. Dahlmann, C. Hopmann, Investigation of the Mechanical Properties of Vinylester-Based Sheet Moulding Compound (SMC) Subject to Particle Recycling, Journal of Composites Science 6 (2022). https://doi.org/10.3390/jcs6030084.

[97] V. Austermann, J. Neuhaus, D. Schneider, R. Dahlmann, C. Hopmann, Investigation of the Mechanical Properties of Vinylester-Based Sheet Moulding Compound (SMC) Subject to Particle Recycling, Journal of Composites Science 6 (2022). https://doi.org/10.3390/jcs6030084.

[98] S. Utekar, S. V K, N. More, A. Rao, Comprehensive study of recycling of thermosetting polymer composites – Driving force, challenges and methods, Compos B Eng 207 (2021). https://doi.org/10.1016/j.compositesb.2020.108596.

[99] J.A.T. Palmer, Mechanical Recycling of Automotive Composites for Use as Reinforcement in Thermoset Composites, 2009.

[100] S.J. Pickering, Recycling technologies for thermoset composite materials—current status, Compos Part A Appl Sci Manuf 37 (2006) 1206–1215. https://doi.org/10.1016/j.compositesa.2005.05.030.

[101] R. Morales Ibarra, Recycling of thermosets and their composites, in: Thermosets: Structure, Properties, and Applications: Second Edition, Elsevier, 2018: pp. 639–666. https://doi.org/10.1016/B978-0-08-101021-1.00020-4.

[102] A.M. Cunliffe, P.T. Williams, Characterisation of products from the recycling of glass fibre reinforced polyester waste by pyrolysis, Fuel 82 (2003) 2223–2230. https://doi.org/10.1016/S0016-2361(03)00129-7.

[103] K. Radhakrishnan, P. Senthil Kumar, G. Rangasamy, L. Praveen Perumal, S. Sanaulla, S. Nilavendhan, V. Manivasagan, K. Saranya, A critical review on pyrolysis method as sustainable conversion of waste plastics into fuels, Fuel 337 (2023). https://doi.org/10.1016/j.fuel.2022.126890.

[104] M.A. Nahil, P.T. Williams, Recycling of carbon fibre reinforced polymeric waste for the production of activated carbon fibres, J Anal Appl Pyrolysis 91 (2011) 67–75. https://doi.org/10.1016/j.jaap.2011.01.005.

[105] S.H. Patel, K.E. Gonsalves, S.S. Stivala, L. Reich, D.H. Trivedi, Alternative procedures for the recycling of sheet molding compounds, Advances in Polymer Technology 12 (1993) 35–45. https://doi.org/10.1002/adv.1993.060120104.

[106] A.M. Cunliffe, N. Jones, P.T. Williams, Pyrolysis of composite plastic waste, Environmental Technology (United Kingdom) 24 (2003) 653–663. https://doi.org/10.1080/09593330309385599.

[107] R. Bottom, Thermogravimetric Analysis, in: Principles and Applications of Thermal Analysis, Wiley, 2008: pp. 87–118. https://doi.org/10.1002/9780470697702.ch3.

[108] S. Ray, R.P. Cooney, Thermal degradation of polymer and polymer composites, in: Handbook of Environmental Degradation Of Materials: Third Edition, Elsevier Inc., 2018: pp. 185–206. https://doi.org/10.1016/B978-0-323-52472-8.00009-5.

[109] D. Titus, E. James Jebaseelan Samuel, S.M. Roopan, Nanoparticle characterization techniques, in: Green Synthesis, Characterization and Applications of Nanoparticles, Elsevier, 2018: pp. 303–319. https://doi.org/10.1016/B978-0-08-102579-6.00012-5.

[110] A. Uda, S. Morita, Y. Ozaki, Thermal degradation of a poly(vinyl alcohol) film studied by multivariate curve resolution analysis, Polymer (Guildf) 54 (2013) 2130–2137. https://doi.org/10.1016/j.polymer.2013.02.030.

[111] H. Kuhn, D. Medlin, eds., Mechanical Testing and Evaluation, ASM International, 2000. https://doi.org/10.31399/asm.hb.v08.9781627081764.

[112] N. Saba, M. Jawaid, M.T.H. Sultan, An overview of mechanical and physical testing of composite materials, in: Mechanical and Physical Testing of Biocomposites, Fibre-Reinforced Composites and Hybrid Composites, Elsevier, 2019: pp. 1–12. https://doi.org/10.1016/B978-0-08-102292-4.00001-1.

[113] S. Kangde, V. Shitole, A.K. Sahu, Suspension Strain Correlation Using Flex Bodies in MBD, in: 2014. https://doi.org/10.4271/2014-01-0763.

[114] C. Wen, B. Xie, Z. Song, Z. Yang, N. Dong, J. Han, Q. Yang, J. Liu, Methodology for designing tractor accelerated structure tests for an indoor drum-type test bench, Biosyst Eng 205 (2021) 1–26. https://doi.org/10.1016/j.biosystemseng.2021.02.007.

[115] P.T. Williams, A. Cunliffe, N. Jones, Recovery of value-added products from the pyrolytic recycling of glass-fibre-reinforced composite plastic waste, Journal of the Energy Institute 78 (2005) 51–61. https://doi.org/10.1179/174602205X40504.

[116] R. DeRosa, E. Telfeyan, G. Gaustad, S. Mayes, Strength and microscopic investigation of unsaturated polyester BMC reinforced with SMC-recyclate, Journal of Thermoplastic Composite Materials 18 (2005) 333–349. https://doi.org/10.1177/0892705705049560.

[117] A. Torres, Recycling by pyrolysis of thermoset composites: characteristics of the liquid and gaseous fuels obtained, Fuel 79 (2000) 897–902. https://doi.org/10.1016/S0016-2361(99)00220-3.

[118] P. Pánek, B. Kostura, I. Čepeláková, I. Koutník, T. Tomšej, Pyrolysis of oil sludge with calcium-containing additive, J Anal Appl Pyrolysis 108 (2014) 274–283. https://doi.org/10.1016/j.jaap.2014.04.005.

[119] M.E. Simonsen, C. Sønderby, Z. Li, E.G. Søgaard, XPS and FT-IR investigation of silicate polymers, J Mater Sci 44 (2009) 2079–2088. https://doi.org/10.1007/s10853-009-3270-9.

[120] M.I. Loría-Bastarrachea, W. Herrera-Kao, J. V. Cauich-Rodríguez, J.M. Cervantes-Uc, H. Vázquez-Torres, A. Ávila-Ortega, A TG/FTIR study on the thermal degradation of poly(vinyl pyrrolidone), J Therm Anal Calorim 104 (2011) 737–742. https://doi.org/10.1007/s10973-010-1061-9.

APPENDICES

A. GC-MS Results

Table A.1 GC-MS Results

Peak No.	RT (min)	Area (%)	Library/ID
1	1.71	0.28	Acetone
2	1.89	1.02	2-Propen-1-ol
3	2.77	3.85	Acetic acid
4	2.96	3.41	Acetic acid
5	3	0.14	1-Butanol
6	3.36	0.71	Acetic acid, 2-propenyl ester
7	3.49	0.28	1,4-Dioxane
8	4.93	3.87	Toluene
9	5.51	0.98	1,3-Dioxolane, 2-ethyl-4-methyl-
10	5.68	0.66	Cyclopentanone
11	5.83	0.5	1,3-Dioxolane, 2-ethyl-4-methyl-
12	8.35	5.72	Ethylbenzene
13	9.7	19.35	Styrene
14	10.04	0.98	1,2-Propanediol, 2-acetate
15	10.12	0.7	1,2-Propanediol, 2-acetate
16	10.19	0.59	1,2-Propanediol, 2-acetate
17	10.71	1.35	Benzene, (1-methylethyl)-
18	11.47	0.61	Benzene, 1-ethenyl-2-methyl-
19	11.75	0.65	Benzene, propyl-
20	11.99	0.56	Benzaldehyde
21	12.91	7.18	α.-Methylstyrene
22	13.16	0.99	Phenol
23	14.33	1.09	Benzene, l-ethenyl-2-methyl-

Table A.1 (Cont'd)

24	14.71	3.44	1,2-Propanediol, diacetate
25	14.92	0.88	Benzene, 3-butenyl-
26	15.41	0.39	Benzene, (1-methylenep ropyl)-
27	15.82	3.09	Acetophenone
28	17.31	0.35	Benzene, (2-methyl-2-propenyl)-
29	17.51	0.6	3-Hexanol, 2,3-dimethyl-
30	18.41	0.41	2-Methylindene
31	18.98	0.34	1-Propanone, 1-phenyl-
32	19.47	0.85	Naphthalene
33	21.01	0.43	2-Butanone, 3-phenyl-
34	21.31	0.55	Benzoic acid, 2-propenyl ester
35	22.03	0.54	Naphthalene, 2-methyl-
36	22.11	0.37	Benzene, 1-cyclopenten-1-yl-
37	22.37	0.75	Naphthalene, 2-methyl-
38	22.52	1.06	Phthalic anhydride
39	22.59	1.49	Phthalic anhydride
40	23.02	0.36	2-Pentanone, 5-phenyl-
41	23.57	0.89	Naphthalene, 2-ethenyl-
42	23.71	0.19	1-Tetradecene
43	23.9	0.44	Diphenylmethane
44	24.21	0.47	Naphthalene, 2,7-dimethyl-
45	24.41	0.89	Diphenylmethane
46	24.56	0.36	Benzoic acid, methyl ester
47	25.18	0.72	1,1'-Biphenyl, 4-methyl-
48	25.29	0.6	1,1'-Biphenyl, 3-methyl-
49	25.61	0.44	Ethylene, 1,1-diphenyl-
50	25.69	0.85	Bibenzyl
51	25.92	0.33	Dibenzofuran
52	26.11	0.35	Benzene, (1-bromoethyl)-

Table A.1 (Cont'd)

53	26.24	0.26	Benzeneacetic acid, .alpha.-oxo-, ethyl ester
54	26.49	0.16	7-Hexadecene, (Z)-
55	26.52	0.45	1,1'-Biphenyl, 3,4'-dimethyl-
56	26.75	0.33	Benzene, 1-methyl-2-(2-phenylethenyl)-
57	27.43	6.22	Benzene, 1,1'-(1,3-propanediyl)bis-
58	27.56	0.49	Bicyclo[4.2.1]nona-2,4,7-triene, 7-phenyl-
59	27.63	0.29	2-Hydroxyfluorene
60	27.67	0.54	Benzene, 1,1'-(3-methyl-1-propene-1,3-diyl)bis-
61	27.73	0.52	Benzene, 1,1'-(1-methyl-1,3-propanediyl)bis-
62	28.03	0.78	1,2-Diphenylethylene
63	28.17	1.52	1-Benzyl-1,2,3-triazole
64	28.31	1.56	Bicyclo[4.2.1]nona-2,4,7-triene, 7-phenyl-
65	28.53	0.39	Benzene, 1,1'-(1,4-butanediyl)bis-
66	28.77	0.48	Benzene, 1,1'-(3-methyl-1-propene-1,3-diyl)bis-
67	28.9	0.32	Phenanthrene
68	29.04	0.85	Benzene, 1,1'-(3-methyl-1-propene-1,3-diyl)bis-
69	29.7	0.25	Benzene, 1-chloro-2,4-dinitro-
70	29.96	0.18	2-Heptadecanone
71	30.57	0.58	n-Hexadecanoic acid

Table A.1 (Cont'd)

72	30.86	0.59	Naphthalene, 2-phenyl-
73	31.65	0.37	1H-2-Pyrrolone, 4-methoxy-
74	31.93	0.31	2-Nonadecanone
75	32.1	0.39	Naphthalene, 2-(phenylmethyl)-
76	32.45	0.5	Octadecanoic acid
77	32.51	0.48	m-Terphenyl
78	32.67	0.25	1,1':3',1"-Terphenyl, 5'-methyl-
79	33.36	0.33	1,1':3',1"-Terphenyl, 5'-methyl-
80	33.45	0.52	Octadecanoic acid, 2-propenyl ester
81	34.23	0.06	Azetidine-2-carboxylic acid
82	34.96	0.57	Pregna-5,17(20)-dien-3-ol
83	35.05	1.03	Benzene, 1,1'-[1-(2,2-dimethyl-3-butenyl)-1,3-propanediyl]bis-
84	35.83	0.17	Butanedioic acid, dibutyl ester
85	35.86	0.14	2-Oxazolidinone, 3-methyl-
86	38.66	0.23	1,1':3',1"-Terphenyl, 5'-phenyl-

B. XRF SQX Calculation Results for Laboratory-Scale Recycling Processes

Table B.1 XRF SQX Calculation Result for Pyrolysis Products

No.	Component	Result (wt%)	Det.limit	El.line	Intensity	w/o normal
1	CaO	74.90	0.04367	Ca-KA	129.6149	44.9276
2	SiO_2	14.70	0.03798	Si-KA	10.5797	8.8203
3	Al_2O_3	4.40	0.02228	Al-KA	3.5896	2.6361
4	TiO_2	1.84	0.07157	Ti-KA	0.3675	1.1048
5	MgO	1.79	0.03539	Mg-KA	0.5951	1.0709
6	Fe_2O_3	0.82	0.02024	Fe-KA	1.0797	0.4927
7	ZnO	0.47	0.01286	Zn-KA	2.0538	0.2833
8	CuO	0.46	0.01339	Cu-KA	1.453	0.2751
9	SrO	0.24	0.00846	Sr-KA	3.6247	0.1462
10	SO_3	0.15	0.00867	S-KA	0.1873	0.0896
11	P_2O_5	0.11	0.00642	P-KA	0.188	0.0681
12	K_2O	0.11	0.00810	K-KA	0.3227	0.0628

Table B.2 XRF SQX Calculation Result for Oxidation Products

No.	Component	Result (wt%)	Det.limit	El.line	Intensity	w/o normal
1	CaO	90.80	0.01635	Ca-KA	1410.8238	51.0111
2	SiO_2	2.64	0.00589	Si-KA	16.7665	1.4855
3	MgO	2.08	0.01195	Mg-KA	5.6646	1.1666
4	TiO_2	1.87	0.03516	Ti-KA	2.5053	1.0503
5	Al_2O_3	0.91	0.00425	Al-KA	6.0907	0.5089
6	BaO	0.55	0.08741	Ba-KA	0.3319	0.3081
7	Fe_2O_3	0.50	0.00963	Fe-KA	4.3096	0.2792
8	ZnO	0.30	0.0051	Zn-KA	8.6719	0.1679
9	SrO	0.10	0.00345	Sr-KA	9.6273	0.0547
10	P_2O_5	0.10	0.0018	P-KA	1.5499	0.0544
11	SO_3	0.10	0.00269	S-KA	1.2003	0.0534
12	Cl	0.04	0.00397	Cl-KA	0.3337	0.0234
13	K_2O	0.02	0.00256	K-KA	0.6802	0.0125

C. XRD Peak Lists for Laboratory-Scale Recycling Processes

Table C.1 XRD Peak List for Pyrolysis Products

No.	2θ, °	Height, cps	FWHM, °	Int. I., cps°	Int. W., °	Size, Å
1	23.035(3)	9172(151)	0.150(2)	1758(13)	0.192(5)	565(9)
2	29.388(14)	110288(598)	0.144(11)	20619(65)	0.1870(16)	592(4)
3	30.879(5)	3333(84)	0.143(5)	646(10)	0.194(8)	602(21)
4	31.431(5)	2403(69)	0.166(6)	541 (9)	0.225(10)	519(19)
5	33.451(10)	174(8)	0.100(2)	19(3)	0.109(19)	847(175)
6	35.264(8)	258(12)	0.090(3)	36(6)	0.140(3)	926(266)
7	35.964(15)	13769(209)	0.145(15)	2695(10)	0.196(4)	598(6)
8	37.314(17)	352(16)	0.117(19)	49(6)	0.140(2)	746(124)
9	39.412(16)	19140(252)	0.154(17)	4034(15)	0.211 (4)	571(6)
10	40.890(3)	174(9)	0.170(9)	32(15)	0.180(9)	521 (281)
11	41.074(7)	1004(40)	0.134(10)	143(15)	0.140(2)	662(49)
12	43.168(16)	16870(242)	0.146(19)	3366(15)	0.200(4)	611(8)
13	44.881(15)	403(18)	0.113(15)	49(7)	0.120(2)	797(106)
14	47.130(3)	5274(119)	0.194(7)	1395(30)	0.265(12)	467(16)
15	47.527(2)	16625(227)	0.191(3)	4340(37)	0.261 (6)	474(7)
16	48.520(2)	17872(245)	0.180(3)	4441 (21)	0.248(5)	505(7)
17	50.513(10)	341(16)	0.220(3)	93(10)	0.270(4)	426(58)
18	51.027(10)	539(26)	0.151(19)	125(7)	0.230(2)	608(78)
19	54.281 (8)	292(15)	0.110(13)	36(4)	0.120(2)	845(101)
20	56.587(5)	2980(88)	0.182(7)	787(11)	0.264(11)	517(19)
21	57.420(3)	7079(153)	0.194(4)	1973(15)	0.279(8)	487(11)
22	58.136(7)	903(38)	0.148(13)	186(11)	0.210(2)	641(55)

Table C.2 XRD Peak List for Oxidation Products

No.	2θ, °	Height, cps	FWHM, °	Int. I., cps°	Int. W., °	Size, Å
1	8.720(4)	148(6)	0.160(4)	25(8)	0.170(6)	516(119)
2	23.038(3)	9821(160)	0.147(2)	1812(13)	0.185(4)	576(8)
3	28.420(6)	375(14)	0.150(4)	98(18)	0.260(6)	579(168)
4	29.393(12)	129886(652)	0.144(8)	23605(66)	0.181(14)	594(3)
5	30.894(5)	3369(87)	0.139(8)	713(11)	0.212(9)	619(34)
6	31.440(6)	2885(78)	0.156(5)	590(10)	0.205(9)	551(18)
7	33.451 (3)	132(6)	0.125(8)	17.5(7)	0.133(11)	693(44)
8	35.300(3)	228(11)	0.130(3)	36(6)	0.160(4)	660(147)
9	35.970(14)	14433(216)	0.147(12)	2737(9)	0.190(3)	592(5)
10	37.320(19)	257(13)	0.170(3)	56(7)	0.220(4)	527(92)
11	39.414(13)	21852(275)	0.144(14)	4264(14)	0.195(3)	612(6)
12	41.084(8)	860(36)	0.124(11)	159(6)	0.184(15)	716(63)
13	43.172(14)	19423 (262)	0.135(17)	3584(17)	0.185(3)	657(8)
14	44.902(9)	472(23)	0.121(17)	75(7)	0.160(2)	744(105)
15	47.131(19)	5878(129)	0.163(5)	1326(24)	0.226(9)	55417)
16	47.529(17)	19954(261)	0.178(2)	4917(31)	0.246(5)	510(6)
17	48.524(19)	20372(267)	0.177(2)	4830(20)	0.237(4)	515(6)
18	50.457(6)	453(22)	0.140(2)	89(7)	0.200(3)	658(102)
19	51.001(8)	384(20)	0.250(4)	138(8)	0.360(4)	361(50)
20	56.593(5)	3293(99)	0.170(6)	773(12)	0.235(11)	554(19)
21	57.427(2)	8445(174)	0.177(3)	2105(14)	0.249(7)	536(9)
22	58.111(10)	899(38)	0.184(12)	203(8)	0.226(19)	515(34)